

Quasicrystals: structure and stability

K. F. Kelton

Since their discovery in 1984, several thousand papers have been published dealing with various aspects of quasicrystals. Despite this flurry of activity, questions concerning the development, structure, and physical properties of this new phase remain only partially answered. This article reviews investigations of the formation and stability of quasicrystals. A pedagogical approach is taken. A brief survey of atomic and structural models, defects, and metallurgical properties of selected systems is provided as necessary background. While most attention is focused on the icosahedral quasicrystalline phase, one section is devoted to another common quasicrystal, the decagonal phase. Aluminium based quasicrystals are most common and are reviewed here; the first review of titanium based quasicrystals is also provided.

IMR/243

© 1993 The Institute of Materials and ASM International. Professor Kelton is in the Department of Physics, Washington University, St Louis, MO, USA.

Introduction

The three dimensional (3D) analogue to the pentagon is the icosahedron, first introduced by Plato¹ as one of the divine geometrical forms now known as the Platonic solids. It is characterised by fivefold, threefold, and twofold rotational symmetries (Fig. 1). Nature abounds with examples of pentagonal and icosahedral symmetry, particularly in biological systems. For example, some fossilised remains of the blastoid, an extinct member of the echinoderm phylum (containing the modern day starfish) that lived approximately 255 million years ago, during the Mississippian (or lower Carboniferous) period form an almost perfect icosahedron.²

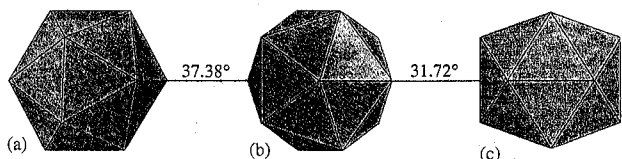
Despite their prevalence in biological systems, these rotational symmetries are conspicuously absent among crystals. Fundamental arguments demonstrate that they are incompatible with translational periodicity.^{3,4} While local atomic configurations with an icosahedral symmetry are found in some large unit cell crystals and are postulated to occur in liquids and glasses, the diffraction patterns show the allowed crystalline or amorphous features. No patterns are obtained with a strict icosahedral symmetry. Twinned assemblies of crystallites can produce diffraction patterns with a pseudo-fivefold symmetry; a careful examination, however, shows that all spots can be indexed to the crystal phases.

In 1984, Shechtman *et al.*⁵ astounded the scientific community by reporting the existence of a metallic solid, Al₈₆Mn₁₄, that produced an electron diffraction pattern with sharp spots (traditionally taken to indicate translational periodicity) arrayed in a tenfold rotationally symmetric arrangement (Fig. 2). Further diffraction studies confirmed that this new phase

demonstrated the full rotational symmetry of the icosahedral point group. Now called the icosahedral phase, or *i*-phase, it has been found in a variety of systems, appearing to be a candidate for the most common structure in 3d transition metal alloys. Other phases that produce similarly sharp diffraction patterns with different, but still classically forbidden, symmetries have also been discovered. Most notable is the decagonal phase, having one periodic axis orthogonal to two non-periodic axes. Collectively, these non-periodic phases are called quasicrystals; they are the subject of this review.

Linus Pauling^{6–8} and others^{9–13} have sought a conventional explanation for these anomalous diffraction patterns in terms of large unit cell crystals or multiply twinned crystalline phases. Both approaches, however, are incapable of explaining the diffraction data. Figure 3b shows a selected area diffraction (SAD) pattern taken from multiply twinned domains of an orthorhombic and monoclinic phase mixture in rapidly quenched Al₇₄Mn₂₆ (Ref. 14) (bright field image in Fig. 3a). Unlike the diffraction pattern from *i*(AlMn) shown in Fig. 2, the ten spots around the central spot are actually clusters of spots. The diffraction pattern from any individual domain is crystalline and it is possible to index the pattern by assuming an overlap of properly oriented crystalline patterns. No such reduction is possible for the *i*-phase. Dark field images,¹⁵ high resolution transmission electron microscopy (HREM),^{16–21} convergent beam studies,^{22,23} X-ray diffraction,²⁴ and field ion microscopy^{25,26} all agree; the icosahedral phase cannot be explained as an ensemble of multiply twinned crystallites. To explain the high resolution X-ray diffraction spectra in terms of a complex crystal structure would require a unit cell edge length of ~7 nm (Ref. 27), a cell containing more than 10 000 atoms! No evidence for such an enormous unit cell has been found in HREM studies of the icosahedral phase.

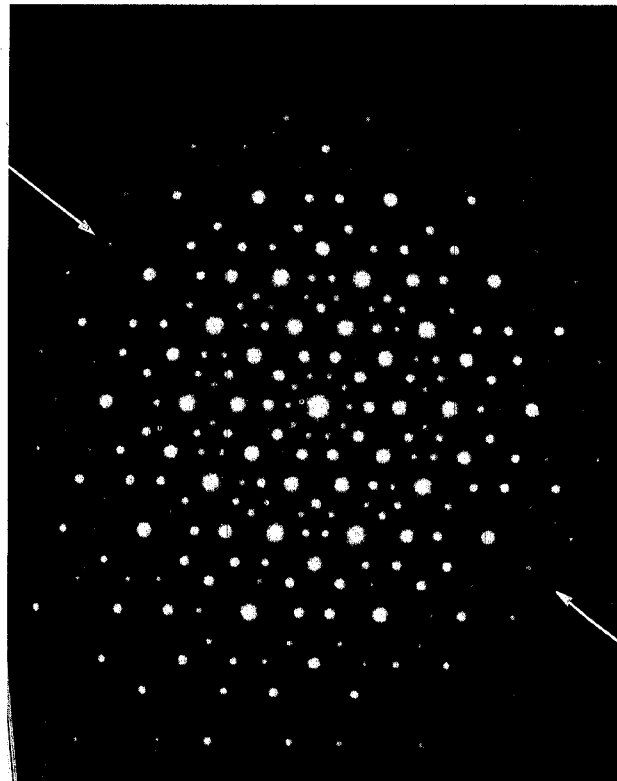
The evidence is then overwhelming that quasicrystals are not like traditional crystals, neither are they random on a large scale like glasses or liquids. They constitute a new class of condensed matter characterised by a non-crystallographic orientational symmetry. They are also quasiperiodic. The most familiar example of a one dimensional (1D) quasiperiodic function is the Fibonacci series,²⁸ resulting originally from the solution to an idealised problem related to the proliferation of rabbits. Representing a baby rabbit by *S* and an adult rabbit by *L*, and applying the simple substitution rule that each month a baby rabbit will be born to each adult, while all existing baby rabbits will reach adulthood, will result in the sequence ... SLSLLSLSL ... With repeated iterations, the ratio *L/S* equals precisely τ , the golden mean [$\tau = (1 + \sqrt{5})/2$]. Like periodic functions, a quasiperiodic function can be written as a trigonometric series. For periodic functions, the length scales



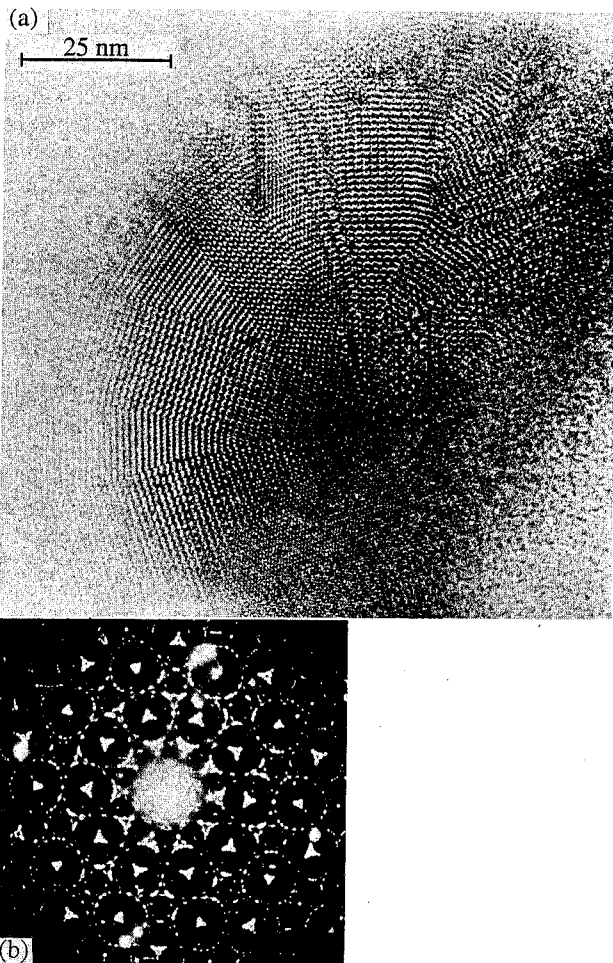
1 An icosahedron viewed along a threefold axis, *b* fivefold axis, and *c* twofold axis: rotation angles between these orientations are indicated

for the terms can be expressed as multiples of a number (equal to the dimensionality) of fundamental length scales. While also finite for a quasiperiodic function, that number is larger than the dimensionality; a simple example is $f(x) = \cos x + \cos \alpha x$, where α is any irrational number such as π or $\sqrt{2}$. Quasicrystals are not the first example of physical systems exhibiting quasiperiodicity; incommensurate crystals also have this property. Quasicrystals are set apart by their non-crystallographic orientational symmetry.

Despite their anomalous diffraction characteristics, these new phases have many features in common with crystallographic phases. They presumably contain the equivalent of a Bravais lattice with atoms decorating that lattice, they contain lattice type defects and they show evidence of chemical ordering. Many important differences, however, may lead to novel behaviour. Quasicrystals support new hydrodynamic modes, phasons, that have no analogue in ordinary crystals. Some models predict that reciprocal space may be



2 Selected area diffraction pattern of icosahedral phase in rapidly quenched $\text{Al}_{86}\text{Mn}_{14}$, taken along fivefold direction. Sighting figure at a glancing angle along radial direction indicated in figure reveals slight positional deviations of weaker diffraction spots due to phason strain



3 *a* high resolution image of multiply twinned multiphase grain of $\text{Al}_{74}\text{Mn}_{26}$ composed of alternating domains of an orthorhombic and a monoclinic phase radiating from central core; *b* SAD pattern from *a*, showing a pseudo-tenfold rotational symmetry resulting from twinning (Adapted from Figs. 10 and 13 of Ref. 14)

densely filled, possibly leading to exotic electronic properties, since the density of states should contain a dense population of gaps. Finally, unusual magnetic behaviour may result from the extremely high symmetry about certain atomic sites. Five years after their initial discovery, however, the most basic questions are only partially answered:

1. What is the correct model for the lattice structure?
2. Where are the atoms?
3. Why does such a non-periodic phase form?
4. What is the degree of stability or metastability?
5. What is the similarity between the quasicrystal structure and that of intermetallic crystalline phases of similar composition, or the undercooled liquid?
6. What are the physical properties that result from this novel structure?

It is not possible to provide an exhaustive review of a field, even one as young as this, in one article. Instead a pedagogical approach is chosen. Selected topics are illustrated by choosing representative alloy systems; no attempt is made to cover all topics, or to discuss all quasicrystals. The reportedly stable

Table 1 Reported aluminium based icosahedral phase alloys

Binary alloys		Ternary alloys		Quaternary alloys			
<i>i</i> -phase	Ref(s.)	<i>i</i> -phase	Ref(s.)	<i>i</i> -phase	Ref(s.)		
Al ₈₆ Co ₁₄	29, 30	Al ₈₀ Cr ₁₃ Co ₇	39	Al _{98-x} Mg _x Au ₂ (38 ≤ x ≤ 48)	58	Al ₆₅ Cr _{20-x} Fe _x Ge ₁₅ (x ≤ 15)	71
Al _{100-x} Cr _x (7 ≤ x ≤ 20)	5, 15, 24, 31	Al ₈₆ Cr ₁₂ Er ₂	40	Al ₇₈ Mg ₁₃ Cr ₉	59	Al ₆₁ Cu _{12.5} Li _x Mg _{36.5} (x = 0, 16.5, 25.9)	72
Al _{100-x} Fe _x (14 ≤ x ≤ 25)	5, 12, 15, 24	Al ₈₆ Cr _{14-x} Fe _x (3 ≤ x ≤ 14)	42, 43	Al _{98-x} Mg _x Ni ₂ (40 ≤ x ≤ 48)	58	Al ₉₂ Fe ₄ Cr ₃ Cu	43
Al _{100-x} Mn _x (12 ≤ x ≤ 23)	5, 12, 15, 24	Al ₈₆ Cr ₇ Ni ₇	44	Al _{98-x} Mg _x Pd ₂ (33 ≤ x ≤ 45)	58	Al ₇₅ Mn ₁₅ Cr ₅ Si ₅	73
Al ₉₂ Mo ₈	32	Al ₆₀ Cr ₂₀ Si ₂₀	41	Al _{98-x} Mg _x Pt ₂ (38 ≤ x ≤ 48)	58	Al ₄₀ Mn ₂₅ Fe ₃ Cu ₇ Ge ₂₅	74
Al ₈₆ Ni ₁₄	29, 30	Al ₆₈ Cu ₂₀ Cr ₁₅	45, 46	(Al,Zn) ₄₉ Mg ₃₂	48, 49, 60	Al _{75.5} Mn _{21.5-x} Ru _x Si ₃ (x = 4, 6)	76, 77
Al _{100-x} Pd _x (20 ≤ x ≤ 25)	33	Al ₆₈ Cu ₂₀ Fe ₁₅	45-47	Al ₈₄ Mn ₁₄ B ₂	61	Al ₇₂ Mn ₁₅ TM ₅ Si ₈ (TM = Ti, V, Cr, Mn, Fe, Co, Ni, Cu, Zr, Nb, Mo, Ru, Rh, Pd, Ag)	78
Al ₈₆ Pt ₁₄	24	Al ₆₈ Cu ₂₀ Mn ₁₅	45, 46	Al _{94-x} Mn _x Cr ₆	62, 63	Mg ₃₂ (Al,Zn,Cu) ₄₉	79
Al _{100-x} Re _x (14 ≤ x ≤ 22)	32, 34	Al ₆₈ Cu ₂₀ Os ₁₅	46	Al _{80-x} Mn ₂₀ Ge _x (x = 2, 6)	64, 65	Al ₇₀ Mn ₁₀ Pd ₂₀	66
Al ₇₈ Mn ₁₂ V ₁₀ (2.5 ≤ x ≤ 20)	35	Al ₇₈ Fe ₂₈ Ce ₇	45, 46, 51, 52	Al ₇₉ Mn ₁₇ Ru ₄	32	Al ₇₂ Mn ₂₈ Ti ₁₀	68
Al _{100-x} V _x (12 ≤ x ≤ 18)	36-38	Al ₈₀ Fe ₁₁ Mo ₉	55	Al _{94-x} Mn _x Si ₆	67	Al _{98.1} Mn _{3.6} Zr _{0.3}	69
		Al ₇₀ Fe ₂₀ Ta ₁₀	56			Al ₇₀ Pd ₂₀ Re ₁₀	70
		Al ₆ Li ₃ Au	48				
		Al ₆ Li ₃ Cu	48, 49				
		Al ₅₁ Li ₃₂ Zn ₁₇	48				
		Al _x Mg _{85-x} Ag ₁₅ (10 ≤ x ≤ 50)	48, 57				

Al-Cu-Fe icosahedral phase and the Al-Cu-Co decagonal phase are of considerable current interest and are discussed at some length. The similarities and differences between the rapidly quenched aluminium and titanium based icosahedral phases are also discussed extensively. A general discussion of the icosahedral phase, showing quasiperiodic order in three dimensions, is presented in the second section. Two and one dimensional quasicrystals are discussed in the third section. Quasicrystal structures, atomic decorations, and defects are discussed in the fourth and fifth sections. Their formation and stability are discussed in the sixth section.

Icosahedral phase – a three dimensional quasicrystal

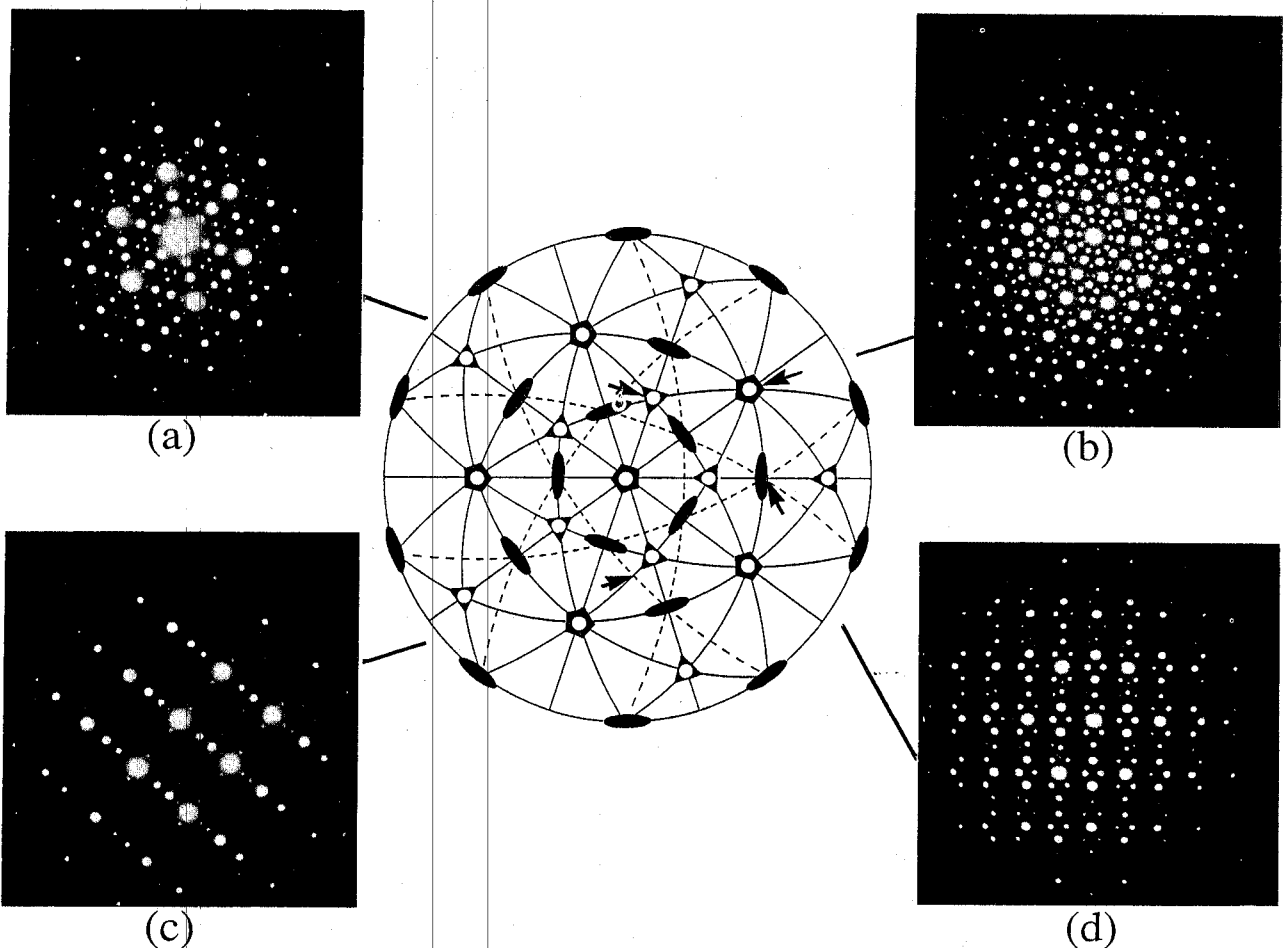
The icosahedral phase forms most readily in aluminium-3d transition (Al-TM) and titanium-3d transition (Ti-TM) metal alloys; partial lists of alloys

reported to contain the *i*-phase are presented in Tables 1 and 2. In most cases the *i*-phase is metastable relative to competing crystalline phases; its formation requires that the occurrence of these other phases be kinetically inhibited. While it is generally reported in alloys that have been quenched rapidly from the liquid phase, it has also been found in samples prepared by devitrification of glasses,¹⁰⁰⁻¹⁰² vapour condensation,^{103,104} solidification under high pressure,¹⁰⁵ electrodeposition,^{106,107} solid state precipitation,^{108,109} interdiffusion of multilayers,¹¹⁰ mechanical alloying,¹¹¹ and ion implantation.¹¹² Evidence suggests that *i*(AlLiCu), *i*(GaMgZn), and *i*(AlCuFe) may be stable and that a 2D quasicrystal, the decagonal phase, is the stable phase in an Al-Cu-Co alloy. Diffraction and metallurgical properties of the metastable Al-TM and Ti-TM *i*-phases and the stable Al-Cu-Fe icosahedral phase are reviewed in this section. The general features of the 2D and 1D quasicrystals are discussed in a following section.

Table 2 Reported non-aluminium based icosahedral phase alloys

Ti-based alloys		Other alloys	
<i>i</i> -phase	Ref.	<i>i</i> -phase	Ref(s.)
Ti ₂ Co	80	Cd ₃ Cu ₄	89
Ti _{68-x} Cr ₃₂ Si _x (6 ≤ x ≤ 18)	81	Co ₈₀ Er ₂₀	90, 91
Ti ₂ Fe	82	Cr ₇₁ Ni ₂₉	39
Ti ₆₁ Mn ₃₇ Si ₂	80	Fe _{100-x} Cu _x (x = 15, 40)	92
Ti ₅₆ Ni ₂₈ Si ₁₆	83	Fe ₄₀ Mo ₆₀	93
Ti ₅₃ Ni ₂₀ Zr ₂₇	84	Fe ₆₂ Nb ₄₈	94
Ti _{73-x} V _x Si _x (13 ≤ x ≤ 25)	85	Ga ₁₆ Mg ₃₂ Zn ₅₂	95
(Ti _{1-x} V _x) ₂ Ni	86	Mn ₅₀ Ni ₃₃ Si ₁₇	96
Ti ₅₆ Ni ₂₃ Fe ₅ Si ₁₆	87	Pd _{68.8} U _{20.6} Si _{20.6}	97
Ti ₆₃ Mn _{37-x} TM _x Si ₂ *	88	Pb ₇₂ Bi ₂₈	40
(TM = V, Cr, Fe, Co, Ni, Cu)		V ₄ Ni ₃₆ Si ₂₃	99
		Fe _{63.1} Cr ₂₁ Ni _{8.3} Mo _{1.6} Si _{4.4} Cu ₁ Nb _{0.6} Co _{0.1} (duplex stainless steel)	98

*Value of x depends on the 3d transition metal added.



4 Selected area diffraction patterns taken by TEM from icosahedral phase in rapidly quenched $\text{Al}_{86}\text{Mn}_{14}$. Lines are drawn from patterns to zone axes on stereographic projection for which they are approximately aligned. Following the notation of Chattopadhyay *et al.*,¹¹³ the zone axes for the patterns can be indexed as: *a* threefold – $[\bar{\tau}^2\bar{1}0]$, *b* fivefold – $[\bar{1}\tau0]$, *c* $[\bar{\tau}10]$, and *d* twofold – $[010]$

Electron microscopy and X-ray diffraction

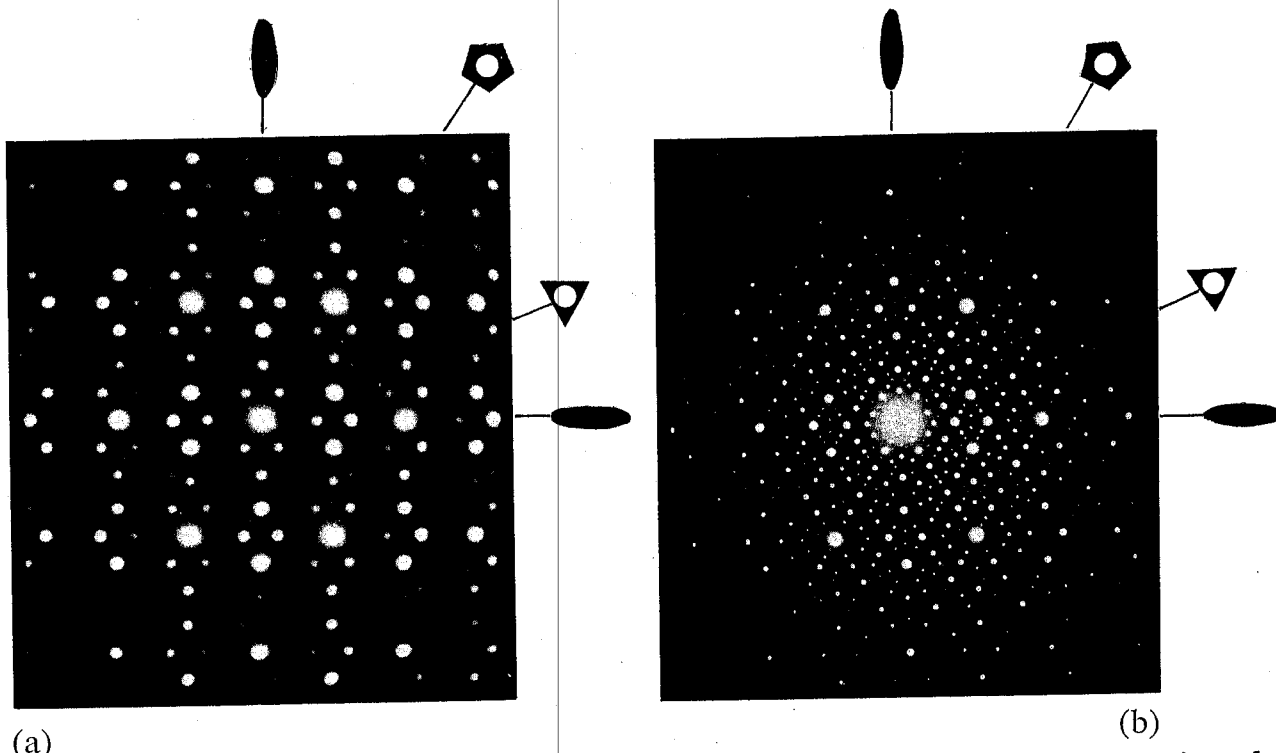
Transmission electron microscopy (TEM) rotation studies about axes that are 36° apart produce a different sequence of diffraction patterns, indicating that the apparent tenfold symmetry in Fig. 2 is actually a fivefold inversion symmetry.⁵ As demonstrated in Fig. 4, the locations and symmetries of these diffraction patterns agree with the elements of the icosahedral point group, $m\bar{3}5$, showing the expected fivefold, threefold, and twofold rotational symmetries. The zone axis is indexed following Chattopadhyay *et al.*¹¹³ Several high symmetry mirror patterns are also observed; one of these, the $[\bar{\tau}10]$, is included in Fig. 4. The icosahedral point group is inconsistent with any crystallographic space group. This structure then represents a radically new type of condensed phase that possesses an extended orientational order, but lacks the expected translational symmetry.

Unlike diffraction patterns taken from periodic phases, along a particular radial direction the distances between the spots are not in integer ratios, but are powers of the golden mean, τ . Along a prominent radial direction the spots can be indexed using two length scales, l and τl , suggesting an incommensurate structure. Most icosahedral phases show a τ^3 scaling of the distances between prominent diffraction spots along the fivefold direction of a diffraction pattern

taken in a twofold orientation (Fig. 5*a*). The expected spots at τ and τ^2 are forbidden by parity constraints.¹¹⁴ Twofold diffraction patterns from *i*(AlCuFe) contain these forbidden spots showing a τ progression along the fivefold direction (Fig. 5*b*).¹¹⁵

For most *i*-phases, the fundamental structure is masked by a high density of defects such as slightly misoriented microdomains,^{116,117} phason strains,¹¹⁸⁻¹¹⁹ localised diffuse scattering,^{120,121} and dislocations;^{116,117,122-129} *i*(AlCuFe), however, is largely defect free. Unlike the stable *i*(AlLiCu) (Ref. 130) and *i*(GaMgZn) (Ref. 131), the Kikuchi bands taken with convergent beam in TEM from *i*(AlCuFe) are fully symmetric.¹¹⁵ Similarly, deviations from perfect icosahedral symmetry in the TEM diffraction patterns are much smaller than those observed from other icosahedral phases^{95,115,132,133} and the diffraction spots are observed for small g , indicating a longer ranged icosahedral order.¹³³

The *i*-phase occurs as part of a fine multiphase mixture in Al-TM and Ti-TM alloys; consequently, only powder X-ray diffraction studies are possible. The positions of the diffraction lines agree with the TEM diffraction studies,^{24,134} demonstrating that the unusual rotational symmetry observed there is not due to multiple scattering. The peaks are broad, particularly in the Ti-TM alloys,^{135,136} indicating



5 a SAD pattern taken along a twofold direction in *i*(AlMn), a simple (P) icosahedral phase; b twofold SAD pattern from *i*(AlCuFe), a body centred (I) icosahedral phase

considerable disorder; powder and single crystal diffraction studies of *i*(AlLiCu) produce similar results.^{137,138} While X-ray diffraction studies on rapidly quenched *i*(AlCuFe) samples show peak widths that are comparable to those observed in other icosahedral phases,^{139,140} measurements on well annealed samples show spectacularly narrowed peaks,^{141–143} in some cases giving resolution-limited widths, implying a coherence length for quasiperiodic long range order that exceeds 800 nm (Ref. 144). X-ray measurements on the isomorphic *i*(AlCuRu) give similar results.¹⁴⁵ These results demonstrate that disorder is not an inherent property of quasicrystals, and are important for choosing the correct lattice geometry (see the section 'Lattice models and basic quasicrystallography' below).

High energy transmission electron microscopy images of the *i*-phase show lattice fringes that follow a quasiperiodic sequence.^{20,146–148} These have been used widely to formulate structural models of quasicrystals,^{17,147,149} however, comparisons with proposed structures can be made only if the sample thickness and degree of defocus of the microscope are well known.^{150,151} While the lattice images of most quasicrystals contain jogs and shifts caused by dislocations, disclinations, and phason strain, *i*(AlCuFe) shows a uniform distribution of lattice fringes in agreement with the order indicated in the X-ray and electron diffraction studies.

Indexing schemes

Owing to the two incommensurate length scales, six numbers are required to specify, or index, uniquely each diffraction peak of the *i*-phase. Two indexing schemes are used most frequently. One, due to

Elser,¹¹⁴ emphasises the structural relation to the icosahedron, while the other, due to Cahn,¹⁵² emphasises the relation to cubic symmetry. The Elser scheme is used in this review.

A basis composed of six unit vectors \mathbf{e}_{\parallel}^n pointing to the upper vertices of an icosahedron is chosen (Fig. 6a). These can be written as

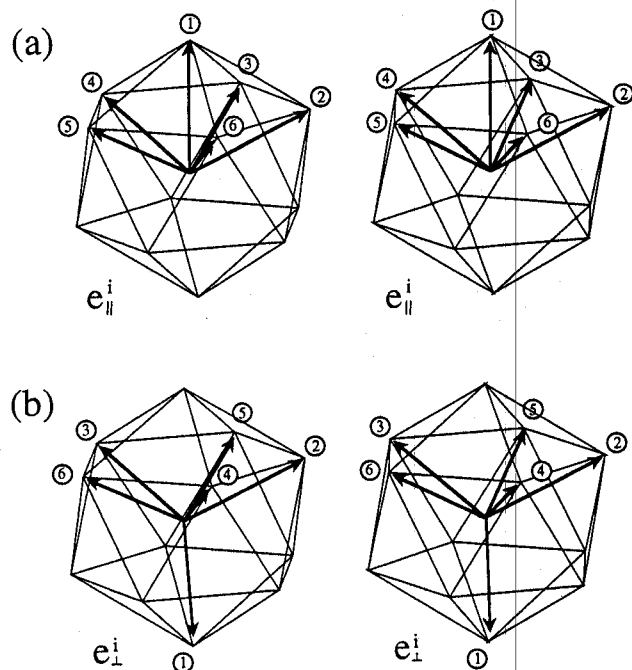
$$\begin{aligned}\mathbf{e}_{\parallel}^1 &= (0, 0, 1) \\ \mathbf{e}_{\parallel}^n &= \left[\sin \beta \cos \left(\frac{2\pi(n-2)}{5} \right), \right. \\ &\quad \left. \sin \beta \sin \left(\frac{2\pi(n-2)}{5} \right), \cos \beta \right]\end{aligned}$$

where $\cos \beta = 5^{-1/2}$ and $n = 2, \dots, 6$. The Bragg vector \mathbf{g} for each diffraction peak can be expressed as an integer linear combination of these vectors

$$\mathbf{g}_{\parallel} = \frac{\pi}{a_R} \sum_{n=1}^6 n_i \mathbf{e}_{\parallel}^n$$

The scale is set by a_R , defined as the quasilattice constant, representing the edge length of rhombohedral, structural, building, blocks (see the section 'Lattice models and basic quasicrystallography' below). A list of the prominent spots in TEM diffraction patterns from the *i*-phase in Al-Mn ($a_R = 0.46$ nm) is provided in Ref. 114. A similar indexing scheme, introduced by Bancel *et al.*,²⁴ is related to Elser's scheme by a scale factor of τ^{-3} .

These basis vectors can be obtained by a projection from a 6D cubic lattice into normal 3D space (see the section 'Lattice models and basic quasicrystallography' below). Another vector set \mathbf{e}_{\perp}^n is obtained on projecting into the remaining three dimensions,



6 Stereopair showing icosahedral basis vectors used in Elser indexing scheme: *a* for parallel space and *b* for perpendicular space: this stereopair may also be viewed with stereoglasses if the figure is photocopied and members of pair are exchanged (Courtesy of T. L. Daulton)

forming a dual or perpendicular space; they are related to e_{\parallel}^i as shown in Fig. 6b. Each Bragg vector has a corresponding vector in the dual space

$$\mathbf{g}_{\perp} = \frac{\pi}{a_R} \sum_{n=1}^6 n_i \mathbf{e}_n^i$$

As discussed in the section 'Lattice models and basic quasicrystallography' below, the intensities of a primitive quasilattice are strictly functions of \mathbf{g}_{\perp} ; since the quasilattice is decorated with atomic clusters, real systems show a \mathbf{g}_{\parallel} dependence also. A determination of the correct atomic decoration by quantitatively predicting the diffraction peak intensities, subject to the appropriate density and stoichiometric constraints, remains one of the central problems in the study of quasicrystals (see the sections 'Lattice models and basic quasicrystallography' and 'Atomic decorations' below).

Nelson and Sachdev¹⁵³ calculated the expected diffraction patterns from a superposition of density waves using vectors pointing to the 20 faces, 12 vertices, or 30 edges of a regular icosahedron. These three classes can also be viewed as projections into three dimensions from a 6D simple cubic (P), face centred cubic (F), or body centred cubic (I), 6D Bravais lattice, respectively.¹⁵⁴ The P reciprocal lattice has even and odd parity vectors depending on the parity of the sum of their indices. The indices for the I-type are all even or all odd, the sum of the indices is even for the F-type reciprocal lattice. The F reciprocal lattice can also be viewed as a superlattice of the P-type, by placing two kinds of icosahedral clusters at even and odd vertices. The predicted diffraction patterns from these classes are indistinguishable along the fivefold

and threefold directions, but important differences are predicted along the twofold directions. Most icosahedral phase diffraction patterns index to the P reciprocal lattice. Ebalard and Spaepen¹¹⁵ pointed out that *i*(AlCuFe) was the first example of an I reciprocal lattice. Chattopadhyay *et al.*¹⁵⁵ had earlier reported an F reciprocal lattice in rapidly quenched Al₈₆Mn₁₄ alloys.

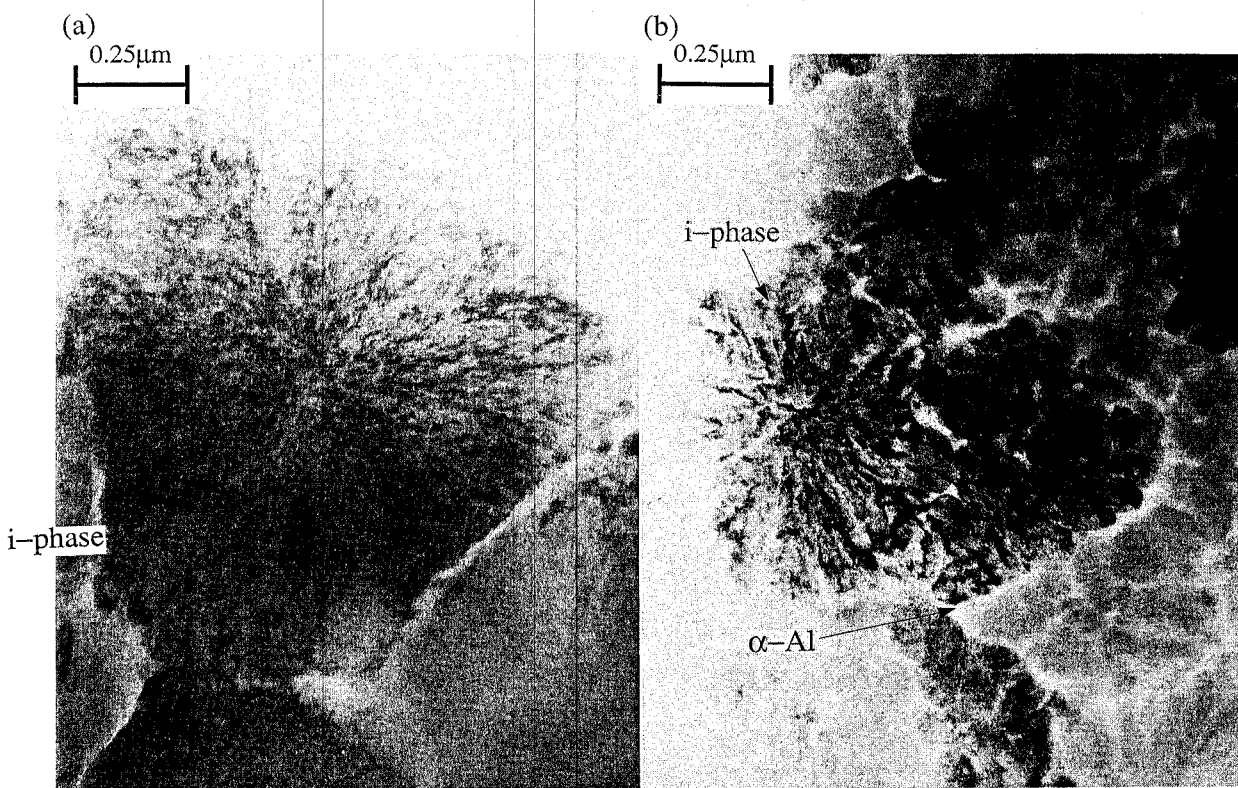
Metallurgy and microstructure

Metallurgical studies have concentrated on the Al-TM alloys; a detailed discussion is given in Ref. 156. The phase diagrams for these quasicrystals often contain a series of intermetallic compounds formed by peritectic reactions on the Al-rich side.¹⁵⁷ The attainment of equilibrium is sluggish, leading to easy metastable phase formation.¹⁵⁸ The common features of the titanium based quasicrystals are less clear. It appears that Si may be critical for *i*-phase formation,¹⁵⁹⁻¹⁶² however, few features of the equilibrium Ti-TM-Si phase diagrams are known in the appropriate concentration ranges.

In rapidly quenched Al-TM and Ti-TM alloys, the *i*-phase grains are mottled and have a coral like, weakly dendritic shape, typically 1–2 μm in diameter (Fig. 7).^{5,15,22} The origin of the mottled texture is unknown, though chemical disorder,¹⁶³ a distribution of regions with a slight misorientation,¹⁶⁴ and density fluctuations¹⁶⁵ have been suggested. The *i*(AlCuFe) grains are smooth and featureless,¹³³ again indicating a low density of defects. They are strongly faceted showing no significant dendritic character.^{47,166}

The aluminium composition of the *i*-phase in Al-TM alloys is close to 80 at.-%.^{38,157,167,168} Owing to the preferred formation of additional phases, particularly the decagonal phase (see the section 'One and two dimensional quasicrystals' below), in alloys of this composition, however, Al-richer systems are more favourable for *i*-phase formation. The growth rate of the *i*-phase from the liquid is therefore typically limited by the diffusion of excess Al from the interface. The microstructures of most rapidly quenched Al-TM alloys are similar suggesting a similar growth process; all *i*-phase grains are surrounded by α-Al (Fig. 7b). X-ray studies show that the spacing between the most strongly reflecting planes changes,¹⁵⁷ indicating that the *i*-phase can exist over some range of compositions. This agrees with studies by Zhang *et al.*¹⁶⁹ on room temperature annealed, rapidly quenched Al₉₆Mn₄ samples; in which the *i*-phase composition was close to 87 at.-% Al. The microstructures of most titanium based icosahedral phases are also similar (Fig. 7a).^{80-82,85} The secondary phase surrounding the *i*-phase, however, is β-Ti, a bcc solid solution. In *i*(TiMnSi), the Mn concentration is fixed at 37 at.-%, though up to 20 at.-% Si can be substituted for the Ti.¹⁷⁰

Frequently, the *i*-phase grows with a strong orientational relation to complex crystalline phases; an understanding of these relationships can provide information about their structural similarities. Koskenmaki *et al.*¹⁷¹ and Guyot and Audier¹⁷² showed that when they formed together, the symmetry



7 Bright field TEM image of typical grain of *i*-phase in *a* $Ti_{60}Cr_{32}Si_8$ and *b* $Al_{83}Cr_{17}$: note mottled appearance of both grains and more dendritic character of $Al_{83}Cr_{17}$ grain (Ref. 81)

axes of the icosahedra in α -(AlMnSi) (a large unit cell, cubic, crystalline, phase¹⁷³) were aligned with the corresponding icosahedral symmetry axes of *i*(AlMnSi): $\langle 100 \rangle_{bcc} \parallel$ 2-fold_{*i*-phase}, $\langle 111 \rangle_{bcc} \parallel$ 3-fold_{*i*-phase} and $\langle 532 \rangle_{bcc}$ approximately parallel with the *i*-phase fivefold zone. A similar relation was reported between *i*(AlMgZn) and the Bergmann phase, a rather large unit cell bcc phase.¹⁷⁴ Zhang and Kelton⁸⁵ recently reported this relation between *i*(TiVSi) and a previously unknown, large unit cell, bcc structure; the overlapping diffraction patterns are shown in Fig. 8. Dong *et al.*¹⁷⁵ reported this earlier for a large unit cell bcc phase nucleating on the boundary between the *i*-phase and β -Ti in rapidly quenched Ti-Fe alloys.

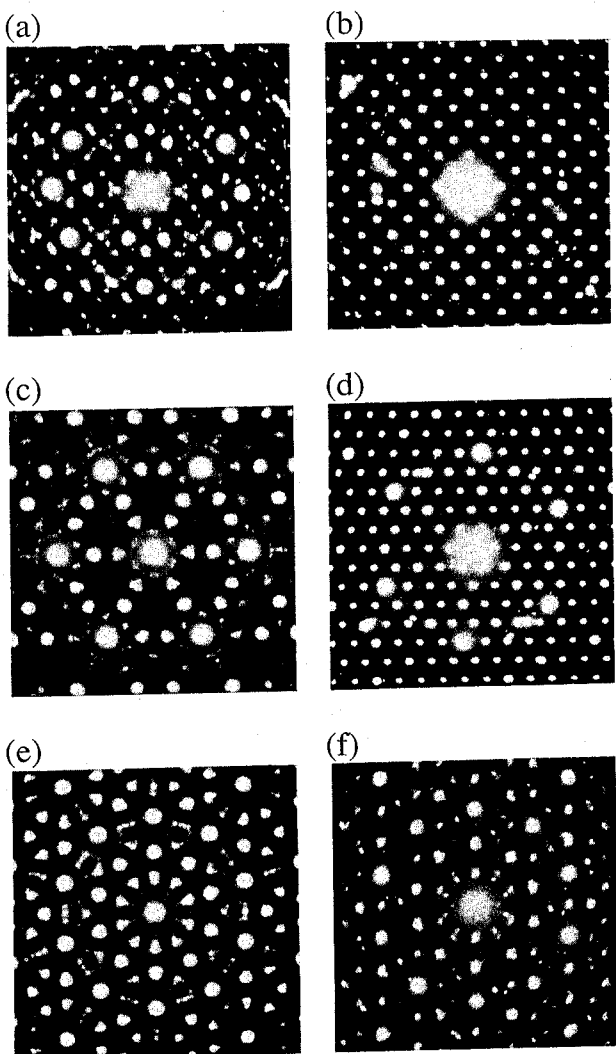
Precipitates frequently show an orientational relationship with the solid solution phase, forming a coherent interface to minimise the interfacial energy. Samples prepared by implanting Al with Mn ions followed by low temperature annealing show that the twofold symmetry axis of the *i*-phase aligns with the $\langle 001 \rangle$ and $\langle \bar{1}10 \rangle$ of the Al.¹⁷⁶ This relation was also observed in dilute Al-Mn (Ref. 169) and Al-Mn-Zr (Ref. 69) alloys. A different relation was found between *i*(AlLiCu) and fcc Al,¹⁷⁷ where the twofold axes of the icosahedron are parallel to the $\langle 110 \rangle$ directions of the Al.

The morphological form for crystalline systems is related to the space group; this was the basis for the early developments in crystallography. The equilibrium shape is determined by surface energy considerations,¹⁷⁸ though in many cases, a non-equilibrium morphology, dictated by growth kinetics, occurs.¹⁷⁹ Surprisingly, strongly faceted forms are found in many quasicrystalline systems, in spite of their lack of

translational periodicity and thermodynamic stability. Several theoretical investigations, however, demonstrate the possibility for faceting in quasiperiodic systems.¹⁷⁹⁻¹⁸⁴

Scanning electron microscopy (SEM) and TEM studies indicate a strong tendency for a pentagonal dodecahedral (PD) growth morphology in rapidly quenched Al-Mn alloys^{164,185} and in dilute Mn alloys, annealed at room temperature¹⁶⁹ or 600 K.¹⁰⁸ *i*-phase precipitates in $Al_{91}Mn_4B_5$, initially claimed to show an icosahedral shape,¹⁸⁶ were later shown to also have a PD morphology.¹⁸⁷ The most striking facets are observed in large grains of the stable *i*-phase materials: a pentagonal dodecahedron for *i*(GaMgZn) (Ref. 95) and *i*(AlCuFe) (Ref. 47) and a rhombic triacontahedron for *i*(AlLiCu).¹⁸⁸

For most quasicrystals, the most rapid growth from the liquid is along the threefold direction.^{185,187,189} This is demonstrated in Fig. 9*a* showing as quenched alloys of dilute Mn concentration (≤ 6 at.-% Mn), displaying a flower-like shape, suggestive of planar cuts through dendrites growing along the threefold directions. The lack of an orientational relation with α -Al^{185,190} and the strong dendritic character indicate that these grains nucleated and grew from the liquid. With increasing Mn, the microstructure develops into that of faceted, interconnected grains with a pentagonal dodecahedral morphology.^{187,191,192} Room temperature annealed samples of $Al_{96}Mn_4$ indicate that the threefold direction is also the fast growth direction from the α -Al solid solution.¹⁶⁹ In *i*(AlLiCu) (Ref. 188) and *i*(TiFeMnSi) (Ref. 193) the fivefold growth direction is fastest. This is illustrated in Fig. 9*b* showing a TEM bright field image of a dendritic cluster taken



a along twofold icosahedral direction coincident with *b* the [001] zone axis; *c* along threefold direction, coincident with *d* the [111] zone axis; *e* along fivefold icosahedral direction, nearly coincident with *f* the [530] cubic zone axis

8 Selected area diffraction patterns of icosahedral bcc phase mixture along prominent zone axes of *i*-phase (Ref. 85)

along the fivefold zone axis of rapidly quenched *i*(TiFeMnSi).

Phase formation

The local atomic structure of the *i*-phase is postulated to be similar to that for liquids and glasses;¹⁹⁴ a study of amorphous structures might therefore illuminate the formation criteria for the *i*-phase. Since the work of Fahrenheit, it has been known that liquids can be cooled considerably below their equilibrium melting temperature without crystallisation.¹⁹⁵ Frank argued that atoms were arranged with a tetrahedral coordination in the undercooled liquid;¹⁹⁶ this order could take the form of an icosahedron, constructed from 20 regular tetrahedra. Because close packed crystalline structures are dominated by local octahedral configurations, the tetrahedral coordination must first be destroyed on crystallisation, constituting a barrier to nucleation. While no direct experimental evidence in support of Frank's hypothesis exists, molecular

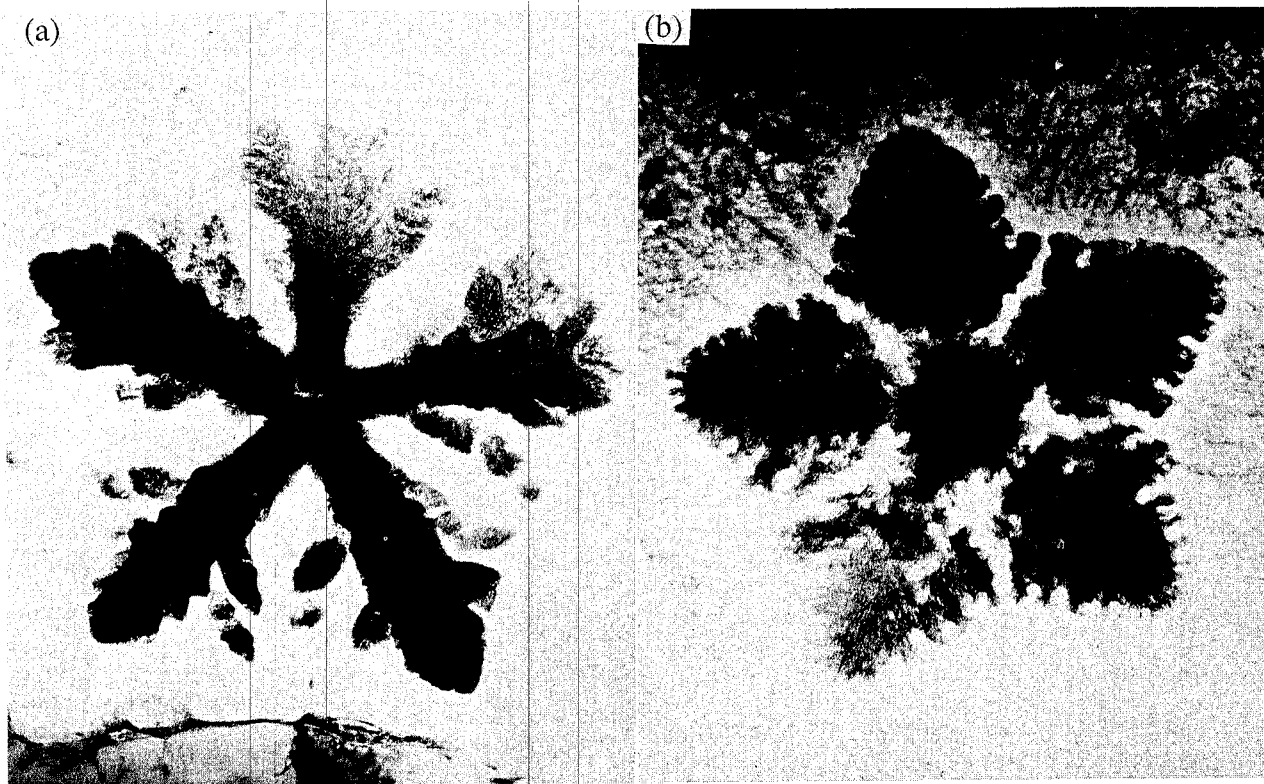
dynamics studies of ensembles of particles interacting under a central potential, show a dramatic increase in the icosahedral configuration, over that found in the equilibrium liquid, as the system is undercooled below the melting point.¹⁹⁷⁻²⁰⁰ Earlier, Bernal²⁰¹ and Finney²⁰² had noticed a predominance for Voronoi polyhedra around each sphere in a dense random packing with five edges per face, indicating a strong tendency towards local fivefold coordinations.

Sachdev and Nelson¹⁹⁴ suggested that the formation of the *i*-phase is favoured over that of competing crystalline phases because less atomic reconstruction is required. This argument is supported by the occurrence of a dense population of very small grains of the *i*-phase with thermal annealing of PdUSi metallic glasses,^{203,204} and by ion mixing processes.²⁰⁵

Some 'amorphous' metals may actually be composed of extremely fine grained, randomly oriented, quasicrystals. Bendersky and Ridder²⁰⁶ argued that rapidly quenched droplets of Al₈₆Mn₁₄ solidify to a 'micro-quasicrystalline' structure with grain sizes as small as 1 nm. Robertson *et al.*²⁰⁷ have shown that the X-ray diffraction of a sputter deposited amorphous Al₇₂Mn₂₂Si₆ film can be explained in terms of a 2.5 nm grain diameter microquasicrystalline structure. Differential scanning calorimetry (DSC) measurements by Chen and Spaepen²⁰⁸ support this, demonstrating that sputter deposited Al_{82.6}Mn_{17.4} and Al₈₂₋₈₃Fe₁₇₋₁₈ films that produced amorphous diffraction patterns, transformed by grain coarsening instead of nucleation and growth, suggesting a fine dispersion of icosahedral grains.

Chen and Spaepen's results indicate an extremely high nucleation rate from the liquid. The devitrification of rapidly quenched Pd_{58.8}U_{20.6}Si_{20.6} produced a fine grained (~100 nm) *i*-phase, also suggesting a large nucleation rate. Transmission electron microscopy and DSC indicate that the transformation is first order, proceeding by nucleation and growth. Based on a detailed analysis of TEM, DSC, and resistivity measurements of the transformation of Al-Cu-V metallic glasses to quasicrystals of the same composition, Holzer and Kelton²⁰⁹ recently determined the temperature dependent nucleation rate. From that they obtained the first estimate of the interfacial energy between the *i*-phase and the undercooled liquid, or glass, $0.002 \leq \sigma \leq 0.015 \text{ J m}^{-2}$. Such a low interfacial energy demands that the atomic structure of the two phases on either side of the interface be similar. Comparable interfacial energies have only been obtained previously for polymeric liquids, where the chain structure in the liquid and the crystal are identical.²¹⁰

Since not all liquids form quasicrystals when they solidify, a criterion other than the similarity between the *i*-phase and liquid atomic configurations is required. Hundreds of intermetallic crystalline compounds have complex structures containing icosahedral units, presumably indicating a strong tendency for icosahedral clustering in the undercooled liquid (see the section 'Atomic decorations' below). When cooled sufficiently slowly, a structure that preserves this atomic coordination on a local scale while introducing other polyhedra to establish long range periodicity may result. These crystalline phases (crystal



9 Bright field images of icosahedral phase grains taken along fivefold direction *a* from *i*(AlMn), where growth is most rapid in threefold direction and *b* from *i*(TiMnFe), where growth is most rapid in fivefold direction: grain morphology reflects underlying icosahedral symmetry

approximants), then, approximate locally the atomic structure of the icosahedral phase; their diffraction patterns are often similar to those taken from the *i*-phase. Quasicrystals frequently form if these liquid alloys are rapidly quenched, suggesting that the kinetics are insufficient to establish the long range periodicity. Instead the icosahedral clusters are packed so as to maintain orientational order without long range translational order. This idea forms the basis of the icosahedral glass model (see the section 'Icosahedral glass' below), and has been successfully used to discover new icosahedral phases by quenching alloys that form crystalline phases with significant local icosahedral order.

For crystals, quasicrystals, and glasses, the fundamental question remains: why is icosahedral order so strongly preferred in some cases? Answers must come from considerations of atomic size, strain, and electronic effects. While enjoying some success, searches for Hume-Rothery type criteria^{211–213} remain phenomenological and speculative. Some fundamental studies of the stability of local structures based on electronic energy configurations are more promising. Since Bloch's theorem is inapplicable, inferences must be drawn from calculations on small clusters, crystal approximants, or quasicrystal structures of finite extent. Several universal features emerge:

1. Total energy calculations have shown that the Mackay icosahedron (cf Fig. 18a) is a particularly stable configuration, supporting its use in structural models.

2. The density of states is characterised by pronounced peaks and a dip near the Fermi surface.²¹⁴

3. Angular dependent forces seem to be responsible for stabilising the titanium based *i*-phases.²¹⁵

4. At least for Al-transition metal (TM) quasicrystals, interactions beyond nearest neighbours are important for stabilising the structure.²¹⁶

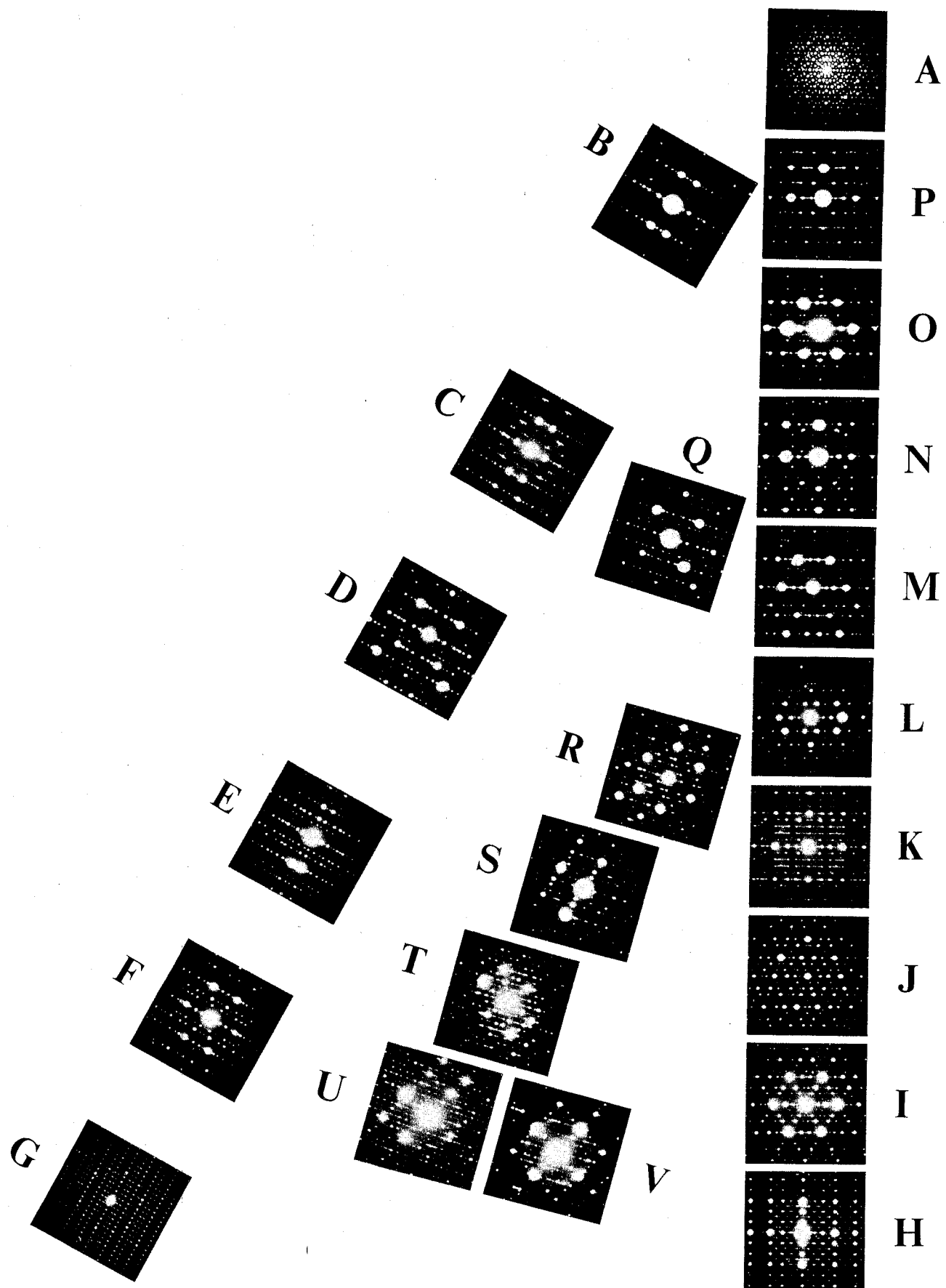
These electronic structure calculations have been reviewed recently.²¹⁷

One and two dimensional quasicrystals

Quasicrystals that display forbidden eightfold, tenfold, and twelvefold rotational symmetries in two dimensions but are periodic in the third have also been discovered. Additionally, 1D quasicrystals that are periodic in two dimensions but are quasiperiodic in the third have been reported. These quasicrystals are discussed briefly in this section. The best studied 2D quasicrystal is the decagonal phase, showing a tenfold rotational symmetry perpendicular to the periodic direction. This is discussed in detail here; a review of 2D quasicrystals with other rotational symmetries can be found elsewhere.^{218,219}

Decagonal phase

Sastray *et al.*²²⁰ reported the discovery of an unknown complex crystalline phase showing anomalous diffraction in a slowly cooled Al₆₀Mn₁₁Ni₄ alloy. Shechtman *et al.*²²¹ noticed a similar phase in rapidly quenched Al-Mn alloys with annealing. Chattopadhyay *et al.*²²⁵ and Bendersky²²² identified this phase as a new, 2D quasicrystal, now known as



10 Experimentally measured 18° stereographic section of decagonal phase showing SAD patterns for all prominent zone axes, determined from Kikuchi band crossings (Ref. 14)

the decagonal phase. Decagonal phase formation has been reported subsequently in many alloys; some are listed in Table 3. As is the case for the icosahedral quasicrystals, most decagonal phases occur in aluminium based alloys. In particular, though quasicrystal formation is now known to be prominent in the titanium alloys, there have been no substantiated reports of decagonal phase formation there.

Electron diffraction

The prominent zone axes from the decagonal phase are shown in Fig. 10. While similar to the diffraction patterns from the *i*-phase, there are important differences. Along one direction (*A* in Fig. 10), a tenfold rotational symmetry with quasiperiodic diffraction spots is obtained. A rotation to the position of an equivalent fivefold pattern for the *i*-phase, however, reveals an inequivalent, pseudo-fivefold pattern (pattern *J* in Fig. 10). Rotating to the position of threefold icosahedral patterns reveals pseudo-threefold patterns (*M* and *I* in Fig. 10). Further, convergent beam patterns taken along the tenfold direction show higher order Laue zones (HOLZ) that are absent in patterns taken from the *i*-phase.

On rotation by 90° from the tenfold pattern, two distinctly different twofold patterns, separated by 18°, are observed (*G* and *H* in Fig. 10). The diffraction spots along the tenfold zone axes in these two diffraction patterns are periodic; they follow a Fibonacci series in the perpendicular directions. This structure is then quasiperiodic in two dimensions but periodic in the third. On the basis of convergent beam diffraction studies, Bendersky²²² established the point group of this new phase as 10/m or 10/mmm, both disallowed crystallographic symmetries. It belongs to the cylindrical family of groups G₁.¹⁵⁵ The space group for the Al-Pd decagonal phase differs from others; it is P-10₅/mm, containing a screw axis and a glide plane.

As first noted by Bendersky,²²² the twofold patterns of the decagonal phase in Al-Mn show prominent streaking, indicating sheets of diffuse intensity in the plane of the zero-order Laue zone. The degree of streaking varies for different alloys and production methods. With the exception of the decagonal phase in Al-Fe,²²⁴ the streaking is perpendicular to the periodic axis, suggesting that either cylindrical domains are aligned along the periodic direction or linear chains are arranged in a Penrose 2D packing. High energy transmission electron microscopy images

of the Al-Mn decagonal phase, taken by Perez-Campos *et al.*²⁴² support the chain model, showing periodically twisting molecular-like chains that spiral along the periodic direction. The streaking for Al-Fe lies parallel to the tenfold zone axis, suggesting stacking faults along the periodic direction.

The spacing along the periodic direction in the decagonal phase in Al-Mn is 1.24 nm.^{14,222,243,244} Decagonal phases with different periodicities, however, have also been reported: 0.4 nm in Al-Ni (Ref. 245); 0.8 nm in Al-Cu-TM (TM = Mn, Fe, Co, or Ni),²⁴⁶ and 1.6 nm in Al-Fe.²²⁴ All known decagonal phase periodicities have been reported as a function of composition in alloys of Al-Co (Ref. 247) and Al₆₅Cu₂₀TM₁₅ (TM = Mn, Fe, Co, or Ni),²⁴⁶ they have been reported in the same alloy of slowly cooled Al₆₅Cu₂₀Co₁₅.²⁴⁸ These results suggest that the decagonal phase contains a stacking of identical, equally spaced, planes; the basic periodicity is 0.4 nm in the real space structure. These different periodicities may indicate a type of polytypism in the decagonal phase.²⁴⁹

Indexing schemes

A minimum of five basis vectors are required to index the decagonal phase zone axes and diffraction patterns. The striking similarities between the diffraction patterns of the decagonal and icosahedral phases suggest that they are structurally related. Motivated by this, attempts to understand the crystallography of the decagonal phase have proceeded by systematic alterations of the crystallography of the icosahedral phase. Fung *et al.*²²² have suggested that the symmetry of the decagonal phase can be obtained from that of the icosahedral phase, either by the addition of a set of five mirror planes intersecting a fivefold axis and bisecting the angles between the mirror planes of the fivefold axis, or by a mirror plane placed normal to the fivefold axis (see also Bendersky²²⁸). These schemes fail, however, to predict accurately the observed Kikuchi band crossings from precision measurements of the prominent zone axes.²⁵⁰ Ho²⁵¹ and others^{192,252} proposed that the periodicity in the tenfold direction can be obtained by distorting the icosahedral vertex vector basis (Fig. 6) to a pentagonal bipyramid edge vector basis.^{192,251,252}

An alternate method, similar to the four vector, indexing scheme commonly used to index hexagonal crystals, proposes a six vector basis. A set of five

Table 3 Reported decagonal phase alloys

Al-based binary alloys		Al-based ternary alloys				Non-Al-based alloys	
<i>i</i> -phase	Ref(s.)	<i>i</i> -phase	Ref(s.)	<i>i</i> -phase	Ref(s.)	<i>i</i> -phase	Ref(s.)
Al _{100-x} Co _x (14 ≤ x ≤ 32)	223	Al ₆₅ Cu ₁₅ Co ₂₀	230, 231	Al-Mn-(Cr,Zr)*	225	Fe ₅₂ Nb ₁₈	240
Al _{100-x} Fe _x (14 ≤ x ≤ 25)	224	Al-Cu-(Fe,Ni)*	230	Al ₆₉₋₇₈ Mn ₉₋₁₅ Fe ₂₋₇	236, 237	Ti ₂ Fe _{1-x} Si _x	241
Al-Ir*	225	Al ₆₉ Cu ₁₉ Mn ₁₂	230, 232	Al-Mn-Ge*	225	(0.01 ≤ x ≤ 0.05)	
Al _{100-x} Mn _x (14 ≤ x ≤ 22)	155, 221, 222	Al ₆₅ Cu ₁₅ Rh ₂₀	231	Al ₈₀ Mn ₁₀ Ni ₁₀	225, 227	V ₄₁ Ni ₃₆ Si ₂₃	231
Al _{100-x} Ni _x (14 ≤ x ≤ 20)	226	Al ₇₅₋₈₆ Co ₁₅₋₂₀ Ni ₁₀₋₁₅	233	Al _{70.5} Mn _{16.5} Pd ₁₃	238		
Al-Os*	225	Al ₇₅ Co ₂₀ Si ₅	234	Al ₇₀ Ni ₁₈ Co ₁₅	239		
Al _{100-x} Pd _x (14 ≤ x ≤ 25)	134, 227-229	Al ₆₅ Cr ₇ Ni ₇	44	Al ₆ Ni(Si)	226		
Al ₈₆ Pt ₁₄	229	Al ₆₂ Cr ₁₉ Si ₁₉	235	Al ₇₅₋₈₅ Rh ₁₅₋₂₀ Cu ₁₀₋₁₅	233		
Al-Rh*	225	Al ₆₅ Fe ₂₈ Ce ₇	53, 54, 225	Al ₇₅₋₈₅ Rh ₁₅₋₂₀ Ni ₁₀₋₁₅	233		
		Al ₇₅₋₈₅ Fe ₁₅₋₂₀ Ni ₁₀₋₁₅	233				

* Composition data not available.

reciprocal lattice vectors \mathbf{a}_j are arranged in the basal plane, separated by 72° ; the sixth vector \mathbf{a}_6 is normal to the plane and points along the decagonal periodic axis. When first proposed by Takeuchi and Kimura,²⁵³ fractional indices were used; Choy *et al.*²⁵⁴ modified the system to use integers only. Their vectors are defined as

$$\mathbf{a}_j^* = a^* R_j(\theta) \mathbf{x} \quad (j = 1-5)$$

$$\mathbf{a}_6^* = c^* \mathbf{z}$$

where $R_j(\theta)$ represents a rotation about the z -axis through the positive (counterclockwise) angle $(j-1)\theta$. This indexing system has been used successfully to index the diffraction patterns and zone axes of the 1.24 nm periodic Al-Mn,^{24,25,42,43} the 0.8 nm periodic Al-Co,²⁵⁵ and the 1.6 nm periodic Al-Pd (Ref. 14) decagonal phases. An inherent ambiguity exists in this scheme, however, leading to several proposed methods for consistently choosing the indices.^{14,256,257}

As for the icosahedral phase, it is natural to view the decagonal phase as a projection from some higher dimensional periodic space (see the section 'Lattice models and basic quasicrystallography' below) though the best projection method is debatable. Ho²⁵¹ originally suggested an oblique lattice in a 6D space; Mandal and Lele²⁵⁸ proposed a 6D tetragonal lattice. In light of the 2D quasiperiodicity, a projection from a 5D space might be expected, however Muller²⁵⁹ showed that this projection produces a lattice of point group symmetry C_5 , lacking the observed mirror plane symmetry. Muller²⁶⁰ also demonstrated that two 6D representations, the pentagonal bipyramid representation proposed by Ho²⁵¹ or the pentagonal cylindrical representation proposed by Choy *et al.*,²⁵⁴ led to the indexing schemes discussed in this section, thus describing most of the observed crystallographic features of the decagonal phase.

Metallurgy and microstructure

In Al-Mn alloys, the decagonal phase grows in competition with the *i*-phase; formation is favoured in melt spun samples containing greater than 20 at.-%Mn. The largest volume fractions are found in the thicker regions of the ribbon that are cooled more slowly. In agreement, electron beam melting studies demonstrate that decagonal phase formation is preferred at slower solidification velocities; it appears to grow epitaxially on the icosahedral phase.^{157,261} There, the *H* twofold zone axis of the decagonal phase (Fig. 10) is aligned parallel to a twofold zone axis of the icosahedral phase; the tenfold zone axis of the decagonal phase is aligned with one of six possible fivefold axes of the icosahedral phase, allowing six possible growth variants. The same orientational alignment between these two phases is also found in rapidly quenched ribbons, again suggesting that the icosahedral phase forms directly from the melt, and the decagonal phase nucleates on those grains.²⁶² Decagonal phase formation in Al-Mn is critically dependent on the concentration of Si; the addition of only a few atomic percent can completely suppress its formation.²¹⁸ Taking advantage of the much greater solubility of Si in the icosahedral phase,

nearly single phase icosahedral samples of Al-Mn-Si can be produced. Interestingly, the addition of Ge in Al-Mn alloys results in a single phase decagonal material.²⁶³

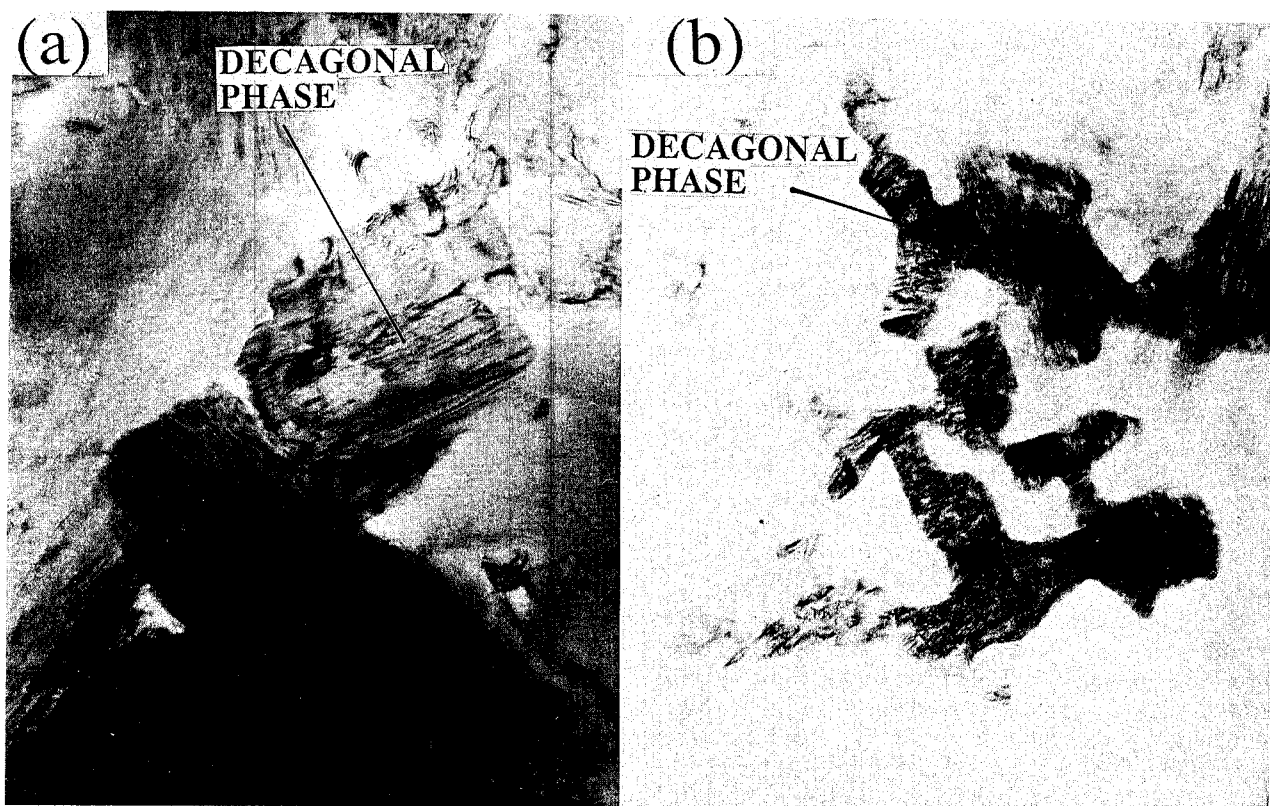
In rapidly quenched alloys the decagonal phase occurs as a component of a multiphase mixture of *i*-phase, solid solution phases, and frequently, complicated monoclinic and orthorhombic crystalline phases. The grain size varies from 0.1 μm to a few micrometres depending on the nominal composition and the sample preparation conditions.

The microstructure of rapidly solidified Al-Mn alloys is strongly dependent on the nominal composition and quench rate. Blocky, faceted, grains in $\text{Al}_x\text{Mn}_{100-x}$ ($82 \geq x \geq 76$) alloys quenched on to a copper wheel rotating at $\sim 30 \text{ m s}^{-1}$ (Fig. 11a)^{14,155,157,222,228} are replaced by interlocking, non-faceted grains when the wheel speed is increased to $\sim 60 \text{ m s}^{-1}$ (Fig. 11b). Decagonal grains typically show striations that vanish when viewed along the tenfold zone axis, suggesting planar defects in agreement with the streaks in the diffraction patterns. Ledges or steps are frequently observed, suggesting a lateral growth mechanism.^{19,21}

Below ~ 76 at.-%Al, the decagonal phase is replaced by Al_3Mn , often taken as an orthorhombic phase that is a crystalline approximant to the decagonal phase.²⁴ Daulton *et al.*,¹⁴ however, show evidence suggesting that Al_3Mn is actually a multiply twinned phase mixture of the orthorhombic phase and a new monoclinic phase. The orthorhombic phase appears to nucleate directly from the melt and the monoclinic phase nucleates and grows coherently on the orthorhombic/melt interface (Fig. 3a). A similar microstructure was observed in Al-Mn-Cu alloys.²⁶⁴

The decagonal phase appears to be a eutectic constituent in rapidly quenched Al-Pd alloys.²⁶⁵ Decagonal prisms have been reported in this system, indicating a strong tendency for facetting. The decagonal phase in rapidly quenched Al-Co alloys shows rosette, nodular, and cellular-dendritic morphologies.^{36,266,267} Defects, including twins, dislocations, dislocation loops, and planar faulting, have been observed.^{247,266} Plate-like and rosette decagonal phase morphologies have also been observed in rapidly quenched Al_4Ni and $\text{Al}_6\text{Ni}(\text{Si})$ alloys.²⁴⁵

The most beautiful grain morphologies are observed in slow cooled samples of (Al,Si)-Cu-Co, where decagonal prismatic needles several millimetres in length are observed.^{268,269} Long prismatic facets form in the longitudinal direction; ten edges are observed at the ends of these needles. The addition of Si was reported to improve the decagonal phase formation in this system.²⁷⁰ More detailed studies in as cast alloys made without Si of the phase generally taken to be the decagonal phase demonstrate that it is actually one of several complex crystalline phases with extremely large unit cells (of the order of 10 nm or more).^{271-274a} The X-ray and TEM diffraction patterns and the stereographic projections from these phases are almost identical to those of the decagonal phase. Annealing the as cast material results in a large number of new, complex, crystalline phases, but does not lead to the decagonal phase.^{273,274,274a} A minimum of 2.5 at.-%Si is required for decagonal



a blocky, faceted grains for alloys quenched at $\sim 30 \text{ m s}^{-1}$; *b* interlocking, less-faceted grains in alloys quenched at $\sim 60 \text{ m s}^{-1}$

11 Bright field TEM images of Al-Mn decagonal phase, illustrating quench rate dependence of microstructure

phase formation,^{274,274a} above 4.5 at.-% a 1D quasicrystal is formed (see the section 'Indexing schemes' above). Interestingly, a decaprismatic growth morphology is observed for this true decagonal phase as well as for the decagonal approximant phases.²⁷⁵

One dimensional quasicrystal

Al–Cu–Ni alloys form structures containing vacancy ordered layers intergrown with occupied layers.^{276,277} Chattopadhyay *et al.*,²⁷⁸ pointed out that the number of layers and the packing order of partially vacant layers follow a truncated Fibonacci sequence, concluding that the structural variants are periodic approximants of a 1D quasicrystal. Zhou *et al.*²⁷⁹ reported small regions within a nodule of the *i*-phase in V₄₁Ni₃₆Si₂₃ showing local translational order in one, two, or three twofold directions. This was taken as the initial stage of transformation of the icosahedral quasicrystal to the stable phase.

He *et al.*²⁸⁰ reported the first example of an extended region of a 1D quasicrystal, occurring as a transformation product of the decagonal phase. Daulton *et al.*^{274,274a} recently reported 1D quasicrystal formation with increasing Si in an Al–Cu–Co alloy. While the 1D quasicrystalline phases produce SAD patterns that on casual inspection appear to be identical to those expected for the decagonal phase, a careful examination shows that they are quasiperiodic along one twofold axis only. Depending on the alloy, the periodicity along the pseudo-tenfold direction is an integer multiple (1–4) of 0.4 nm, identical to the decagonal phase periodicities. The diffraction

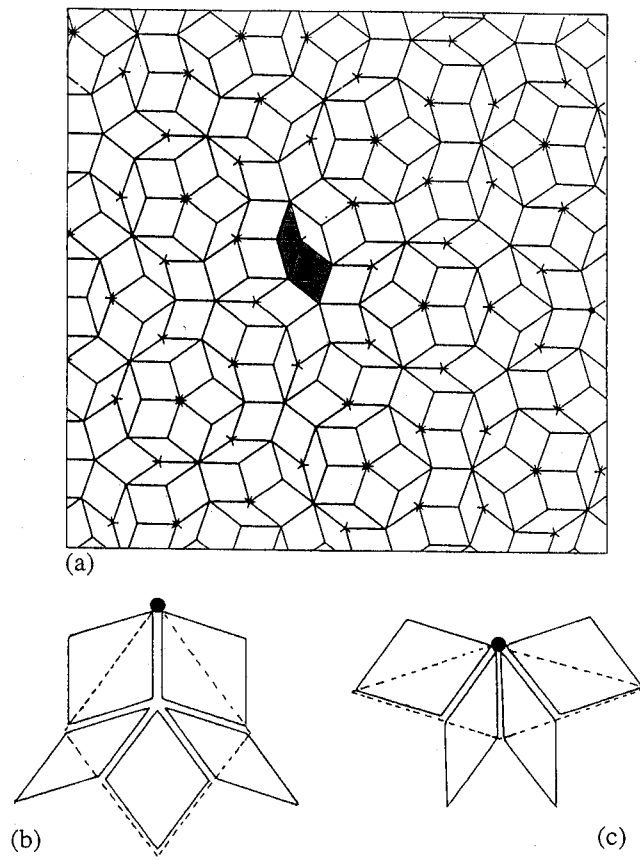
spot intensities along the new periodic direction are strongly modulated, following the Fibonacci sequence.^{274,274a,280}

Lattice models and basic quasicrystallography

Following the methods of standard crystallography, quasiperiodic crystals are often defined by first constructing a geometry, equivalent to the Bravais lattice in normal crystals, and then decorating that geometry with a basis. A crystal lattice can be decomposed into a packing of a single unit cell that preserves long range translational periodicity and a crystallographic orientational symmetry of the lattice points. In two dimensions, this can be viewed as a tiling problem; a square lattice can for example be formed by packing square tiles along their edges in a regular way. By analogy a quasilattice can be constructed, where the lattice points are arranged in patterns with a non-crystallographic orientational symmetry. In this section, different models for constructing the quasilattice are discussed. The atomic structure of quasicrystals, involving the decoration of the quasilattice, is discussed in the section 'Atomic decorations' below.

There are several ways to generate quasilattices deterministically:

1. Inflation and deflation of a small number of unit cells.
2. Tilings with matching rules.
3. Superposition of quasiperiodically spaced grids.
4. Projection from a higher dimensional space.
5. Generalised dual or multigrid methods.



12 a 2D Penrose tiling: the two fundamental shapes, acute and obtuse rhombi, are shaded; **b** and **c** prescription for deflation of tiles to construct a Penrose tiling: **b** an acute tile goes to two acute and one obtuse and **c** an obtuse tile goes to one acute and one obtuse (**b** and **c** taken from Ref. 290)

Some of these methods and non-deterministic random methods are discussed below.

Penrose tilings

The earliest theoretical insights into the structure of quasicrystals grew out of the investigation of the icosahedral bond orientational order in undercooled liquids and glasses. Nelson^{281,282} suggested that the glass transition occurred as the liquid phase approached a topologically close packed structure, such as the Frank-Kasper phase. Owing to an entanglement of defects, the liquid falls out of equilibrium, forming a glass. Levine and Steinhardt,²⁸³ argued that though quasiperiodic structures were only known as mathematical models, they might be a better template to understand the structure and dynamics of undercooled liquids and glasses. They hailed the discovery of the icosahedral phase as the first known physical example of such structures.

The Fibonacci series is the most common example of a 1D quasiperiodic structure (see the 'Introduction' above). Penrose tilings are the most common example in two dimensions.^{284,285} Although the original construction used 'kites' and 'darts', an equivalent construction, using acute and obtuse rhombi with angles of 72° and 144°, respectively, is most frequently considered. A similar pattern was produced by

Mackay using pentagons and isosceles triangles.²⁸⁶ A 2D Penrose lattice is shown in Fig. 12a; the two fundamental rhombi are shaded for identification. A large amount of local, pentagonal (or decagonal), orientational symmetry is obvious in this tiling. Further, it is self-similar under an inflation by τ .²⁸⁷⁻²⁸⁹ This pattern was first termed a quasilattice by Mackay, since the vertices of the tiles have coordinates

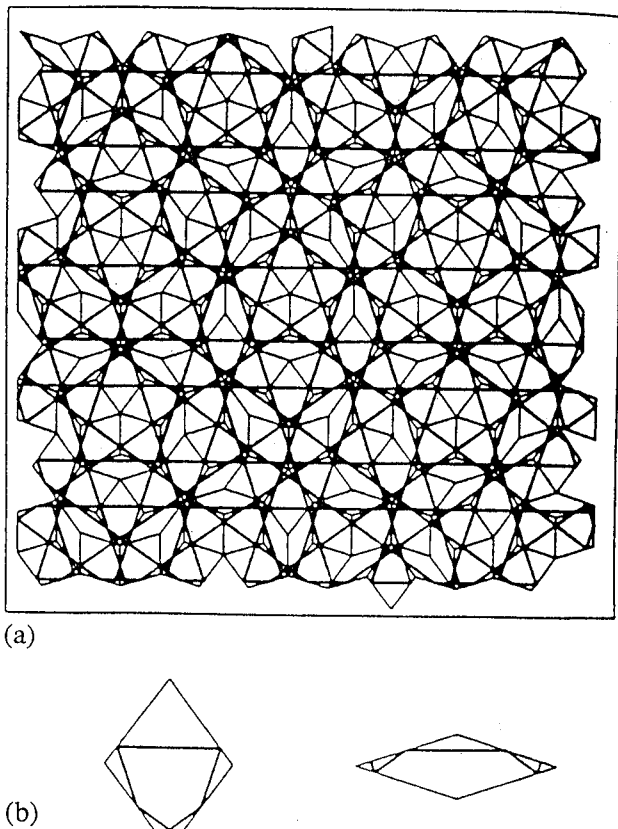
$$\vec{r} = U_1 \vec{a}_1 + U_2 \vec{a}_2 + U_3 \vec{a}_3 + U_4 \vec{a}_4 + U_5 \vec{a}_5$$

where U_i are integers with respect to the five axes (a_i) that are located in the plane and spaced 72° apart. Mackay extended the Penrose construction to 3D, using prolate and oblate rhombohedra, $\alpha = \tan^{-1} \tau = 63.43^\circ$ and its supplement, respectively.²⁹⁰

The Penrose tiling in Fig. 12a was constructed by deflation, a prescription for subdividing each unit cell into small cells of the same shape as shown in Fig. 12b. Here: (a) acute tiles go to two acute and one obtuse tile in the next generation; (b) one obtuse tile goes to one acute and one obtuse. Matching rules whereby the tiles are decorated in a particular manner to force the ways they may join can also be formulated. By changing the matching rules, these tiles can be packed into a crystalline lattice, an infinite number of quasilattices, or a random lattice. Penrose^{284,285} successfully formulated a set of matching rules for his 2D tiles. The matching rules for the 3D Penrose tiling are more complicated; two rhombohedra with the same shape have different matching and inflation rules, and the rules for a given unit cell may depend upon the local tiling configurations. Levine and Steinhardt²⁹¹ suggested an alternative construction based on four unit cells, each of which can be formed from the oblate and prolate rhombohedral bricks: (a) a rhombic triacontahedron formed from ten oblate and ten prolate bricks; (b) a rhombic icosahedron formed from five oblate and five prolate bricks; (c) a rhombic dodecahedron formed from two oblate and two prolate bricks; and (d) a prolate rhombohedron.

It is often difficult to determine the correct matching rules. Further, the local matching rules do not guarantee a perfect packing; the system appears to require a more global set. Since the rules apparently arise from short ranged, chemical interactions, this requirement for subtle interactions over large distances has led to the argument that it is extremely difficult, if not impossible, to grow a perfect quasicrystal. Elser has argued that a disordered structure might be a more realistic model, stabilised by the large entropic contribution to the free energy²⁹² (see the section 'Random tiling models' below).

Three years before the discovery of the icosahedral phase, Mackay obtained a tenfold optical diffraction pattern from a mask with holes located at the vertices of a Penrose tiling.²⁹³ Sharp diffraction spots, indicating long range translational order, were obtained with a tenfold non-crystallographic symmetry, similar to the patterns from the *i*-phase (Fig. 2) and the decagonal phase (Fig. 10, pattern *A*). Levine and Steinhardt²⁸³ computed the first diffraction patterns from a 3D Penrose tiling. Their published fivefold and threefold patterns are identical to those observed in Fig. 4; no twofold patterns were published.



13 *a* 2D Penrose tiling constructed using tiles with Ammann decoration; *b* continuous lines illustrate translational order present in quasiperiodic lattice; the lines are not periodically spaced, but follow a Fibonacci sequence (Ref. 294)

As is obvious from the sharp diffraction spots, quasiperiodicity should not be equated with disorder. The Penrose lattice is a fully ordered structure; the entropy per tile vanishes in the thermodynamic limit. The long range translational correlation is therefore perfect, though not periodic. This translational quasiperiodicity is illustrated in Fig. 13*a* where the Penrose tiles have been decorated with line segments as prescribed by Ammann (Fig. 13*b*).^{288,291,294} When laid into a Penrose tiling, these line segments join to form a grid of continuous lines that are parallel to each of the equivalent five pentagonal orientations. Along any pentagonal direction, the spacing of the grids follows a perfect Fibonacci sequence.

Projection from higher dimensional space

As first demonstrated by de Bruijn,²⁹⁵ a quasiperiodic lattice can be viewed as a projection from a higher dimensional periodic lattice on to a projected space that has an irrational orientation to the original lattice. The vertices of the Penrose tilings were obtained by projecting from a 5D lattice to a 2D subspace. Kramer and Neri²⁹⁶ later used that technique to construct the 3D Penrose lattice by projecting from a 12D space. As recognised by Elser,^{114,297} Kalugin *et al.*,²⁹⁸ and Katz and Duneau²⁹⁹ this approach provides a powerful tech-

nique for calculating Fourier transforms of quasicrystal lattices, which are directly related to the observed diffraction patterns. Their approach has been called the strip projection method. The icosahedral phase is obtained by projecting a segment of a 6D cubic lattice to a 3D space, generally called the parallel space, and denoted as x_{\parallel} . The 3D space perpendicular to the projection space is termed the perpendicular space x_{\perp} . As discussed above, corresponding parallel q_{\parallel} and perpendicular q_{\perp} reciprocal spaces also exist (see the section 'Indexing schemes' above). Since the hypercubic lattice is characterised by a single length, there should exist a corresponding quasilattice constant.¹¹⁴ Further, it becomes clear why six indices are required to index the quasicrystal diffraction patterns successfully. This technique enables the systematic introduction of disorder into the quasilattice and the construction of large unit cell crystal approximants to the quasicrystal.

Figure 14*a* illustrates the use of the strip projection technique to obtain a 1D incommensurate crystal (here the Fibonacci sequence) by projecting from a 2D square lattice \mathbf{R}^2 . The projection space, x_{\parallel} , is an axis that lies with an irrational slope to the periodic square lattice; x_{\perp} is perpendicular to x_{\parallel} . Two lines, parallel to x_{\parallel} , are constructed, (the window or strip, denoted by $\mathbf{W}(x_{\perp})$). All points of the 2D lattice that lie between these lines are projected on to x_{\parallel} . The size of the window must be chosen to match the density. If the strip is too narrow, 'holes' appear in the projected lattice; if it is too wide, too many points are obtained. It is generally chosen so that it contains exactly one unit cell of the original lattice. With this choice, there exists a unique lattice path that best approximates the incommensurate slope. The shape of the window function necessarily becomes more complicated as the dimensionality of the projection increases; for the 3D quasicrystal, it is a tri-contahedron.

The Fourier transform of the projected structure can also be obtained using the strip projection technique. Since only a subspace, \mathbf{Z}^2 , of \mathbf{R}^2 chosen, truncated by the boundaries of the window

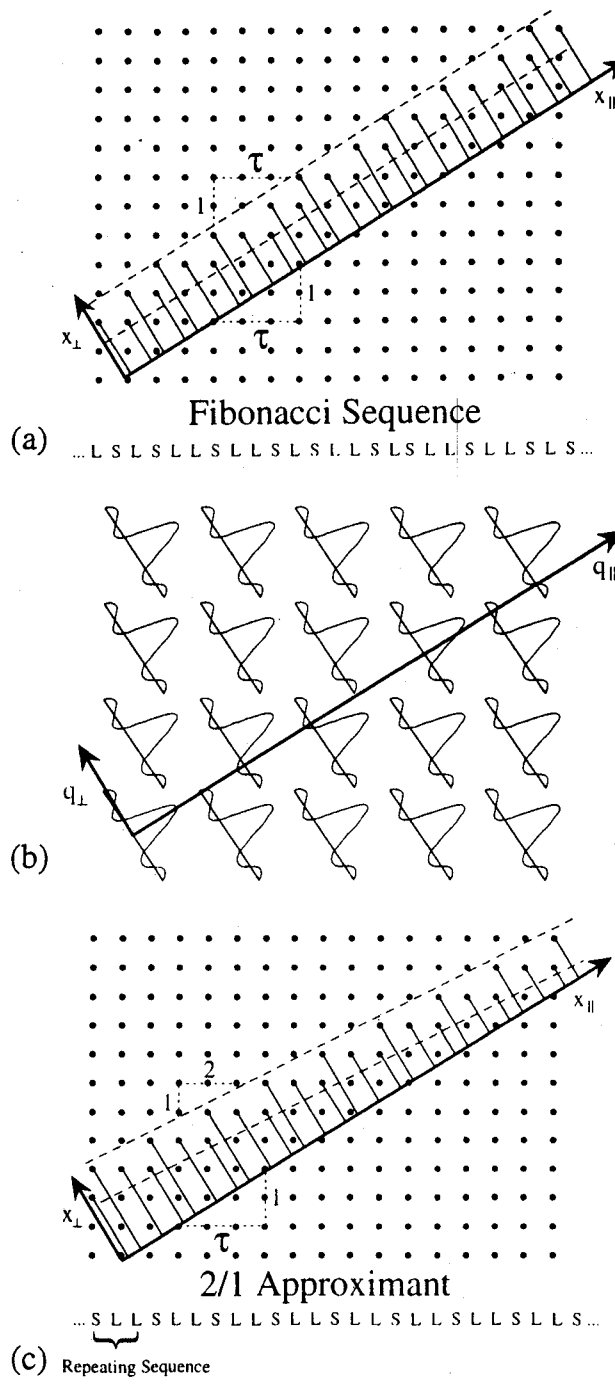
$$\mathbf{Z}^2 = \mathbf{R}^2(x, y) \times \mathbf{W}(x_{\perp})$$

the reciprocal lattice is given by

$$\mathbf{Z}'^2 = F[\mathbf{Z}^2] = F[\mathbf{R}^2(x, y)] \otimes F[\mathbf{W}(x_{\perp})]$$

This is illustrated in Fig. 14*b*. Along q_{\parallel} , the Fourier transform of each lattice point is a Dirac delta function, predicting true Bragg diffraction peaks; along q_{\perp} , it is a smooth function $f(q_{\perp}) = (\sin q_{\perp})/q_{\perp}$, within normalisations and phase factors. The Fourier transform of the projection is then given by the intersection of $f(q_{\perp})$ with q_{\parallel} . The intensity of a diffraction spot is determined by its distance from the projection space; intense spots have small values of g_{\perp} while weak spots have large values. Although the projection reciprocal space is densely filled with points, in practice spots with g_{\perp} greater than some value will not be detectable due to experimental limitations.

If the projection window and x_{\parallel} are constructed with an irrational slope to the hyperlattice, the projected sequence of points never repeats; if the slope is τ^{-1} (as in Fig. 14*a*), the Fibonacci sequence is



a projection in real space from a 2D periodic lattice of points lying within the window on to a line inclined with slope equal to τ^{-1} ; b projection in reciprocal space showing intensity distribution about each reciprocal lattice point due to Fourier transform of window function; c projection in real space when window is inclined with a slope that is a rational approximate to τ , here $3/2$; resulting 1D structure approximates a segment of a Fibonacci sequence in each repeat distance

14 Illustration of projection method from two to one dimensions

obtained. As illustrated in Fig. 14c, if the slope of the window is instead taken as a rational ratio that approximates τ^{-1} , the projected sequence of points repeats with a long period; locally, the spots follow the Fibonacci sequence. The strip projection approach then additionally provides a powerful method for generating crystal structures that have a local order identical to that in quasicrystals. Because of their method of generation, these crystals are called rational

approximants. Their diffraction patterns can be generated following the method illustrated in Fig. 14b; they will clearly resemble those obtained for the quasicrystal.

The strip projection has several limitations. It can only produce a limited subset of the possible quasilattices (see Ref. 300 for a discussion of possible quasilattices), and except for special cases, it cannot be used to find the diffraction pattern of a decorated quasilattice. A more general approach, the cut projection method, has been proposed by Bak.³⁰¹ As for a regular crystalline lattice, a basis is associated with the higher dimensional lattice. The projected density is then obtained by the intersection of the lower dimension projection space (a line, x_{\parallel} in this simple case) with the basis embedded in the higher dimensional space. Clearly, the strip projection method is a limiting case of this technique, corresponding to the basis of a line segment perpendicular to the projection space. More complicated structures are allowed within this method. For example, depending on the slope of the cut, a modulated crystal or quasicrystal can be constructed by modulating the Al and Mn hyperplane. Further, the hyperplanes are not constrained to be continuous; they might have a fractal structure for example. Possible chemical decorations are also more readily included (see the section 'Atomic decorations' below). Surprisingly, the drawbacks of this method are related to its generality; it is frequently difficult to discern whether modulated or regular quasicrystals have been constructed and to distinguish between the different local isomorphism classes generated by this method.³⁰⁰

Random tiling models

If the experimentally observed quasicrystalline phases are actually stabilised by the energetic constraints embedded in the matching rules, then the ideal quasicrystal is the ground state and exotic electronic or phonon spectra can be expected because of the dense filling of reciprocal space with Bragg peaks. With a few possible exceptions, however, no hint of such exotic properties exists. Further, since many quasicrystals are metastable, produced by cooling the liquid at rates of over 10^6 K s^{-1} , it is difficult to imagine how the many subtle matching rules required for a successful quasiperiodic tiling can be satisfied. Indeed, studies of Al–Cu–Fe, where the *i*-phase is stable at high temperatures, indicate a transition to a crystalline phase at about 670°C (see the 'Concluding remarks' below), supporting the prejudice that for sufficiently low temperatures, the ground state of any condensed system should be periodic.³⁰²

In reality, the formability of any phase, crystalline or otherwise, depends on thermodynamic stability, and on kinetic constraints of the phase nucleation and growth. If the kinetics of formation are sufficiently fast to ensure the formation of the stable phase, the balance of energy and entropy will determine true equilibrium. Elser³⁰³ first suggested that an energetically preferred, perfect Penrose tiling could become unstable at finite temperatures due to the large entropy associated with local violations of the matching rules. This condition can be formulated

equivalently in terms of a projection where the projection strip is allowed to fluctuate about an average slope. Depending on the severity of these fluctuations, if the projection window remains continuous, the projected pattern of tiles will still tessellate the space. The tiling may retain periodic or quasiperiodic long range translational order, depending on the average slope of the cut. Despite the disorder associated with the large number of tile rearrangements, transfer matrix and Monte Carlo calculations have confirmed that quasiperiodic long-range positional order remains; Bragg diffraction peaks are therefore predicted. If the projection window does not remain continuous, but develops tears, the projection will not fill space and the correlation lengths for translational order will be finite, though the orientational symmetry may be preserved. This is the case for an icosahedral glass (see the section 'Icosahedral glass' below); Bragg diffraction peaks are not predicted for that case.

Since clusters with a local icosahedral configuration appear in both crystalline and quasicrystalline phases of the same alloys, the cluster-cluster interactions are likely to be small on the scale of the energy binding the atoms within the clusters. Henley³⁰⁴ proposed that the free energy is purely entropic. Assuming that the entropy is an analytic function of the phason strain, $\mathbf{h}_i(\mathbf{r})$ (see the section 'Phason strain' below), Henley proposed a square gradient, entropic free energy F given (in the absence of dislocations) by

$$\frac{F}{k_B T} = \frac{K}{2} \int [\vec{\nabla}_i \mathbf{h}_i(\mathbf{r})]^2 d^3 r$$

where K is called the phason stiffness.

Since a non-zero average phason strain lowers the rotational symmetry and a large non-zero phason strain will lead to a crystalline approximant, with zero entropy, the entropy density has a global maximum when the average phason strain is zero.

Several Landau theories demonstrate that the proper choice of particular phenomenological parameters will stabilise quasicrystals in 2D and 3D.^{305–308} There is no known route, however, for obtaining the actual atomic arrangements and interactions from these parameters. Instead, most arguments of phase stability are based on numerical simulations of systems of particles interacting via idealised potentials. Such calculations have demonstrated the mechanical stability of the ideal Penrose tiling,^{291,309} though it has not yet proven possible to grow such tilings from a given initial particle configuration. In 2D, several authors have demonstrated that particles acting under simple Lennard-Jones interactions chosen to favour local decagonal order, form quasicrystals.^{310,311} Allowing these particles to relax under a Monte Carlo simulation led to a quasiperiodic tiling that was intermediate between the Penrose tiling and a decagonal glass. The inflation and deflation symmetries of the Penrose tiling were absent, but sharp diffraction peaks remained. At low temperatures, evidence pointed to a structural transformation to another unknown phase. Molecular dynamics³¹² and transfer matrix³¹³ calculations confirm these features.

Icosahedral glass

There is a considerable evidence for the existence of atomic clusters with an icosahedral symmetry in the i -phase. Icosahedral clusters have been postulated in undercooled liquids and glasses (see the section 'Phase formation' above) and occur in many large unit cell crystalline phases. This suggests that if an alloy melt is cooled sufficiently quickly, the icosahedral clusters might have insufficient time to pack periodically. Instead, they would pack with the correct local symmetry, but with a reduced coordination number, forming an orientationally ordered, but translationally disordered, random cluster packing often called the icosahedral glass.

To preserve a long range orientational order, the icosahedra can pack in one of three ways: (a) vertex to vertex; (b) edge to edge; and (c) face to face. Shechtman and Blech¹⁵ proposed a packing of icosahedra along edges, however this disagreed with the observed diffraction peak positions taken along the twofold zone axis of $i(\text{AlMn})$. Bancel *et al.*²⁴ first measured the diffraction peak widths in high resolution X-ray diffraction studies on samples of rapidly quenched Al–Mn. Based on those data they determined that the translational coherence was limited to ~ 0.5 nm, roughly the radius of one icosahedral cluster, though the orientational coherence extended much farther. Stephens and Goldman³¹⁴ found that a random face packing of icosahedra with the icosahedra rotated by 60° around the threefold direction gave diffraction peaks with non-zero peak widths that were in reasonable agreement with experimental measurements in $i(\text{AlMn})$.

Predictions from the simple icosahedral glass model agree only qualitatively with experimental measurements. Measured diffraction peak widths increase linearly with increasing $|\mathbf{g}_{\perp}|$,^{315,316} in disagreement with the icosahedral glass prediction¹⁸⁴ that the peak widths should scale as $|\mathbf{g}_{\perp}|^2$. The icosahedral glass is unstable to dendritic growth modes since the number of possible packing sites is greatest on the end of branches. This leads to an unacceptably low density, $\sim 60\%$ of that for a bcc packing. Finally, recent diffraction studies in $i(\text{AlCuRu})$ and $i(\text{AlCuFe})$, both reputed to be stable, report resolution limited diffraction peaks, much narrower than the icosahedral glass predictions.

Two approaches have been offered to circumvent these difficulties. Elser^{317,318} developed a dynamical growth algorithm that simulated the growth of the interface, propagating at a constant velocity. As icosahedra attached themselves to the interface, they were allowed to diffuse to maximise the number of cluster linkages. This has the advantages of invoking local growth algorithms only and following a plausible mode of phase growth. To avoid dendritic branching, Robertson and Moss^{319–321} included both local environment and non-local surface growth constraints. A packing fraction equal to $\sim 90\%$ of that for a bcc packing was obtained, similar to the result obtained by Elser and by Henley's canonical tiling method.³²²

While adjustments of the growth constraints for random cluster models will improve the agreement with experiment, all models predict non-zero peak

widths. The recent studies on well annealed samples of Al–Cu–Fe and Al–Cu–Ru, showing resolution limited peak widths, are in apparent conflict with these predictions. Since as cast samples of those alloys often have finite peak widths, Robertson and Moss offer an intriguing suggestion. The random cluster model offers a growth mode producing a non-equilibrium random tiling favouring icosahedral clusters and containing a great deal of phason strain. If the temperature is increased to the point where the diffusion kinetics are sufficiently rapid, this structure can relax via dynamical phason modes to an equilibrium random tiling model, without long wavelength phason strain, giving true Bragg peaks.

Which is the correct geometry?

More discriminating tests are required to determine unambiguously whether *i*-phase alloys are best described by the perfect quasiperiodic tiling, the random tiling, or the icosahedral glass models. Scattering experiments on *i*(AlCuFe) appear to eliminate the icosahedral glass model for those systems, though recent work by Robertson and Moss³²¹ suggests that a properly constrained random cluster packing may provide an accurate description of the diffraction data. Both the perfect quasicrystal and the random tiling models predict resolution limited Bragg diffraction peaks. Below $\sim 670^\circ\text{C}$, there is considerable evidence for a structural transformation to a crystalline phase in that system (see the section 'Stability' below). This is consistent with random tiling predictions. Since the free energy is assumed to be entirely entropic, the phason elastic constant is expected to be temperature independent. This is in contrast to the perfect quasiperiodic model where the structure is presumed favoured on energetic grounds. There the phason–phonon coupling should be strong and the elastic constant is expected to be temperature dependent. Using Monte Carlo simulation on an ensemble of particles interacting via a Lennard-Jones potential, Strandburg *et al.*³²³ found a reduced phason elastic constant as expected from a random tiling model. Experimental studies of the temperature dependence of the Debye–Waller factors and the diffuse scattering could probe the phason elastic constants.³²⁴ Such studies are clearly desired. On the basis of a random tiling mode, Hatwalne and Ramaswamy³²⁵ make predictions of other measurable physical properties: the temperature dependence and free energy of the grain boundary structure, the nature of the elastic instability, and the form of sound damping near the instability. The last prediction appears to be the most readily measurable quantity. More detailed studies of the temperature dependent scattering and of these other physical properties are essential for resolving this important question. Also, predictions based on constrained random cluster packings are essential for comparison with other model predictions.

Phason strain

The diffraction peaks from the *i*-phase are often shifted from their ideal positions. Viewing the tenfold

pattern for *i*(AlMn) shown in Fig. 2 on edge, the spots appear to 'wander' about the line drawn from the central spot. The less intense spots, corresponding to diffraction peaks with the largest values of g_\perp , deviate most from their expected positions. The diffraction peak widths also scale with $|g_\perp|$. These features can be explained by phason strain, a disorder not found in periodic crystals.

In incommensurate systems at low temperatures, six hydrodynamical modes (Goldstone modes) arise because of the broken translational symmetry (phonons), and the incommensurability (phasons). It is natural to expect similar modes in a quasicrystal. The essential features of phasons in quasicrystals can be obtained using a density functional approach based on six density waves, though more density waves are needed for a discussion of stability in terms of Landau theory. The mass density of atoms may be expressed as a Fourier series by^{326,327}

$$\rho(\mathbf{r}) = \sum_{\mathbf{q}} \rho_{\mathbf{q}} \exp(i\mathbf{q} \cdot \mathbf{r}) \\ = \sum_{\mathbf{q}} |\rho_{\mathbf{q}}| \exp(i\phi_{\mathbf{q}}) \exp(i\mathbf{q} \cdot \mathbf{r})$$

Since $\rho(\mathbf{r})$ is real, $\rho_{\mathbf{q}}^* = \rho_{-\mathbf{q}}$, and $\phi_{\mathbf{q}} = -\phi_{-\mathbf{q}}$.

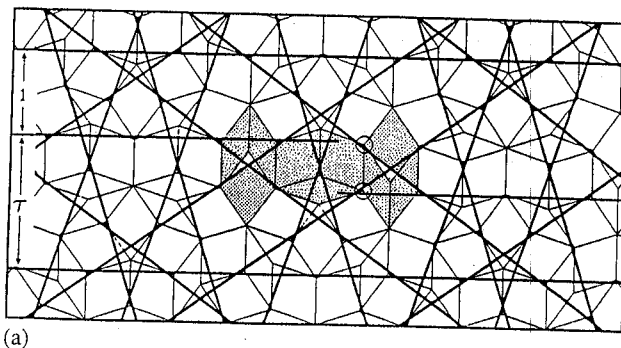
At low temperatures, the important fluctuations will be phase fluctuations of the density wave order parameters. Minimising the free energy with respect to the phases of the density waves fixes all $|\rho_{\mathbf{q}}|$ and all phases, save six. These phases are generally expressed in terms of the six possible degrees of freedom

$$\phi_{\mathbf{q}} = \sum_{i=1}^3 q_{||}^i u_i + \sum_{i=1}^3 q_\perp^i w_i$$

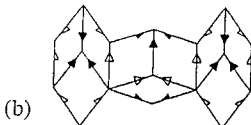
where $q_{||}^i$ are the components of the real space (parallel) reciprocal lattice vectors and q_\perp^i are the components in the perpendicular space. The u_i are displacements in the parallel space, corresponding to the normal phonon field familiar in crystals, and w_i are the displacements in the perpendicular space, corresponding to the phason field.

Spatially uniform displacements lead only to a change in the phase of the density waves and therefore do not modify the diffraction patterns. As in crystals, uniform displacements in the parallel space simply result in a lattice translation, while uniform displacements in the perpendicular space result in the formation of a locally isomeric quasicrystal. If the free energy is independent of the phase of the density waves, uniform displacements cost no energy.

In the parallel space, a non-uniform displacement produces an elastic deformation that is energetically unfavourable. Similarly, Socolar *et al.*³²⁸ have shown within the quasilattice model, that non-uniform displacements in the perpendicular space modify the local tiling arrangements. As shown in Fig. 15 a decorated tile that has been flipped, breaks the long range quasiperiodicity and carries an energy penalty. Hydrodynamic theory predicts that strain in the parallel space, will relax quickly by phonon modes, however phasons relax slowly, requiring diffusion of the atoms to correct the mismatched tiling.³²⁷ Any phason fields resulting from the sample preparation should therefore remain unchanged.



(a)



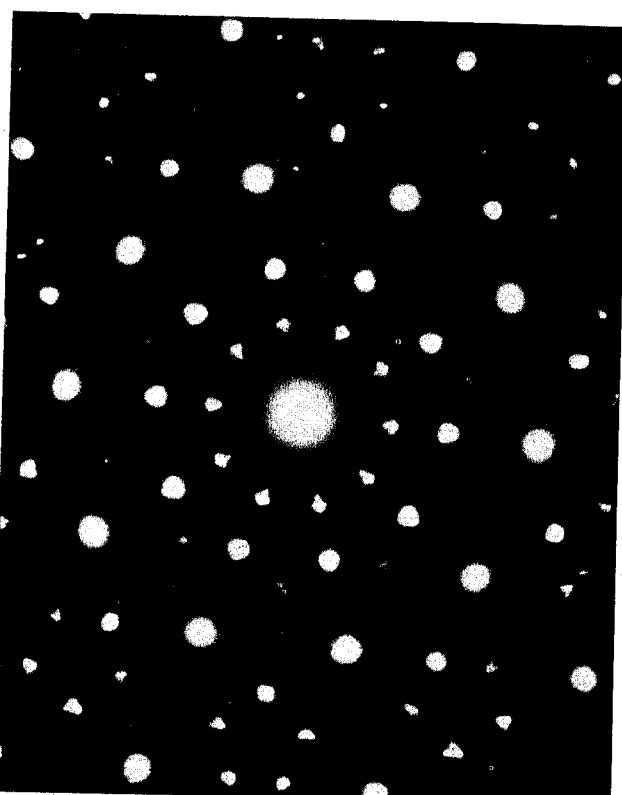
15 Illustration of disorder introduced into long range translational order of Ammann quasilattice due to a tile flipping from a phason strain (Ref. 328)

Deviations in the expected diffraction positions and the anomalously large peak widths can be explained in terms of a linear variation in the phason field, w (Ref. 329). Assuming that $w = M \cdot r$, where M is a second rank tensor, the scattered intensity is given by

$$I(\mathbf{q}) \approx \int d^3r d^3r' \langle \rho(\mathbf{r}) \rangle_w \langle \rho(\mathbf{r}') \rangle_w \exp[-i\mathbf{q} \cdot (\mathbf{r} - \mathbf{r}')] \\ = V^2 \sum_{\mathbf{q} \in L_R} |\langle \rho_{\mathbf{q}} \rangle|^2 \delta_{\mathbf{q}, \mathbf{q} + \Delta\mathbf{q}}$$

where $\Delta\mathbf{q} = \mathbf{q}_\perp \cdot \mathbf{M}$. So, a linear strain in the phason field shifts the peak in proportion to its value of \mathbf{g}_\perp in contrast to peak shifts proportional to $\mathbf{g}_{||}$, because of elastic strain arising from variations of the phonon field.³³⁰ A quadratic or higher power of the strain, in the phason field leads to an anisotropic peak broadening. Similarly, for linear phason strain the peak widths increase monotonically with $|\mathbf{g}_\perp|$. X-ray scattering measurements of peak widths in $i(\text{AlMn})$ and $i(\text{AlLiCu})$ are consistent with a linear phason strain; the $|\mathbf{g}_\perp|^2$ dependence predicted by the face packed icosahedral glass is inconsistent.³³¹ Constraints on the random packing of icosahedra, however, can produce better agreement with peak width data.³²¹

The diffraction spots from icosahedral phases frequently have an anisotropic, typically triangular (or 'T'), shape (see for example, the tenfold pattern from $i(\text{TiCrSi})$ shown in Fig. 16). While diffraction spot anisotropy seems to be most common in titanium based alloys,^{80,81,85} it has also been observed in studies of aluminium-transition metal and related alloys,^{332,333} and in $i(\text{AlLiCu})$.³¹⁶ Annealing $i(\text{AlCuFe})$ at low temperatures, causes the spots to become more anisotropic (see the section 'Reversible structural transformations' below). Within a phason strain model, these spot shapes could arise from anisotropic broadening resulting from non-linear modulation, or from a superposition of shifted peaks from different domains of the sample with different phason strain fields. The latter view is supported by diffraction experiments showing that diffraction patterns from small domains show no spot anisotropy;



16 TEM SAD pattern taken from i -phase in $\text{Ti}_{61}\text{Mn}_{37}\text{Si}_2$ showing strong anisotropy for weaker, lower q_\perp diffraction peaks

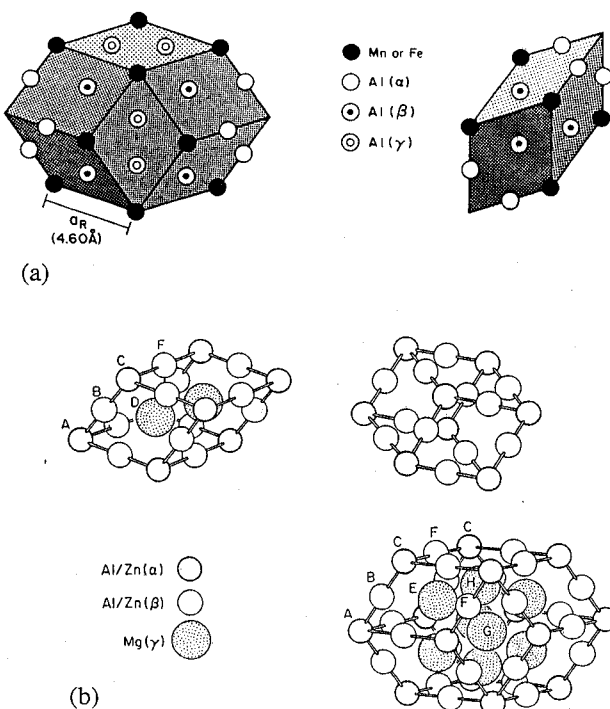
the spots are instead shifted as predicted by a linear phason strain. Diffraction patterns taken from larger regions, presumably containing several domains, show no evidence for diffraction peak shifts, but contain triangularly shaped spots.

Assuming an icosahedrally symmetric phason strain field arising from continuous linear strains, Socolar and Wright³³⁴ calculated the composite diffraction pattern produced by overlapping diffraction patterns from regions corresponding to the 20 different face vectors of an icosahedron. The observed triangular shapes at wave vectors along icosahedral edge directions are predicted, as well as a double peak observed in radial scans through peaks with vertex symmetry in samples of $i(\text{AlLiCu})$.³¹⁶

Audier and Guyot^{335,336} have argued that the spot shape anisotropy arises from an extremely fine grained multiply twinned rhombohedral structure. This is supported by recent calculations by Ishii^{337,338} of the spot shape arising from an instability of the i -phase against a rhombohedral deformation. Since phason disorder can be viewed as a continuous change in the slope of the projection from the hyperspace, these views may be equivalent for such small domain sizes.

Atomic decorations

Many crystal structures contain clusters of atoms that are tetrahedrally coordinated; in some cases, these form relatively undistorted icosahedra. Often these icosahedra are joined by other polyhedra. In the bcc crystal structure of MoAl_{12} , for example, one icosahedral cluster is centred at the origin of the cubic unit cell and is linked to the cluster at the body centre by



17 *a* decoration of rhombic dodecahedron and prolate rhombohedron by Al and Mn or Fe atoms in $\alpha(\text{AlMnSi})$ or $\alpha(\text{AlFeSi})$ structures; the $\text{Al}(\beta)$ and $\text{Al}(\delta)$ atoms are not shown (Ref. 346); *b* decorations of prolate rhombohedron, oblate rhombohedron, and rhombic dodecahedron by Al and Mg atoms in $(\text{Al}, \text{Zn})_{49} \text{Mg}_{32}$ structure (Ref. 347)

an octahedron; WAl_{12} , ReAl_{12} , TcAl_{12} , and MnAl_{12} also form with this structure.^{339,340} The tetrahedrally close packed (tcp) structures (or Frank-Kasper phases) contain only tetrahedral interstices.^{341–343}

Diffraction patterns from these crystalline phases often bear a strong resemblance to those from the *i*-phase. Their diffraction patterns contain sharp, periodically spaced, peaks reflecting the allowed crystalline symmetries, but have an intensity modulation dictated by the icosahedral clusters. These observations indicate that the local atomic configurations must be similar in the *i*-phase and these related crystal structures. Proposed atomic structures for representative icosahedral alloys, *i*(AlMnSi), *i*(AlLiCu), *i*(AlMgZn), and *i*(TiTMSi), TM = 3d transition metals, are discussed in this section. These are the best studied systems and serve to illustrate essential features of the common decoration schemes.

Quasiperiodic lattice decorations

Al–Mn–Si

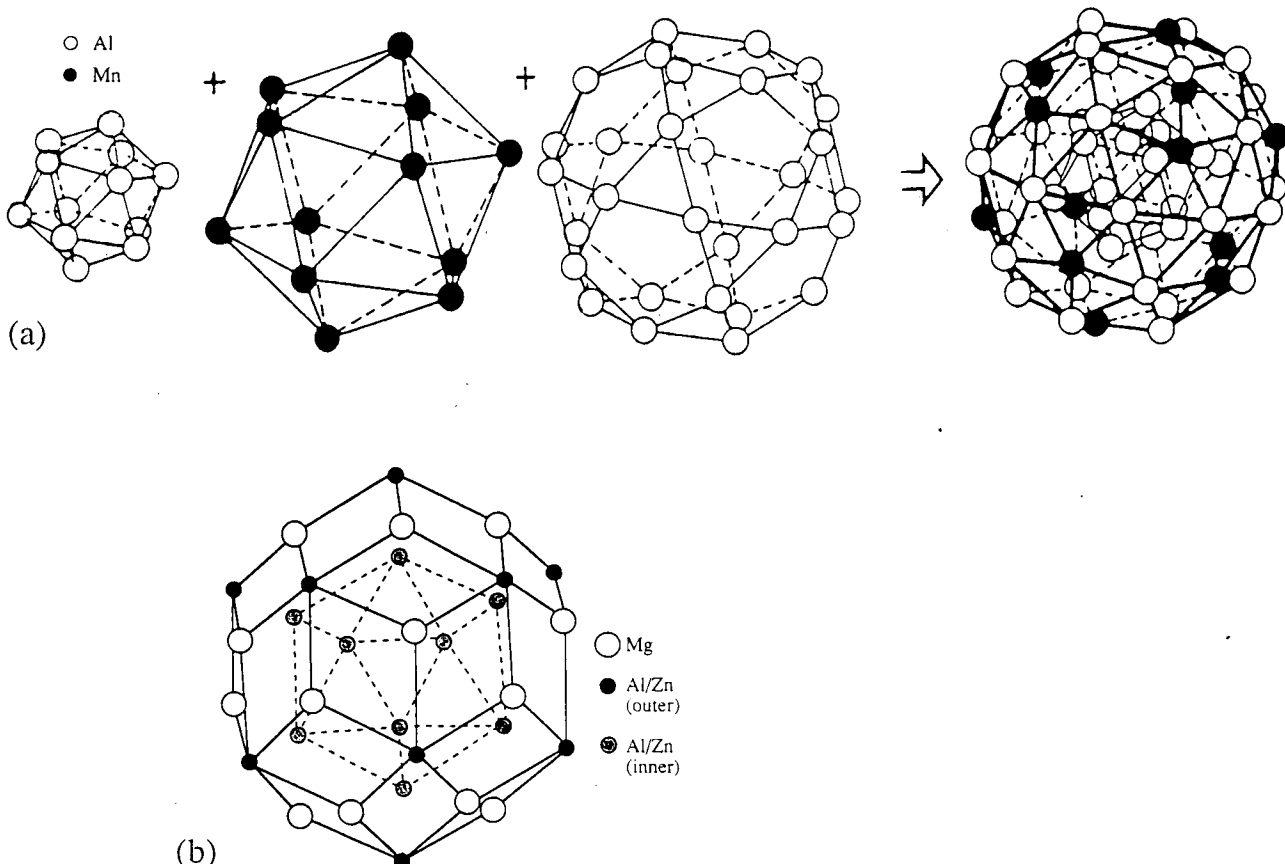
The $\alpha(\text{AlMnSi})$ structure (simple cubic, space group $\text{Pm}\bar{3}$, with $a = 1.268 \text{ nm}$, Ref. 344) is probably related to that of the AlMnSi *i*-phase. The crystalline diffraction patterns, for example, show intensity modulations that correspond to the locations of the prominent diffraction peaks for the *i*-phase. The best *i*(AlMnSi) composition is $\text{Al}_{74} \text{Mn}_{20} \text{Si}_6$,⁶⁷ giving sharp diffraction peaks, more uniform contrast in TEM images, and a crystallisation temperature almost 200 K higher than in other alloys;⁶⁷ the composition of $\alpha(\text{AlMnSi})$

is very near this value, $\text{Al}_{72.5} \text{Mn}_{17.4} \text{Si}_{10.1}$.³⁴⁴ Confirmation of the structural similarity was provided in a rapidly quenched $\text{Al}_{74.2} \text{Mn}_{20} \text{Si}_{5.8}$ ribbon, showing a crystallographic orientational relationship between the *i*-phase and the α -phase, identical to that obtained subsequently in *i*(TiVSi) (see the section 'Indexing schemes' above).^{171,345}

As first demonstrated by Elser and Henley,³⁴⁶ $\alpha(\text{AlMnSi})$ can be obtained by a 1/1 projection from the same 6D hypercubic lattice used to construct the *i*-phase. The crystalline atomic structure can also be constructed from two decorated tiles (Fig. 17a), prolate rhombohedra (PR), found in the 3D Penrose (or Ammann) tiling, and rhombic dodecahedron (RD), constructed from two prolate rhombohedra and two oblate rhombohedra (also found in the Penrose lattice).³⁴⁶ Each tile has an edge parallel to one of the centre to vertex vectors of an imaginary icosahedron. Viewing the almost bcc $\alpha(\text{AlMnSi})$ structure as two interpenetrating simple cubic lattices, each simple cubic edge is the long axis of a RD. Other symmetry axes are aligned with the other [100] directions. The space not filled by the RD is filled by the PR joining the body centres and the corner holes.

There are six classes of sites in this structure: a vacancy, a Mn site, and four Al or Si sites (Fig. 17a). The decoration of the PR is determined by that of the RD since all faces are shared with the RD. The tips of the long axis of the RD are vacant; Mn atoms sit at each of the 12 remaining vertices. The midpoints of all edges joining the vacancies to the Mn vertices are occupied by Al(α) atoms. On each of the 8 faces adjoining the vacant tip, an Al(β) atom divides the diagonal from the tip to the far Mn vertex in the ratio $\tau^{-1} : \tau^{-2}$. Two Al(β) atoms are located in the interior on the long axis, spaced at the ratio of $\tau^{-2} : \tau^{-3} : \tau^{-2}$. The remaining four faces are each decorated with two Al(γ) atoms, dividing the long face diagonal into thirds. Since there are vacant sites in the α -phase associated with the body centre, the RD on one of the simple cubic sublattices contains two additional Al(γ) atoms in the interior on the vertical symmetry axis.

Because the tiles can be packed quasiperiodically to form the 3D Penrose tiling, a chemical decoration of the tiles from the periodic packing can be used as a starting configuration for the chemical decoration in the quasicrystal. These atomic clusters, however, should not be viewed as fundamental atomic building blocks of the *i*-phase. Owing to the considerable evidence for clusters with an icosahedral symmetry, the Mackay icosahedron (MI) is a better candidate.³⁴⁶ As shown in Fig 18a, this cluster contains 54 atoms, consisting of an inner icosahedron of 12 Al atoms with a vacant centre, surrounded by a double sized icosahedron containing Mn on the vertices, capped by 30 Al atoms located slightly out of the middles of the Mn icosahedron edges forming an icosidodecahedron. While commonly called the Mackay icosahedron, this differs slightly from the original one proposed by Mackay where the 30 Al atoms were on the Mn icosahedron edges.³⁵⁰ Most of the atom sites of $\alpha(\text{AlMnSi})$ can be described by Mackay icosahedra joined face to face along the $\langle 111 \rangle$ of a cube and separated by octahedra (Fig. 19). Since these

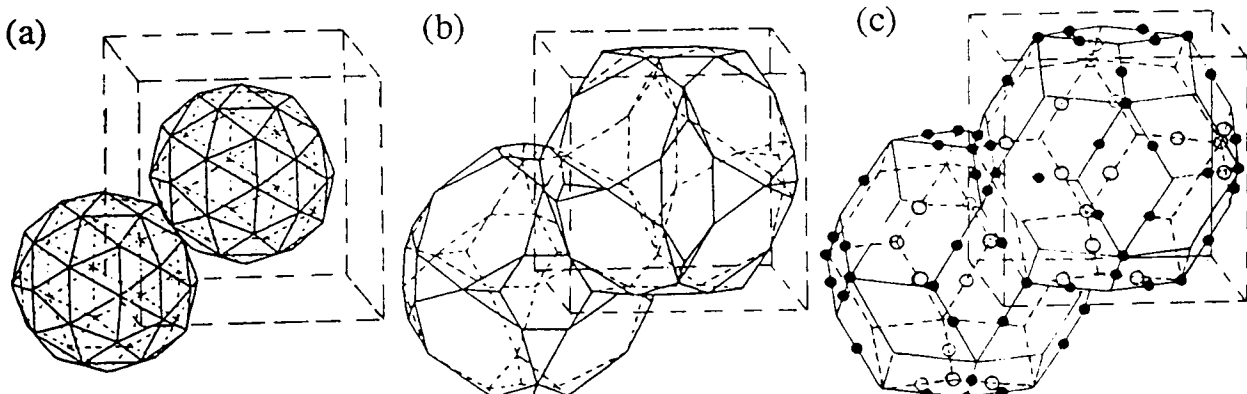


18 *a* construction of 54 atom Mackay icosahedron for *i*(AlMn), from an inner icosahedron of Al atoms plus a double sized Mn icosahedron and an Al icosidodecahedron; atom types are indicated; for this alloy, the central site is vacant (Ref. 348); *b* illustration of Pauling triacontahedron, the fundamental cluster in *i*(AlMgZn); atom types are indicated (Ref. 349)

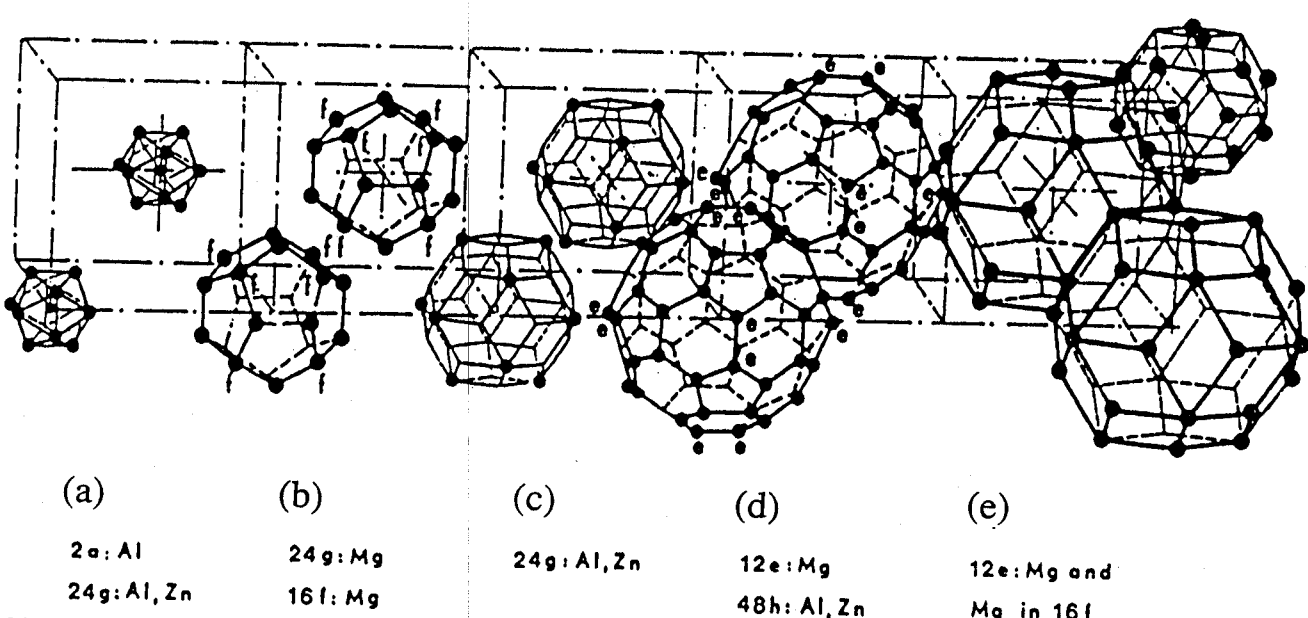
icosahedra fail to account for all atoms; an atomic layer surrounding each cluster must also be added. In simple cubic α (AlMnSi), some of the atomic sites for this layer associated with the body centred cluster are vacant; they are filled in the bcc phase, α (AlFeSi).³⁵¹

Audier and Guyot^{352,353} constructed a 3D Penrose tiling with icosahedral or triacontahedral clusters, joining the clusters along their threefold axes. Large rhombohedra are decorated by Mackay icosahedra; four of the eight vertices of both tiles are occupied. The acute rhombohedron contains one interior icosahedron, located at τ of the distance from the occupied vertex to the unoccupied one along the main body diagonal. The obtuse rhombohedron is empty. A crystalline packing is precluded since the opposite faces of the rhombohedra are inequivalent. Unfortunately, such constructions, based on a single type of cluster, packed with no overlap, result in improbably low densities and disagree with diffraction data.³⁵⁴

Even in the best packings for the *i*-phase, icosahedral clusters account for only $\sim 2/3$ of the total number of atoms. Typically the space between the



19 Atomic structure of α (AlMnSi) phase, showing *a* Mackay icosahedra joined along $\langle 111 \rangle$ cubic direction and *b* Al(Si) atomic layers surrounding Mackay icosahedra; these atomic sites can be taken to define some vertices and middle edge positions of a triacontahedron *c* (Ref. 348)



20 Illustration of $(\text{Al},\text{Zn})_{49}\text{Mg}_{32}$ bcc structure showing *a* an icosahedra centred at (000) and at $(\frac{1}{2}, \frac{1}{2}, \frac{1}{2})$; *b* dodecahedra; *c* addition of icosahedra to previous dodecahedra; *d* distorted truncated $\langle 100 \rangle$ directions or through an overlapping volume defining a small oblate rhombohedron along $\langle 111 \rangle$ direction (Ref. 348)

clusters (often called 'glue') is taken to be amorphous, contributing little to the sharp structure in the observed diffraction patterns. That the calculated diffraction patterns, while producing the correct qualitative features, disagree quantitatively with the intensity of measured X-ray and neutron scattering peaks, suggests this is fallacious. Several approaches have been proposed for systematically accounting for these additional atoms. Most suggest a construction based on two or more polyhedra that are allowed to overlap.^{348,355-357}

Al-Mg-Zn and Al-Li-Cu

The classic examples of periodically packed icosahedral clusters occur in the $(\text{Al},\text{Zn})_{49}\text{Mg}_{32}$ (Ref. 358) and the isomorphous Al_5CuLi_3 (Ref. 359) (*R*-phase) structures (bcc, space group $\text{Im}\bar{3}$). A cluster with true icosahedral symmetry, the Pauling triacontahedra (Fig. 18*b*), forms the basic building block of this structure. The construction of the bcc unit cell is illustrated in Fig. 20; only one of the constituent polyhedra, the irregular truncated icosahedron, is not a polyhedron with perfect icosahedral symmetry. Some slowly cooled samples of Al-Mg-Zn and Al-Cu-Li contain a phase mixture of the *i*-phase and this bcc phase with the same orientational relationship as between the $\alpha(\text{AlMnSi})$ *i*-phase and $\alpha(\text{AlMnSi})$.³⁶⁰

Henley³⁴⁷ showed that bcc $(\text{Al},\text{Zn})_{49}\text{Mg}_{32}$ (and the isomorphous *R*-phase) can be described by a different decoration of the same 1/1 cubic projected structure used to describe the $\alpha(\text{AlMnSi})$ (Fig. 17*b*); again different classes of Al atoms are noticed. Following their approach in $\alpha(\text{AlMnSi})$, Audier and Guyot³⁴⁸ generated and decorated a 3D Penrose lattice to construct a compact, extended aggregate. The projected density agreed qualitatively with high resolution images and diffraction patterns, but the predicted intensities differed from X-ray and neutron

measurements on Al_6CuLi_3 single quasicrystals. As for $i(\text{AlMnSi})$, better agreement was obtained by packing two different clusters, now based on the two triacontahedral subshells of the *R*-cluster, a small triacontahedron composed of an (Al,Cu) icosahedron and a Li dodecahedron and a large triacontahedron of pure Li. Katz³⁶¹ recently reported that 14 different decorations for the prolate rhombohedron and 8 different decorations for the oblate one are necessary to enforce the quasiperiodicity of their tiling. Audier and Guyot's scheme requires a unique decoration for each rhombohedron.

Ti-transition metal

The appropriate crystal approximant for the titanium based quasicrystals is less clear than in the quasicrystal systems discussed above. The Ti_2Ni structure was proposed originally as a candidate for the $i(\text{TiNi})$ and $i(\text{TiFe})$.^{82,86} This intermetallic structure forms at the apparent *i*-phase composition, it is fcc, contains 96 atoms in the unit cell and has some local icosahedral atomic configurations. Yang^{356,357} has demonstrated that the local structure in Ti_2Ni is related to the $\alpha(\text{AlMnSi})$ structure, giving a possible model for the quasicrystal structure.

The Ti_2Ni structure does not appear in the equilibrium phase diagram near the compositions of $i(\text{TiMn})$,⁸⁰ $i(\text{TiCr})$,⁸¹ or $i(\text{TiV})$.⁸⁵ Also, a closer inspection of Ti_2Ni indicates that the icosahedra in this unit cell are severely distorted, questioning its use as a good crystal approximant, even in those systems where it does occur. Recent work on titanium alloys demonstrates that silicon is required for *i*-phase formation.^{162,170} As for $i(\text{AlMn})$, then, the crystalline approximants are likely to be found in the ternary transition metal-silicon phase diagrams.

Thermal annealing of the $i(\text{TiMnSi})$ results in the formation of three complex crystalline phases. Nuclear

magnetic resonance (NMR) and TEM studies suggest that these crystals are packing variants of the same icosahedral clusters.³⁶²⁻³⁶⁴ A new bcc phase, the α -phase, with $Im\bar{3}$ and $a = 1.30$ nm, forms on annealing.^{364,365} As illustrated in Fig. 8, this bcc phase occurs with a strong crystallographic orientation relationship to $i(TiVSi)$.⁸⁵ A similar phase has also been reported in rapidly quenched samples of Ti_2Fe ;¹⁷⁵ since no local compositional data were reported, possible Si contamination is unknown. Recently the bcc phase was reported in a slowly cooled ingot of Ti–Cr–Si made at the reported composition of the i -phase.³⁶⁶ This phase is probably the true crystal approximant responsible for i -phase formation in the Ti–transition metal based quasicrystals. The determination of its atomic structure should significantly improve understanding of the formability and structure of titanium based quasicrystals.

Quasicrystal classes

Henley³⁴⁷ has argued that icosahedral alloys may be classified by the ratio of the quasilattice constant a_R , determined from the diffraction patterns, to the typical interatomic spacings \bar{d} , determined from crystalline alloys with the same composition. If $a_R/\bar{d} \approx 2.0$, the i -phase belongs to the (Al,Zn)Mg class; if $a_R/\bar{d} \approx 1.65$, it belongs to the (AlMnSi) class. By this method most quasicrystals appear to belong to the (AlMnSi) class, including $i(PdUSi)$, $i(AlCuV)$, $i(TiMnSi)$, and $i(AlCuFe)$; $i(AlLiCu)$ belongs to the (Al,Zn)Mg class. Recently Kalugin³⁶⁷ has introduced a new scheme that differs from some of the predictions made by Henley's method.

The two primary crystal approximants are constructed from different polyhedra. The Frank–Kasper phase, $(Al,Zn)_{49}Mg_{32}$, contains only tetrahedra, while $\alpha(AlMnSi)$ contains tetrahedra and octahedra. Yang,^{356,357} therefore, proposed an equivalent classification criteria: icosahedral phases of composition close to Frank–Kasper phases should belong to the (Al,Zn)Mg class, while those close in composition to crystal phases containing octahedra and tetrahedra belong to the (AlMnSi) class.

Random cluster packings

The diffraction pattern from a network of chemically decorated, randomly packed, identical, icosahedral, clusters is easily calculated; the square of the Fourier transform of the centres of all the identical clusters is simply multiplied by the square of the Fourier transform of the atom positions in the individual clusters. The cluster decorations can be determined from scattering studies of the appropriate crystalline approximants; computer simulations can produce the random packings (see the section 'Icosahedral glass' above). This approach has been followed by a number of groups, with some success.^{15,184,314,317} For those alloys where the unconstrained icosahedral glass may be appropriate, this approach works as well as others, though it appears incorrect for $i(AlCuFe)$ and $i(AlRuCu)$. Recent work by Robertson and Moss,^{319,321} however, suggests that with proper constraints, it may be applied even there.

For all cases of packed polyhedra, there are regions between the clusters that must be filled. These

intracluster regions are often assumed to be filled by 'glue' atoms arranged in an amorphous configuration that does not affect the prominent diffraction features. That these atoms remain amorphous while all other atoms are strongly coordinated, however, is unlikely, despite the good agreement recently obtained by Robertson and Moss.³²¹ The interstices developed in random packing models are varied and some are quite large. Several heuristic schemes have been followed for filling them with atoms.^{137,368} Following a method originally proposed by Bernal to classify interstices in random close packings of hard spheres, Henley³²² has recently proposed a restriction on the types of possible linkages, faces, and cells in the interstices between networked icosahedra to a canonical set. Comparisons between the predicted diffraction intensities from structures constructed following these rules and measured values are not yet available.

Projection techniques

Assuming that $\alpha(AlMnSi)$ is a 1/1 projection, Cahn *et al.*^{369,370} determined the atomic decoration of the hypercubic lattice from a Patterson map constructed from scattering studies of the α -phase. The atomic structure of $i(AlMnSi)$ was obtained directly by taking the appropriate projection from the same decorated hyperspace. For simplicity, spherical atomic surfaces were assumed. The volumes of the atomic surfaces were determined from the i -phase composition and density, incorporating these in an unambiguous way. Although reasonable agreement between the predicted and measured diffraction intensities was found, the model contains incomplete Mackay icosahedra and many unphysically short bond lengths. Several methods have been proposed to prevent the formation of the wrong bonds.³⁷¹⁻³⁷³ Most schemes, however, are *ad hoc* and lead to a density for the i -phase that is too low.

Choosing polyhedral atomic surfaces instead of the spherical surfaces assumed by Cahn *et al.*, Duneau and Oguey³⁷⁴ avoided short bond lengths without a loss in density. Further, the local atomic structure was similar to that of $\alpha(AlMnSi)$ containing a large number of Mackay icosahedra (~66.6% of the atoms reside in MI compared with 78.3% in the α -phase). The agreement with measured diffraction intensities is very good. Unlike α , the proposed i -phase structure contains some Mn–Mn nearest neighbours. This could account for the magnetic differences between the two phases.^{375,376} This structure is probably the best description for $i(AlMnSi)$ presently available.

One severe criticism of the projection technique is that no account of the diffuse scattering present in the diffraction patterns is taken in the construction of the Patterson map used to determine the atomic decoration in the hypercubic lattice. The resulting unphysical local atomic configurations would be a natural result if the structure were not a strict Penrose tiling, but a random packing.³⁷⁷ Since there is growing evidence that the geometry of many quasiperiodic structures is stabilised entropically, suggesting a random tiling or randomly packed clusters, care must be taken when interpreting predictions from projection methods.

Stability

As discussed above, most quasicrystals are metastable, produced by non-equilibrium processes such as rapid quenching. On thermal annealing at sufficiently elevated temperatures, these will transform to conventional crystals by a first order phase transition, often passing through a series of metastable phases. Recently, quasicrystals that are stable at high temperatures have been observed to undergo reversible structural phase transformations at lower temperatures. These transitions may be driven by a phason softening mechanism similar to the familiar phonon softening in some conventional crystalline transformations. The order of this transformation is unknown; theoretical models predict both first and second order transitions. A transition of higher order is supported by many experiments, some suggesting a continuous transformation between the quasicrystal and various crystalline approximant phases.

A knowledge of the degree of *i*-phase metastability or stability, and the kinetics and morphology of the crystallisation is useful for understanding the formation and structure of quasicrystals. The study of these phase transformations is an increasingly dynamic field with several new papers appearing each month. In this section, an attempt is made to provide an outline of these investigations. Both reversible and irreversible transformations are discussed.

Irreversible structural transformations in metastable quasicrystals

Detailed crystallisation studies have been made only in a few systems, generally concentrating on the *i*-phase. The discussion presented here is brief and limited to the metastable *i*-phase in Al-TM and Ti-TM alloys. A more complete discussion is presented elsewhere.³⁷⁸

Al-transition metal alloys

The Al-transition metal alloys are the best studied. Transmission electron microscopy and X-ray diffraction studies on Al-Mn alloys show that the products of crystallisation depend strongly on the alloy concentration.³⁷⁹⁻³⁸² In Al₈₆Mn₁₄, the *i*-phase transforms directly to Al₆Mn; in Al₈₀Mn₂₀, it transforms first to the decagonal phase, which then transforms to hexagonal Al₄Mn at higher temperatures. Transmission electron microscopy investigations of partially crystallised Al₈₆Mn₁₄ (Refs. 383-385) demonstrate that crystalline Al₆Mn nucleates at the phase boundary between the *i*-phase and α -Al (see the section 'Indexing schemes' above for a discussion of the as quenched sample morphology). Transmission electron microscopy studies also show a different number of nuclei associated with different *i*-phase grains.^{381,382} McAlister *et al.*³⁸¹ asserted that this was evidence for two types of nucleation sites; it is probably, however, a probability effect arising from a low nucleation frequency.^{384,385} The mode of reaction is also strongly composition dependent. Koster and Schuhmacher³⁸⁶ demonstrated that in Al₈₉Mn₁₁, Al₆Mn forms a shell around the periphery of the *i*-phase nodule and grows by a peritectoid reaction into the *i*-phase. That mor-

phology has not been reported in alloys of different composition.

Chen *et al.*³⁸⁷ first determined the kinetics of crystallisation of the *i*-phase in Al₈₆Mn₁₄ by measuring the heat evolved in DSC. They concluded that the transformation was diffusion controlled with a constant nucleation rate. Similar results were obtained by others.^{381,384,385} Fitting isothermal and non-isothermal DSC data and changes in the electrical resistivity, and using the results from TEM studies of the evolving microstructure, Kelton and Holzer^{384,385} made the first estimate of the nucleation rate and growth velocity for the transformation $i\text{-phase} + \alpha\text{-Al} \rightarrow \text{Al}_6\text{Mn}$ in that alloy. As expected, the grain boundary nucleation rate, B_{I_v} , is low; the maximum rate at 700 ± 10 K is $B_{I_v} \approx 10^{22 \pm 1} \text{ m}^{-3} \text{ s}^{-1}$. For a 0.1 μm diameter grain, this corresponds to 0.5-50 nucleation events per second per grain. The peak transformation temperature is 750 ± 10 K. Based on these data, they placed a lower bound for the interfacial energy between the *i*-phase and Al₆Mn at 0.03 J m⁻². This is similar to the interfacial energies of Al and its melt (0.09 J m⁻²) and Mn and its melt (0.21 J m⁻²)^{388,389} and smaller than a typically orientationally averaged interfacial boundary energy between unlike crystalline phases,³⁹⁰ suggesting a similar atomic structure in the liquid and *i*-phase. As discussed in the section 'Phase formation' above, recent measurements of the interfacial energy between the *i*-phase and the glass in Al-Cu-V alloys have confirmed this.²⁰⁹

The stability of the *i*-phase also depends strongly on the composition. Schaefer *et al.*¹⁵⁷ and Chen and Chen⁶⁷ demonstrated that the addition of small amounts of Si stabilised the *i*-phase in Al-transition metal alloys. Similarly, Dunlap and Dini^{29,30} found that the onset temperature for crystallisation in Al₈₆TM₁₄ (TM = Cr, Mn, Fe) alloys decreased (indicating a decreased stability) with increasing 3d electron count. This behaviour could arise from the size of the 3d transition metal or from electronic *d*-band effects.

Transformation studies are valuable for establishing relations between the *i*-phase and crystalline phases. As discussed above, Elser and Henley³⁴⁶ and Guyot and Audier³⁵² first pointed out the close correspondence between the [230] and [100] diffraction patterns in the cubic $\alpha(\text{AlMnSi})$ phase and the fivefold and twofold patterns of the *i*-phase, and suggested a relation between the two structures. Another relation between the *i*-phase and $\alpha(\text{AlMnSi})$ was found in TEM *in situ* heating studies of (Al₆Mn)_{1-x}Si_x ($x = 0.02$ and 0.04).³⁹¹

Ti-transition metal alloys

A differential thermal analysis (DTA) of Ti₆₁Mn₃₇Si₂ shows an endothermic peak at ~1230 K; ΔH_f is 23 ± 5 kcal (g atom)⁻¹, (Ref. 365). The enthalpy values vary significantly for samples obtained from different quenches, suggesting a strong quench rate and compositional dependence. Transmission electron microscopy and X-ray powder diffraction confirm that the endotherm is due to a transformation of the *i*-phase. This suggests that the *i*-phase could be stable in some temperature regime, though attempts to obtain it by slow cooling have been unsuccessful.

Annealing $Ti_{61}Mn_{37}Si_2$ at 973 K for 1 week completely transformed the sample, producing a phase mixture of the μ -phase, a hexagonal (hP) phase of composition $Ti_{67}Mn_{30}Si_3$ with $a = 0.8$ nm and $c = 1.57$ nm, and the λ -phase, an A-face centred orthorhombic (oA) of composition $Ti_{58}Mn_{40}Si_2$ with $a = 3.21$ nm, $b = 2.62$ nm, and $c = 1.01$ nm,^{363,364} and a bcc phase of composition $Ti_{68}Mn_{29}Si_3$ with an edge length of 1.34 nm (the α -phase). A detailed analysis of the intensity modulations in the diffraction spots shows that these phases are constructed from different packings of the fundamental atomic clusters found in the i -phase. Taking the clusters to be icosahedra, their vertices pack along the b -direction of the λ -phase, they pack along edges in the plane and along faces in the c -direction in the μ -phase, and with faces along the $\langle 111 \rangle$ of the α -phase. That the clusters survive the transformation suggests a tendency for stable local icosahedral coordinations, in agreement with recent NMR studies.³⁶²

Reversible structural transformations

X-ray and TEM investigations of the i -phase in Al–Cu–Fe indicate the onset of a structural transformation to a lower symmetry phase at $\sim 670^\circ\text{C}$.^{392–394} The X-ray scattering intensity of the large \mathbf{g}_\perp peaks decreases dramatically with annealing at this temperature, suggesting a phason softening mechanism,³⁹² analogous to the more familiar phonon softening leading to phase transitions in crystals. Transmission electron microscopy diffraction studies of the transformation product show i -phase type diffraction patterns with an extreme spot anisotropy. This could indicate a dramatic increase in phason strain or the transformation of the quasicrystal to an extremely fine grained (~ 10 nm) rhombohedral phase.

As discussed above, non-uniform phason fluctuations in quasicrystals will modify the local atomic configuration. The magnitude of these long wavelength phason fluctuations can be locked to special values to produce periodic approximants to the quasicrystal. Ishii recently enumerated all possible phason induced structural modifications expected for the icosahedral phase.^{337,395} The instability caused by locking into configurations given $I_h \rightarrow D_{3d}$, (icosahedral to rhombohedral point group symmetry) could be responsible for the structural transformations between the icosahedral and rhombohedral phases in Al–Cu–Fe alloys.³³⁸ The ‘T shaped’ peaks observed in $i(\text{AlMn})$, $i(\text{AlLiCu})$, and $i(\text{Ti–transition metal})$ are predicted, suggesting that an instability against the rhombohedral deformation is responsible there also.

The order of this structural transformation is not known, though no evidence for nucleation, signalling the most common first order transformation, has been found. Further, no evidence for a spinodal transformation has been reported. Ishii³³⁸ argues that the transition should be first order since third order terms are present in an expansion of the elastic free energy in the phonon and phason strain fields. Previous discussions of the transformation of $i(\text{AlLiCu})$ to the R-phase (see the section ‘Atomic decorations’ above)

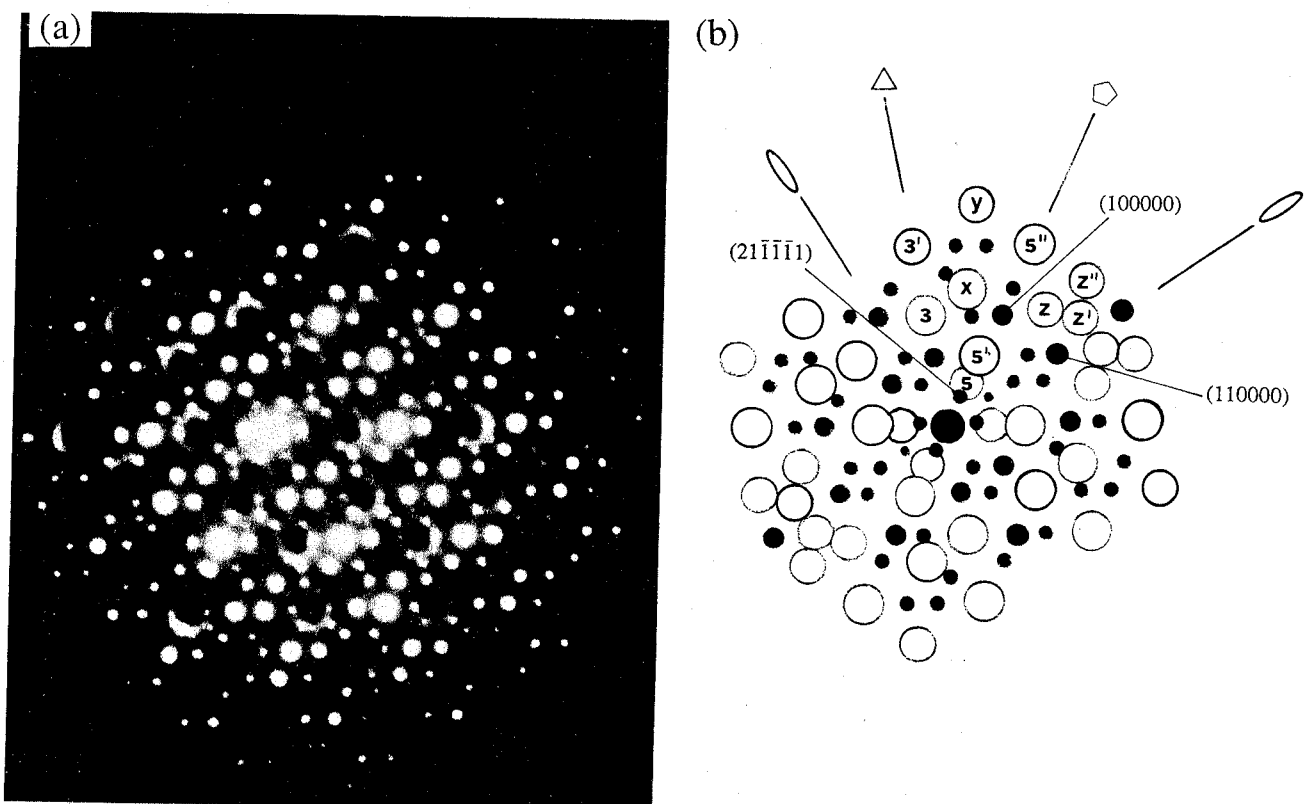
in terms of a continuous variation of the phason strains would imply a second order transition.³⁹⁶ Since the symmetry of the rhombohedral phase is a subgroup of the icosahedral point group this is possible.³⁹⁷

Additional evidence suggesting continuous, phason-based transformations (reversible and irreversible) to periodic approximant structures exists for icosahedral and decagonal phases.^{398–400} The alloy composition and thermal history are important for obtaining the 1D quasicrystal or the decagonal phase.^{274,401} Annealing studies in rapidly quenched Al–Co–Cu suggest a continuous shift in the diffraction spot positions from their quasiperiodic values in the decagonal phase, to a periodic spacing along one direction. This can be modelled in terms of a linear phason strain with increasing amplitude.⁴⁰¹ In support of this model, no evidence currently exists for a phase mixture of 1D and 2D quasicrystals. Pentagonal shaped diffraction spots in the tenfold diffraction pattern of $i(\text{AlNiSi})$ were explained as a superposition of microdomains with the diffraction spots shifted by phason strain.

Localised diffuse scattering

Weak localised diffuse scattering in an icosahedral phase was first observed in Al–Mn, following low temperature aging.¹²⁰ Diffuse scattering has been observed subsequently in TEM studies of a variety of systems including $i(\text{AlCr})$,⁴⁰² $i(\text{AlMnZn})$,¹²¹ $i(\text{TiMnSi})$,^{80,403} $i(\text{AlCuV})$,⁴⁰⁴ $i(\text{TiCrSi})$,⁸¹ and $i(\text{TiVSi})$.⁸⁵ Rings of diffuse scattering were also reported from monochromatic Laue and precession X-ray diffraction studies of $i(\text{AlCuLi})$.^{405,406} The origin of this diffuse scattering is of considerable interest since it may signal a developing instability in the i -phase, leading to atomic ordering or disordering, or to a structural transformation. It could also yield new information about atom locations.

The arcs are most intense in the titanium based icosahedral phases. Gibbons *et al.*⁴⁰⁷ made a detailed study of the arc shapes, locations, and intensity distributions in $i(\text{TiMnSi})$ by taking diffraction patterns at closely spaced points on great circles between the twofold, threefold, and fivefold orientations. Many of the observations made on samples with less intense arcs were confirmed. While not present in the fivefold or threefold orientations, significant diffuse scattering with an approximately circular intensity distribution (arcs) appears in the twofold orientations (Fig. 21). These arcs are centred on the odd-parity spots normally missing in the simple cubic icosahedral reciprocal lattices (see the section ‘Icosahedral phase – a three dimensional quasicrystal’ above). Rotation studies confirm that they are formed by intersections of the Ewald sphere with approximately spherical surfaces of diffuse scattering intensity in reciprocal space, that are invariant under the rotational symmetry of the icosahedral point group. The intensity distribution on the shells, however, is very complicated and bears no simple relation to the symmetry of the quasilattice. On prolonged annealing, superlattice like spots develop on the ring of intensity; the centre remains free of intensity.^{120,403,408}



21 a TEM SAD pattern from $i(\text{TiMnSi})$ $\sim 1^\circ$ from twofold zone axis towards nearby threefold axis; b schematic diagram of diffraction pattern showing prominent spots and major locations of localised diffuse scattering by letters and numbers in first quadrant; the intense peaks are labelled using indexing scheme of Bancel *et al.*:²⁴ symmetry axes in plane of figure are indicated by approximate symbols (Ref. 407)

Chattopadhyay and Mukhopadhyay⁴⁰⁹ suggested that the arcs might be due to an ordering in the 'glue' atoms between the Mackay icosahedra presumably contained within the quasicrystal structure. Henley argued that this is equivalent to ordering in the 6D hypercubic lattice.⁴¹⁰ Supporting this view, Mukhopadhyay *et al.*⁴⁰⁸ recently reported that the arcs were replaced by weak intensity spots after annealing. Taken with the original diffraction spots, a τ scaling was observed, corresponding to an ordered *i*-phase such as *i*(AlCuFe) or *i*(AlCuRu).^{411,412} Initial studies of annealing in *i*(TiMnSi) suggested a change in the arc intensity with annealing at 300°C.⁴⁰³ Recent work by Kelton *et al.*,^{413,414} however, shows no change in arc intensity with annealing. Further, no appearance of the forbidden spots was noted.

Extending the transition state theory developed to explain arcs in crystals,^{415,416} Steinhardt⁴¹⁷ proposed a sum rule for cluster occupation

$$\sum_{k=1}^{S_0} \bar{\sigma}_{j+k} \omega_k W(r_j^j + r_k^k) = \varepsilon_j$$

where $\bar{\sigma}_{j+k}$ are 6D Flinn occupation parameters, W is the window function, ω_k are Fourier coefficients of a series fitting the geometric locus of the diffuse scattering, and ε_j is a residue taking into account that, because of topological constraints, all clusters cannot be chemically ordered. Following Steinhardt, Gibbons *et al.*⁴⁰⁷ assumed an icosahedral cluster defined by the 6D lattice vectors that form a centred icosahedron when projected into $x_{||}:e_k = (000000)$,

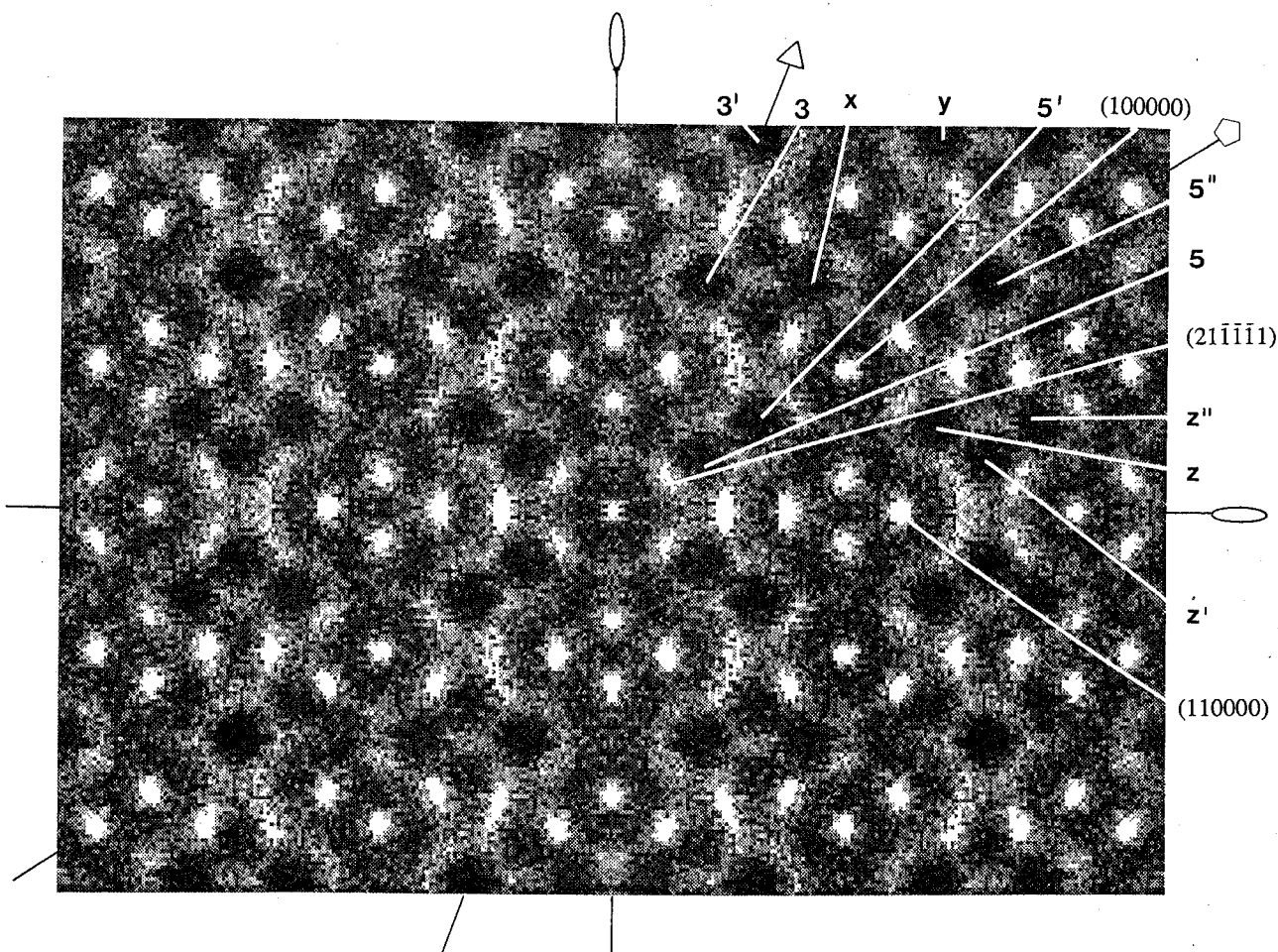
$(100000), (\bar{1}00000), (010000), \dots, (00000\bar{1})$. This gave a specific form for the geometrical locus of diffuse scattering

$$f(\mathbf{q}) = \omega_0 + \sum_{k=1}^{12} \exp(-i\mathbf{q} \cdot \mathbf{e}_{||}^k r_0)$$

where r_0 is the centre to vertex distance in the icosahedral cluster. In agreement with the data, no arcs are predicted in the fivefold or threefold diffraction patterns. Although arcs are predicted in patterns where they exist in the data, quantitative agreement is poor. The arcs in the twofold orientation along the fivefold direction, for example, are not centred around the odd parity spots.

If the diffuse scattering arises from chemical ordering, the nearly identical atomic form factors for titanium and manganese suggest that the arcs should be less intense in those alloys than in Al-Mn. That the opposite is always observed indicates that chemical ordering models are suspect. This argument is supported by recent studies showing no effect of alloying on arc location or intensity in titanium based alloys.⁴¹⁴

Levitov⁴¹⁸ proposed a model where the diffuse scattering originates from a displacement disorder arising from distortions of the triacontahedron strip used to project a quasiperiodic structure from a 6D simple cubic lattice. Jarić and Nelson⁴¹⁹ also suggested a phason origin arguing that the diffuse scattering is closely related to the diffuse scattering around reciprocal lattice points. Neither of these models has



22 Diffraction pattern along twofold axis computed from an icosahedral glass, averaged over six model glasses containing 900 icosahedra each; the intense peaks and localised diffuse scattering are labelled in same manner as for Fig. 21: symmetry axes in plane of pattern are indicated (Ref. 407)

been developed in sufficient detail to test experimentally. Initial calculations based on the qualitative model proposed by Levitov, however, do not agree with the shapes and locations of the arcs observed in *i*(TiMnSi).⁴²⁰

Goldman *et al.*⁴⁰⁶ proposed that the localised diffuse scattering arises naturally from the topological disorder inherent in the icosahedral glass model, for a quasicrystal, relying primarily on nearest neighbour cluster correlations. A comparison of the predictions from a face packed icosahedral glass, assuming one scatterer in the centre of each icosahedron (Fig. 22), with the data from *i*(TiMnSi) (Fig. 21) shows good agreement, suggesting that for some systems, the icosahedral glass may be a reasonable model.

Most proposed models for the diffuse scattering are unique to the icosahedral phase. Diffuse scattering, however, is also common in crystalline phases. Intense arcs of diffuse scattering and additional spots are frequently observed in Ti-, Zr-, and Hf-based solid solutions, for example.⁴²¹ They arise from the ω -phase, a product of a displacement transformation from the solid solutions. Kelton *et al.*⁴¹³ reported the ω -phase in the Ti-Mn solid solution forming with the *i*-phase. Arcs that are located at the same positions relative to the pseudo-icosahedral diffraction spots were also reported in one of the crystalline approxim-

ant phases that form by crystallisation of the icosahedral phase in that system.⁴¹³ The arcs may, therefore, arise from disorder accompanying a structural transformation, possibly resulting from a soft-phason mechanism similar to that proposed for *i*(AlCuFe) or from distortions of a fundamental icosahedral cluster common to the crystalline and quasicrystalline phases. It should be possible to treat the latter possibility within the transition state model.

Concluding remarks

In summary, quasicrystals constitute a new class of condensed matter that challenges many long standing prejudices in crystallography and condensed matter physics. Their diffraction patterns contain sharp spots, indicating extended order, that display a rotational symmetry that is inconsistent with the translational periodicity of ordinary crystals. As for crystals phases, TEM and X-ray studies reveal chemical and topological disorder, but also a new hydrodynamic mode not found in crystals, i.e. phason strain. Like crystals, quasicrystals form from the liquid by a first order phase transition; the barrier to nucleation of the icosahedral phase is very small, demonstrating a similar local atomic structure to that of the undercooled liquid. In some cases there is strong

evidence that the quasicrystal is more stable than competing crystalline phases. The non-periodic structures appears to be stabilised by an increased entropy over competing periodic phases.

As should be clear, many questions remain unanswered. There are at present no definitive tests to choose unambiguously among the possible structural models: the quasicrystal, the random tiling, or the icosahedral glass. There appear to exist fundamental building blocks, fragments, or possibly complete, icosahedral clusters that are common to the undercooled liquid, the icosahedral phase, and the closely related complex crystalline phases. The reasons for a strong tendency toward clustering in some systems are unknown. Such observations also hint of the possibility that the mechanism of crystal growth might be different from the models of single atom incorporation that are normally assumed. Little is known of the mechanism for complex crystal growth, much less for quasicrystal growth.

The future should witness an increased activity in the measurement of physical properties of quasicrystals. There is dearth of data on the electrical, electronic, and mechanical properties of these materials. This may result partially from the intense activity centred around structural models. It is more likely a result, of the lack of good samples. As discussed in this article, most samples are multiphase ribbons formed by rapid solidification. Recently, large, single crystals of a limited number of quasicrystals have become available. Preliminary measurements of the electronic density of states and electron transport show some anomalies.

An assessment of practical applications of quasicrystals must await more extensive measurements of their physical properties. Mechanically, they appear to be hard and brittle, limiting their usefulness as structural materials, though they might prove valuable for dispersion hardening of structural alloys. An exploitation of their high nucleation rate from the liquid to produce an extremely fine grained material potentially make them useful for nanophase materials. Their hardness might be useful for coatings, currently a use of metallic glasses. Quasicrystals frequently occur as precipitates in structural alloys such as Al-Li-Cu and stainless steel, often degrading their performance. One potential application of quasicrystal research might therefore be to learn how to avoid their formation.

Linus Pauling, still sceptical of the existence of quasicrystals, once remarked that the misguided flurry of activity in quasicrystal research has led to a much better understanding of the formation and structure of complicated intermetallic phases. Less direct results of quasicrystal research, include an improved understanding of phase formation, crystallography, and metastable and equilibrium phase diagrams.

Improved sample quality and the application of more powerful probes to the study of quasicrystals places us at the edge of a new frontier, poised for a rapid development in understanding of this novel phase. Whether for practical or basic reasons, the field of quasicrystal research promises a richness for a long time. The discovery of quasicrystals and their study have broken the confines of materials based

only on translationally periodic structures. An endless diversity of ordered structures is now possible.

Note added in proof

Since this review article was completed, there have been many interesting developments in the understanding of quasicrystals and related crystalline phases. Quasicrystals that are even more ordered than the i (AlCuFe) alloys discussed here have been discovered. Measurements of the physical properties of quasicrystals are now beginning to appear, presenting some surprises.⁴²² Finally, studies of crystaline approximants that are closely related to quasicrystals are becoming more numerous, partially owing to the discovery of extremely high order approximants, including 2/1, 3/2, and 5/3 cubic rational approximants, in several alloys.⁴²³ Many of the recent developments were discussed at the 4th International Conference on Quasicrystals, held in St. Louis, MO, during June 1992; the proceedings are published in Ref. 424.

Acknowledgements

I am grateful to P. Gibbons and to my graduate students for their invaluable contributions to the investigations of the stability and formability of the icosahedral phase, particularly in titanium based alloys. I thank A. Carlsson, T. Daulton, and P. Gibbons for useful discussions and a critical reading of this manuscript in various stages of its production. I also thank P. Suntharothok-Priesmeyer for her excellent job of preparing the manuscript and the figures. This work was partially supported by the National Science Foundation under Grant No. DMR 89-03081.

References

- PLATO: 'Timaeus', in 'The collected dialogues of Plato', (trans. B. Jowett; ed. E. Hamilton and H. Cairns), 54c, 1180ff; 1973, Princeton, NJ, Princeton University Press.
- I. THOMPSON: 'The Audubon Society field guide to North American fossils'; 1982, New York, Alfred Knopf.
- C. KITTEL: 'Introduction to solid state physics', 5 edn, Chap. 1; 1976, New York, Wiley.
- B. K. VAINSHTEIN: 'Modern crystallography I', Chap. 2; 1981, Berlin, Springer-Verlag.
- D. SHECHTMAN, I. BLECH, D. GRATIAS, and J. W. CAHN: *Phys. Rev. Lett.*, 1984, **53**, 1951-1953.
- L. PAULING: *Nature*, 1985, **317**, 512-514.
- L. PAULING: *Phys. Rev. Lett.*, 1987, **58**, 365-368.
- L. PAULING: *Proc. Natl Acad. Sci.*, 1988, **85**, 8376-8380.
- M. J. CARR: *J. Appl. Phys.*, 1986, **59**, 1063-1067.
- T. R. ANANTHARAMAN: *Current Sci.*, 1988, **57**, 578.
- T. R. ANANTHARAMAN: in 'Quasicrystals and incommensurate structures in condensed matter', (ed. M. J. Yacaman *et al.*), 199-211; 1989, Singapore, World Scientific.
- R. D. FIELD and H. L. FRASER: *Mater. Sci. Eng.*, 1985, **68**, L17-L21.
- K. S. VECCHIO and D. B. WILLIAMS: *Metall. Trans.*, 1988, **19A**, 2875-2884.
- T. L. DAULTON, K. F. KELTON, and P. C. GIBBONS: *Philos. Mag. B*, 1991, **63**, 687-714.
- D. SHECHTMAN and I. BLECH: *Metall. Trans.*, 1985, **16A**, 1005-1012.
- D. SHECHTMAN, D. GRATIAS, and J. W. CAHN: *CR Acad. Sci. II*, 1985, **300**, 909.
- K. HIRAGA, M. HIRABAYASHI, A. INOUE, and T. MASUMOTO: *Sci. Rep. Res. Inst., Tôhoku Univ. A*, 1985, **32**, 309-314.
- L. BURSILL and J. LIN: *Nature*, 1985, **316**, 50-51.

19. R. PORTIER, D. SHECHTMAN, D. GRATIAS, and J. W. CAHN: *J. Microsc. Spectrosc. Electron (France)*, 1985, **10**, 107.
20. K. M. KNOWLES, A. L. GREER, W. O. SAXTON, and W. M. STOBBS: *Philos. Mag.*, 1985, **B52**, L31–L38.
21. R. GRONSKY, K. M. KRISHNAN, and L. TANNER: *Proc. Electron. Microsc. Soc. Am.*, 1985, **43**, 34.
22. K. F. KELTON and T. W. WU: *Appl. Phys. Lett.*, 1985, **46**, 1059–1060.
23. L. BENDERSKY: *Phys. Rev. Lett.*, 1985, **55**, 1461–1463.
24. P. A. BANCEL, P. A. HEINEY, P. W. STEPHENS, A. I. GOLDMAN, and P. M. HORN: *Phys. Rev. Lett.*, 1985, **54**, 2422–2425.
25. A. J. MELMED and R. KLEIN: *Phys. Rev. Lett.*, 1986, **56**, 1478–1481.
26. H. B. ELSWIJK, P. M. BRONSVELD, and J. Th. M. DE HOSSON: *Phys. Rev. B*, 1988, **37**, 4261–4264.
27. P. BAK and A. I. GOLDMAN: in 'Aperiodicity and order', Vol. 1, (ed. M. V. Jarić), 143–170; 1988, Boston, Academic Press.
28. D. J. STRUIK: 'A concise history of mathematics', 86–87; 1967, New York, Dover.
29. R. A. DUNLAP and K. DINI: *Can. J. Phys.*, 1985, **63**, 1267–1269.
30. R. A. DUNLAP and K. DINI: *J. Phys. F, Met. Phys.*, 1986, **16**, 11–16.
31. D. A. LILLIENFELD, M. NASTASI, H. H. JOHNSON, D. G. ART, and J. W. MAYER: *J. Mater. Res.*, 1986, **1**, 237–242.
32. P. A. BANCEL and P. A. HEINEY: *J. Phys. (Orsay)*, 1986, **47-C3**, 341–350.
33. G. P. VAN BAKEL, P. M. BRONSVELD, and J. Th. M. DE HOSSON: *J. Phys. (Orsay)*, 1989, **50-C8**, 265–269.
34. J. A. KNAPP and D. M. FOLLSTAEDT: in 'Fundamentals of beam-solid interactions and transient thermal processing', (ed. M. J. Aziz et al.), Mater. Res. Soc. Symp. Proc., 1988, **100**, 597.
35. S. M. ANLAGE, B. FULTZ, and K. M. KRISHNAN: *J. Mater. Res.*, 1988, **3**, 421–425.
36. A. INOUE, H. M. KIMURA, and T. MASUMOTO: *J. Mater. Sci.*, 1987, **22**, 1758–1768.
37. K. V. RAO, J. FIDLER, and H. S. CHEN: *Europhys. Lett.*, 1986, **1**, 647–653.
38. A. INOUE, L. ARNBERG, B. LEHTINEN, M. OGUCHI, and T. MASUMOTO: *Metall. Trans.*, 1986, **17A**, 1657–1664.
39. D. W. LAWTHOR, R. A. DUNLAP, and V. SRINIVAS: *Can. J. Phys.*, 1989, **67**, 463–467.
40. D. A. LILLIENFELD: in 'Fundamentals of beam-solid interactions and transient thermal processing', (ed. M. J. Aziz et al.), Mater. Res. Soc. Symp. Proc., 1988, **100**, 45.
41. H. M. KIMURA, A. INOUE, Y. BIZEN, and T. MASUMOTO: *Mater. Sci. Eng.*, 1988, **99**, 449–452.
42. R. A. DUNLAP, D. W. LAWTHOR, and D. J. LLOYD: *Phys. Rev. B*, 1988, **38**, 3649–3652.
43. R. MANAILA, V. FLORESCU, A. JIANU, and A. BADESCU: *Phys. Status Solidi (a)*, 1988, **109**, 61–66.
44. W. L. ZHOU, X. Z. LI, and K. H. KUO: *Scr. Metall.*, 1989, **23**, 1571–1574.
45. A. P. TSAI, A. INOUE, and T. MASUMOTO: *J. Mater. Sci. Lett.*, 1988, **7**, 322–326.
46. A. P. TSAI, A. INOUE, and T. MASUMOTO: *Jpn. J. Appl. Phys.*, 1988, **27**, L1587–L1590.
47. A. P. TSAI, A. INOUE, and T. MASUMOTO: *Jpn. J. Appl. Phys.*, 1987, **26**, L1505–L1507.
48. H. S. CHEN, J. C. PHILLIPS, P. VILLARS, A. R. KORTAN, and A. INOUE: *Phys. Rev. B*, 1987, **35**, 9326–9329.
49. J. C. PHILLIPS and H. S. CHEN: *Phys. Rev. Lett.*, 1986, **57**, 3085–3088.
50. AN-PANG TSAI, A. INOUE, and T. MASUMOTO: *J. Mater. Sci. Lett.*, 1989, **8**, 253–256.
51. A. P. TSAI, A. INOUE, and T. MASUMOTO: *Jpn. J. Appl. Phys.*, 1987, **26**, L1994–L1996.
52. A. INOUE, Y. BIZEN, and T. MASUMOTO: *Metall. Trans.*, 1988, **19A**, 383–385.
53. L. Y. YANG, J. G. ZHAO, W. S. ZHAN, C. Y. YANG, Y. Q. ZHOU, and K. K. FUNG: *J. Phys. F, Met. Phys.*, 1987, **17**, L97–L99.
54. L. M. ANGERS, L. D. MARKS, J. R. WEERTMAN, and M. E. FINE: in 'Materials problem solving with transmission electron microscopy', (ed. L. W. Hobbs et al.), Mater. Res. Soc. Symp. Proc., 1986, **62**, 255.
55. V. SRINIVAS, M. E. McHENRY, and R. A. DUNLAP: *Phys. Rev. B*, 1989, **40**, 9590.
56. A. P. TSAI, A. INOUE, and T. MASUMOTO: *Jpn. J. Appl. Phys.*, 1988, **27**, L5–L8.
57. A. INOUE, K. NAKANO, Y. BIZEN, T. MASUMOTO, and H. S. CHEN: *Jpn. J. Appl. Phys.*, 1988, **27**, L944–L947.
58. A. INOUE, K. NAKANO, T. MASUMOTO, and H. S. CHEN: *Mater. Trans. JIM*, 1989, **30**, 200.
59. N. K. MUKHOPADHYAY: *Mater. Forum*, 1989, **13**, 228.
60. P. RAMACHANDRARAO and G. V. S. SASTRY: *Pramāna*, 1985, **25**, L225–L230.
61. R. GOPALAN, D. AKHTAR, and T. P. RAJASEKHARAN: *Z. Metallkd.*, 1990, **81**, 111–113.
62. A. SADOC: *J. Phys. (Orsay)*, 1986, **47-C3**, 1003.
63. C. ZHENHUA, W. YUN, Z. DUOSAN, and J. XIANGYANG: *Scr. Metall.*, 1990, **24**, 599–604.
64. N. P. LALLA, R. S. TIWARI, O. N. SRIVASTAVA, and S. RANGANATHAN: Personal communication, 1988.
65. N. K. MUKHOPADHYAY, G. N. SUBBANNA, K. CHATTOPADHYAY, and S. RANGANATHAN: in 'Proc. 4th Asia-Pacific conf. workshop on electron microscopy', 187–188; 1988, Bangkok.
66. AN-PANG TSAI, A. INOUE, and T. MASUMOTO: *Philos. Mag. Lett.*, 1990, **62**, 95–100.
67. C. H. CHEN and H. S. CHEN: *Phys. Rev. B*, 1986, **33**, 2814–2816.
68. A. R. YAVARI and J. L. VERGER-GAURY: *J. Mater. Sci.*, 1988, **23**, 3383–3386.
69. T. OHASHI, L. DAI, N. FUKATSU, and K. MIWA: *Scr. Metall.*, 1986, **20**, 1241–1244.
70. A. P. TSAI, A. INOUE, Y. YOKOYAMA, and T. MASUMOTO: *Mater. Trans. JIM*, 1990, **31**, 98.
71. V. SRINIVAS, R. A. DUNLAP, D. BAHADUR, and E. DUNLAP: *Philos. Mag. B*, 1990, **61**, 177–188.
72. Y. SHEN, G. J. SHIFLET, and S. J. POON: *Phys. Rev. B*, 1988, **38**, 5323–5337.
73. S. NANO, W. DMOWSKI, T. EGAMI, J. W. RICHARDSON Jr, and J. D. JORGENSEN: *Phys. Rev. B*, 1987, **35**, 435–440.
74. R. A. DUNLAP and V. SRINIVAS: *Phys. Rev. B*, 1989, **40**, 704–707.
75. M. EIBSCHÜTZ, M. E. LINES, H. S. CHEN, J. WASZCZAK, G. PAPAEFTHYMIOU, and R. B. FRANKEL: *J. Appl. Phys.*, 1988, **63**, 4063–4065.
76. K. KIMURA, T. HASHIMOTO, and S. TAKEUCHI: *J. Non-Cryst. Solids*, 1990, **117/118**, 828–831.
77. P. A. HEINEY, P. A. BANCEL, A. I. GOLDMAN, and P. W. STEPHENS: *Phys. Rev. B*, 1986, **34**, 6746–6751.
78. H. YAMANE, K. KIMURA, and S. TAKEUCHI: *Acta Metall.*, 1988, **36**, 3243–3248.
79. N. K. MUKHOPADHYAY, G. N. SUBBANNA, S. RANGANATHAN, and K. CHATTOPADHYAY: *Scr. Metall.*, 1986, **20**, 525–528.
80. K. F. KELTON, P. C. GIBBONS, and P. N. SABES: *Phys. Rev. B*, 1988, **38**, 7810–7813.
81. Z. ZHANG and K. F. KELTON: *Philos. Mag. Lett.*, 1990, **62**, 265–271.
82. C. DONG, Z. K. HEI, L. B. WANG, Q. H. SONG, Y. K. WU, and K. H. KUO: *Scr. Metall.*, 1986, **20**, 1155–1158.
83. R. CHATTERJEE and R. C. O'HANDLEY: *Phys. Rev. B*, 1989, **39**, 8128–8131.
84. V. V. MOLOKANOV and V. N. CHEBOTNIKOV: *J. Non-Cryst. Solids*, 1990, **117/118**, 789–792.
85. Z. ZHANG and K. F. KELTON: *Philos. Mag. Lett.*, 1991, **63**, 39–47.
86. Z. ZHANG, H. Q. YE, and K. H. KUO: *Philos. Mag. A*, 1985, **52**, L49–L52.
87. R. A. DUNLAP, R. C. O'HANDLEY, M. E. McHENRY, and R. CHATTERJEE: *Phys. Rev. B*, 1988, **37**, 8484–8487.
88. K. F. KELTON and X. ZHANG: *Bull. Am. Phys. Soc.*, 1990, **35**, 523.
89. L. A. BENDERSKY and F. S. BIANCANIELLO: *Scr. Metall.*, 1987, **21**, 531–536.
90. M. E. McHENRY and R. C. O'HANDLEY: in 'Plasma processing and synthesis of materials', (ed. D. Apelian and J. Szekely), Mater. Res. Soc. Symp. Proc., 1987, **98**, 363.
91. L. HUA, J. SHOUTING, O. MIEVING, S. YICHENG, and R. C. O'HANDLEY: *Acta Metall. Sin. (China)*, 1988, **24**, A313.
92. B. X. LIU, C. H. SHANG, R. J. HUANG, and H. O. LI: *J. Non-Cryst. Solids*, 1990, **117/118**, 785–788.
93. C. H. ZHANG, J. LI, H. O. LI, and B. X. LIU: *J. Phys. F, Met. Phys.*, 1988, **18**, L169–L173.
94. A. Q. HE, H. Q. YE, and K. H. KUO: *Scr. Metall.*, 1989, **23**, 533–536.
95. W. OHASHI and F. SPAEPEN: *Nature*, 1987, **330**, 555–556.
96. K. H. KUO, C. DONG, D. S. ZHOU, Y. X. GUO, Z. K. HEI, and D. X. LI: *Scr. Metall.*, 1986, **20**, 1695–1698.
97. S. J. POON, A. J. DREHMAN, and K. R. LAWLESS: *Phys. Rev. Lett.*, 1985, **55**, 2324–2327.
98. Z. W. HU, X. L. JIANG, J. ZHO, and S. S. HSU: *Philos. Mag. Lett.*, 1990, **61**, 115–118.

99. K. H. KUO, D. S. ZHOU, and D. X. LI: *Philos. Mag. Lett.*, 1987, **55**, 33–39.
100. D. A. LILIENFELD, M. NASTASI, H. H. JOHNSON, D. G. AST, and J. W. MAYER: *Phys. Rev. Lett.*, 1985, **55**, 1587–1590.
101. J. C. HOLZER and K. F. KELTON: *Acta Metall. Mater.*, 1991, **39**, 1833–1843.
102. A. P. TSAI, A. INOUE, Y. BIZEN, and T. MASUMOTO: *Acta Metall.*, 1989, **37**, 1443–1449.
103. A. CSANADY, P. B. BARNA, J. MAYER, and K. URBAN: *Scr. Metall.*, 1987, **21**, 1535–1540.
104. Y. SAITO, K. MIHAMA, and H. S. CHEN: *Phys. Rev. B*, 1987, **35**, 4085–4088.
105. J. A. SEKHAR and T. RAJASEKHARAN: *Nature*, 1986, **320**, 153–155.
106. B. GRUSHKO and GERY R. STAFFORD: *Metall. Trans.*, 1989, **20A**, 1351–1359.
107. B. GRUSHKO and GERY R. STAFFORD: *Scr. Metall.*, 1989, **23**, 1043–1048.
108. S. R. NISHITANI, H. KAWAURA, K. F. KOBAYASHI, and H. P. SHINGU: *J. Cryst. Growth*, 1986, **76**, 209–214.
109. W. C. CASSADA, Y. SHEN, S. J. POON, and G. J. SHIFLET: *Phys. Rev. B*, 1986, **34**, 7413–7416.
110. D. M. FOLLSTAEDT and J. A. KNAPP: *Phys. Rev. Lett.*, 1986, **56**, 1827–1830.
111. J. ECKERT, L. SCHULTZ, and K. URBAN: *Appl. Phys. Lett.*, 1989, **55**, 117–119.
112. J. D. BUDAI and M. J. AZIZ: *Phys. Rev. B*, 1986, **33**, 2876–2878.
113. K. CHATTOPADHYAY, S. LELE, R. PRASAD, S. RANGANATHAN, G. N. SUBBANNA, and N. THANGARAJ: *Scr. Metall.*, 1985, **19**, 1331–1334.
114. V. ELSE: *Phys. Rev. B*, 1985, **32**, 4892–4898.
115. S. EBALARD and F. SPAEPEN: *J. Mater. Res.*, 1989, **4**, 39–43.
116. C. H. CHEN, J. P. REMEKA, G. P. ESPINOSA, and A. S. COOPER: *Phys. Rev. B*, 1987, **35**, 7737–7740.
117. D. N. WANG, T. ISHIMASA, H. U. NISSEN, S. HOVMOLLER, and J. RHYNER: *Philos. Mag. A*, 1988, **58**, 737–752.
118. M. TANAKA, M. TERAUCHI, K. HIRAGA, and M. HIRABAYASHI: *Ultramicroscopy*, 1985, **17**, 279–286.
119. K. HIRAGA, M. HIRABAYASHI, A. INOUE, and T. MASUMOTO: *J. Microsc.*, 1987, **146**, 245.
120. N. K. MUKHOPADHYAY, S. RANGANATHAN, and K. CHATTOPADHYAY: *Philos. Mag. Lett.*, 1987, **56**, 121–127.
121. N. K. MUKHOPADHYAY, N. THANGARAJ, K. CHATTOPADHYAY, and S. RANGANATHAN: *J. Mater. Res.*, 1987, **2**, 299–304.
122. K. HIRAGA and M. HIRABAYASHI: *Jpn J. Appl. Phys.*, 1987, **26**, L155–L158.
123. J. MENON: *Scr. Metall.*, 1988, **22**, 1125–1127.
124. Z. ZHANG and K. URBAN: *Philos. Mag. Lett.*, 1989, **60**, 97–102.
125. J. DEVAUD-RZEPSKI, M. CORNIER-QUIQUANDON, and D. GRATIAS: in ‘Quasicrystals and incommensurate structures in condensed matter’, (ed. M. J. Yacaman *et al.*), 498–515; 1989, Singapore, World Scientific.
126. S. EBALARD and F. SPAEPEN: *J. Mater. Res.*, 1990, **5**, 62–73.
127. R. WANG and M. DAI: *Philos. Mag. Lett.*, 1990, **61**, 119–123.
128. Y. HATWALNE and S. RAMASWAMY: *Philos. Mag. Lett.*, 1990, **61**, 169–172.
129. Z. ZHANG, M. WOLLGARTEN, and K. URBAN: *Philos. Mag. Lett.*, 1990, **61**, 125–131.
130. K. S. VECCHIO and D. B. WILLIAMS: *Philos. Mag. B*, 1988, **37**, 535–546.
131. F. SPAEPEN, LI-CHYONG CHEN, and W. OHASHI: *Bull. Am. Phys. Soc.*, 1988, **33**, 604.
132. K. M. KNOWLES and W. M. STOBBS: in ‘Phase transformations ’87’, (ed. G. W. Lorimer), 557–561; 1988, London, The Institute of Metals.
133. K. HIRAGA, B. ZHANG, M. HIRABAYASHI, A. INOUE, and T. MASUMOTO: *Jpn J. Appl. Phys.*, 1988, **27**, L951–L953.
134. P. A. BANCEL and P. A. HEINEY: *Phys. Rev. B*, 1986, **33**, 7917–7922.
135. R. HU, T. EGAMI, J. C. HOLZER, and K. F. KELTON: *Bull. Am. Phys. Soc.*, 1990, **35**, 194.
136. J. L. LIBBERT, K. F. KELTON, and A. I. GOLDMAN: *Bull. Am. Phys. Soc.*, 1991, **36**, 988.
137. Y. SHEN, S. J. POON, W. DMOWSKI, T. EGAMI, and G. J. SHIFLET: *Phys. Rev. Lett.*, 1987, **58**, 1440–1443.
138. A. R. KORTAN, H. S. CHEN, and J. V. WASZCZAK: *J. Mater. Res.*, 1987, **2**, 294–297.
139. W. MALZFELDT, P. M. HORN, D. P. DIVINCENZO, B. STEPHENSON, R. GAMBINO, and S. J. HERD: *J. Phys. (Orsay)*, 1986, **47-C3**, 379–387.
140. Y. CALVAYRAC, J. DEVAUD-RZEPSKI, M. BESSIÈRE, S. LEFEBVRE, A. QUIVY, and D. GRATIAS: *Philos. Mag. B*, 1989, **59**, 439–450.
141. A. P. TSAI, A. INOUE, and T. MASUMOTO: *J. Mater. Sci. Lett.*, 1989, **8**, 470–472.
142. Y. CALVAYRAC, A. QUIVY, M. BESSIÈRE, S. LEFEBVRE, M. CORNIER-QUIQUANDON, and D. GRATIAS: *J. Phys. (Orsay)*, 1990, **51**, 417–431.
143. A. WASEDA, K. EDAGAWA, and H. INO: *Philos. Mag. Lett.*, 1990, **62**, 183–186.
144. P. A. BANCEL: *Phys. Rev. B*, 1989, **63**, 2741–2744.
145. C. A. GURYAN, A. I. GOLDMAN, P. W. STEPHENS, K. HIRAGA, A. P. TSAI, A. INOUE, and T. MASUMOTO: *Phys. Rev. Lett.*, 1989, **62**, 2409–2412.
146. K. CHATTOPADHYAY, S. LELE, S. RANGANATHAN, G. N. SUBBANNA, and N. THANGARAJ: *Current Sci.*, 1985, **54**, 895–903.
147. K. HIRAGA: *JEOL News*, 1987, **25E**, 8–12.
148. T. ISHIMASA, Y. FUKANO, and M. TSUCHIMORI: *Philos. Mag. Lett.*, 1988, **58**, 157–165.
149. M. DUNEAU and A. KATZ: *Phys. Rev. Lett.*, 1985, **54**, 2688–2691.
150. P. BUSECK, J. COWLEY, and L. EYRING: ‘High-resolution transmission electron microscopy and associated techniques’; 1988, New York, Oxford University Press.
151. J. C. H. SPENCE: ‘Experimental high-resolution electron microscopy’; 1988, New York, Oxford University Press.
152. J. W. CAHN: *J. Mater. Res.*, 1986, **1**, 13–26.
153. D. R. NELSON and S. SACHDEV: *Phys. Rev. B*, 1985, **32**, 689–695.
154. D. S. ROKHSAR, N. D. MERMIN, and D. C. WRIGHT: *Phys. Rev. B*, 1987, **35**, 5487–5495.
155. K. CHATTOPADHYAY, S. RANGANATHAN, G. N. SUBBANNA, and N. THANGARAJ: *Scr. Metall.*, 1985, **19**, 767–771.
156. R. J. SCHAEFER and L. A. BENDERSKY: in ‘Aperiodicity and order’, Vol. 1, (ed. M. V. Jarić), 111–142; 1988, Boston, Academic Press.
157. R. J. SCHAEFER, L. A. BENDERSKY, D. SHECHTMAN, W. J. BOETTINGER, and F. S. BIANCANIELLO: *Metall. Trans.*, 1986, **17A**, 2117–2125.
158. J. H. PEREPEZKO and W. J. BOETTINGER: in ‘Alloy phase diagrams’, (ed. L. H. Bennett *et al.*), Mater. Res. Soc. Symp. Proc., 1983, **19**, 223–234.
159. L. A. BENDERSKY and M. J. KAUFMAN: *Philos. Mag. B*, 1986, **53**, L75–L80.
160. R. A. DUNLAP and K. DINI: *J. Mater. Res.*, 1986, **1**, 415–419.
161. A. YAMANE, K. KIMURA, T. SHIBUYA, and S. TAKEUCHI: 1987, Technical Report of IIISP, Ser. A, No. 1848, University of Tokyo.
162. X. ZHANG and K. F. KELTON: *Bull. Am. Phys. Soc.*, 1991, **36**, 987.
163. K. M. KNOWLES and W. M. STOBBS: *J. Microsc.*, 1987, **146**, 267–285.
164. J. L. ROBERTSON, M. E. MISENHEIMER, S. C. MOSS, and L. A. BENDERSKY: *Acta Metall.*, 1986, **34**, 2177–2189.
165. J. A. RAMSEY, P. C. GIBBONS, and K. F. KELTON: *Bull. Am. Phys. Soc.*, 1991, **36**, 987.
166. M. AUDIER, P. GUYOT, and Y. BRECHET: *Philos. Mag. Lett.*, 1990, **61**, 55–62.
167. K. KIMURA, T. HASHIMOTO, K. SUZUKI, K. NAGAYMA, H. INO, and S. TAKEUCHI: *J. Phys. Soc. Jpn.*, 1985, **54**, 3217–3220.
168. K. M. KRISHNAN, R. GRONSKY, and L. E. TANNER: *Scr. Metall.*, 1986, **20**, 239–242.
169. K. YU-ZHANG, J. BIGOT, J. P. CHEVALIER, D. GRATIAS, G. MARTIN, and R. PORTIER: *Philos. Mag. B*, 1988, **58**, 1–13.
170. P. N. SABES, J. C. HOLZER, and K. F. KELTON: *Bull. Am. Phys. Soc.*, 1989, **34**, 407.
171. D. C. KOSKENMAKI, H. S. CHEN, and K. U. RAO: *Phys. Rev. B*, 1986, **33**, 5328–5332.
172. P. GUYOT and M. AUDIER: *Philos. Mag. B*, 1985, **52**, L15–L19.
173. M. COOPER and L. ROBINSON: *Acta Crystallogr.*, 1966, **20**, 614.
174. M. AUDIER, P. SAINFORT, and B. DUBOST: *Philos. Mag. B*, 1986, **54**, L105–L111.
175. C. DONG, K. CHATTOPADHYAY, and K. H. KUO: *Scr. Metall.*, 1987, **21**, 1307–1312.
176. J. D. BUDAI and M. J. AZIZ: *Phys. Rev. B*, 1986, **33**, 2876–2878.
177. A. LOISEAU and G. LAPASET: *Philos. Mag. Lett.*, 1987, **56**, 165–171.
178. C. ROTTMAN and M. WORTIS: *Phys. Rep.*, 1984, **103**, 59–79.
179. A. A. CHERNOV: *Sov. Phys. Usp.*, 1961, **73**, 277.
180. T. L. HO, J. A. JASZCZAK, Y. H. LI, and W. F. SAAM: *Phys. Rev. Lett.*, 1987, **59**, 1116–1119.
181. J. A. JASZCZAK, W. F. SAAM, and B. YANG: *Phys. Rev. B*, 1989, **39**, 9289–9295.

182. K. INGERSENT and P. J. STEINHARDT: *Phys. Rev. B*, 1989, **39**, 980–992.
183. T. L. HO, Y. H. LI, W. F. SAAM, and J. A. JASZCZAK: *Phys. Rev. B*, 1989, **39**, 10 614–10 626.
184. P. W. STEPHENS: in 'Aperiodicity and order', Vol. 3, (ed. M. V. Jarić and D. Gratias), 37–104; 1989, Boston, Academic Press.
185. H. U. NISSEN, R. WESICKEN, C. BEELI, and A. CSANADY: *Philos. Mag. B*, 1988, **57**, 587–597.
186. T. RAJASEKHARAN, R. GOPALAN, D. AKHTAR, and D. BANARJEE: *Scr. Metall.*, 1987, **21**, 289–291.
187. D. MACKO, O. HUDAK, P. DIKO, V. HAJKO Jr, J. BILLY, and P. MAKROCYZ: *Phys. Lett. A*, 1988, **127**, 360–362.
188. F. W. GAYLE: *J. Mater. Res.*, 1987, **2**, 1–4.
189. F. CHENG-GAO, W. ZI-QIN, W. YUAN-SHENG, and T. LING-CHAO: *J. Microsc.*, 1987, **146**, 261.
190. C. BEELI, T. ISHIMASA, and H. U. NISSEN: *Philos. Mag. B*, 1988, **57**, 599–608.
191. B. MIAO, G. YANG, and S. WANG: *Phys. Lett. A*, 1987, **121**, 283–285.
192. N. THANGARAJ, G. N. SUBBANNA, S. RANGANATHAN, and K. CHATTOPADHYAY: *J. Microsc.*, 1987, **146**, 287.
193. Z. ZHANG and K. F. KELTON: *Scr. Metall. Mater.*, 1992, **26**, 393–398.
194. S. SACHDEV and D. R. NELSON: *Phys. Rev. B*, 1985, **32**, 4592–4606.
195. D. B. FAHRENHEIT: *Philos. Trans. R. Soc.*, 1724, **39**, 78.
196. F. C. FRANK: *Proc. R. Soc.*, 1952, **A215**, 43–46.
197. P. J. STEINHARDT, D. R. NELSON, and M. RONCHETTI: *Phys. Rev. Lett.*, 1981, **47**, 1297–1300.
198. P. J. STEINHARDT, D. R. NELSON, and M. RONCHETTI: *Phys. Rev. B*, 1983, **28**, 784–805.
199. J. D. HONEYCUTT and H. C. ANDERSON: *J. Phys. Chem.*, 1987, **91**, 4950.
200. T. L. BECK and R. S. BERRY: *J. Chem. Phys.*, 1988, **88**, 3910–3922.
201. J. D. BERNAL: *Proc. R. Soc.*, 1964, **A280**, 299–322.
202. J. L. FINNEY: *Proc. R. Soc.*, 1970, **A319**, 479–493; 495–507.
203. A. J. DREHMAN, A. R. PELTON, and M. A. NOACK: *J. Mater. Res.*, 1986, **1**, 741–745.
204. Y. SHEN, S. J. POON, and G. J. SHIFLET: *Phys. Rev. B*, 1986, **34**, 3516–3519.
205. J. A. KNAPP and D. M. FOLLSTAEDT: *Phys. Rev. Lett.*, 1985, **55**, 1591–1594.
206. L. A. BENDERSKY and J. D. RIDDER: *J. Mater. Res.*, 1986, **1**, 405–414.
207. J. L. ROBERTSON, S. C. MOSS, and K. G. KREIDER: *Phys. Rev. Lett.*, 1988, **60**, 2062–2065.
208. L. C. CHEN and F. SPAEPEN: *Nature*, 1988, **336**, 366–368.
209. J. C. HOLZER and K. F. KELTON: *Acta Metall. Mater.*, 1991, **39**, 1833–1843.
210. D. TURNBULL and F. SPAEPEN: *J. Polymer Sci.*, 1978, **63**, 237.
211. P. VILLARS, J. C. PHILLIPS, and H. S. CHEN: *Phys. Rev. Lett.*, 1986, **57**, 3085–3088.
212. K. M. RABE, A. R. KORTAN, J. C. PHILLIPS, and P. VILLARS: *Phys. Rev. B*, 1991, **43**, 6280.
213. J. TARTAS and E. J. KNYSTAUTAS: *J. Mater. Res.*, 1991, **6**, 1219–1229.
214. A. P. SMITH and N. W. ASHCROFT: *Phys. Rev. Lett.*, 1987, **59**, 1365–1368.
215. R. B. PHILLIPS, H. DENG, A. E. CARLSSON, and M. S. DAW: *Phys. Rev. Lett.*, 1991, **67**, 3128–3131.
216. H. DENG and A. E. CARLSSON: *Bull. Am. Phys. Soc.*, 1991, **36**, 939.
217. A. E. CARLSSON and R. B. PHILLIPS: in 'Quasicrystals: the state of the art', (ed. D. P. DiVincenzo and P. J. Steinhardt), 361–402; 1991, Singapore, World Scientific.
218. S. RANGANATHAN and K. CHATTOPADHYAY: *Key Eng. Mater.*, 1987, **13–15**, 229–236.
219. K. H. KUO: *J. Non-Cryst. Solids*, 1990, **117/118**, 756–764.
220. G. V. S. SASTRY, C. SURYANARAYANA, M. van SANDE, and G. van TENDELOO: *Mater. Res. Bull.*, 1978, **13**, 1064–1070.
221. D. SHECHTMAN, R. J. SCHAEFER, and F. S. BIANCANIELLO: *Metall. Trans.*, 1984, **15A**, 1987–1997.
222. L. A. BENDERSKY: *Phys. Rev. Lett.*, 1985, **55**, 1461–1463.
223. K. K. FUNG, C. Y. YANG, Y. Q. ZHOU, J. G. ZHAO, W. S. ZHAN, and B. G. SHEN: *Phys. Rev. Lett.*, 1986, **56**, 2060–2063.
224. C. SURYANARAYANA and J. MENON: *Scr. Metall.*, 1987, **21**, 459–460.
225. K. H. KUO: *Mater. Sci. Forum*, 1987, **22–24**, 131–140.
226. X. Z. LI and K. H. KUO: *Philos. Mag. Lett.*, 1988, **58**, 167–171.
227. N. THANGARAJ, K. CHATTOPADHYAY, S. RANGANATHAN, C. SMALL, and H. A. DAVIES: in 'Proc. 11th cong. on electron microscopy', 1986, **11**, 1525–1526.
228. L. BENDERSKY: *J. Phys. (Orsay)*, 1986, **47-C3**, 457–464.
229. S. H. J. IDZIAK, P. A. HEINEY, and P. A. BANCER: *Mater. Sci. Forum*, 1987, **22–24**, 3533.
230. X. HE, Y. K. WU, and K. H. KUO: Unpublished work.
231. K. H. KUO, D. S. ZHOU, and D. X. LI: *Philos. Mag. Lett.*, 1987, **55**, 33–39.
232. S. EBALARD and F. SPAEPEN: *J. Mater. Res.*, 1990, **5**, 62–73.
233. A. P. TSAI, A. INOUE, and T. MASUMOTO: *Mater. Trans. JIM*, 1989, **30**, 463.
234. J. MENON and C. SURYANARAYANA: *Mater. Trans. JIM*, 1989, **30**, 878.
235. H. ZHANG, D. H. WANG, and K. H. KUO: *J. Mater. Sci.*, 1989, **24**, 2981–2986.
236. R. J. SCHAEFER: *Scr. Metall.*, 1986, **20**, 1187–1192.
237. R. XU, R. D. WERKMAN, I. VINCE, P. J. SHURER, and F. VAN der WOUDE: *Hyperfine Interact.*, 1988, **45**, 403.
238. C. BEELI, H. U. NISSEN, and J. ROBADEY: *Philos. Mag. Lett.*, 1991, **63**, 87–95.
239. A. P. TSAI, A. INOUE, and T. MASUMOTO: *Mater. Trans. JIM*, 1989, **30**, 463–465.
240. A. Q. HE, Q. B. YANG, and H. Q. YE: *Philos. Mag. Lett.*, 1990, **61**, 69–75.
241. P. MANDAL, R. S. TIWARI, and O. N. SRIVASTAVA: *Mater. Res. Bull.*, 1990, **25**, 277–282.
242. P. PEREZ-CAMPOS, J. G. PEREZ-RAMIREZ, A. GOMEZ, R. HERRERA, and M. JOSE-YACAMAN: *Scr. Metall.*, 1986, **20**, 401–405.
243. J. D. FITZGERALD, R. L. WITHERS, A. M. STEWART, and A. CALKA: *Philos. Mag. B*, 1988, **58**, 15–33.
244. J. MAYER, A. CSANADY, and K. URBAN: *J. Mater. Res.*, 1990, **5**, 57–61.
245. X. Z. LI and K. H. KUO: *Philos. Mag. Lett.*, 1988, **58**, 167–171.
246. L. X. HE, Y. K. WU, and K. H. KUO: *J. Mater. Sci. Lett.*, 1988, **7**, 1284–1286.
247. J. MENON and C. SURYANARAYANA: *Phys. Status Solidi(a)*, 1988, **107**, 693–708.
248. L. X. HE, Z. ZHANG, Y. K. WU, and K. H. KUO: in 'International Physics Conf. Ser. '93', Vol. 2, Chap. 13, 501–502; 1988.
249. J. MENON, C. SURYANARAYANA, and G. SINGH: *J. Appl. Crystallogr.*, 1989, **22**, 96–99.
250. T. L. DAULTON, K. F. KELTON, and P. C. GIBBONS: *Philos. Mag. B*, 1991, **63**, 687–714.
251. TIN-LUN HO: *Phys. Rev. Lett.*, 1986, **56**, 468–471.
252. B. KOOPMANS, P. J. SCHURER, F. VAN der WOUDE, and P. BRONSVELD: *Phys. Rev. B*, 1987, **35**, 3005–3008.
253. S. TAKEUCHI and K. KIMURA: *J. Phys. Soc. Jpn.*, 1987, **56**, 982–988.
254. T. C. CHOY, J. D. FITZGERALD, and A. C. KALLONIATIS: *Philos. Mag. B*, 1988, **58**, 35–46.
255. G. van TENDELOO, J. MENON, A. SINGH, and S. RANGANATHAN: *Phase Transitions*, 1989, **16–17**, 59–65.
256. N. K. MUKHOPOADHYAY, K. CHATTOPADHYAY, and S. RANGANATHAN: in 'Quasicrystals and incommensurate structures in condensed matter', (ed. M. Yacaman *et al.*), 212–221; 1989, Singapore, World Scientific.
257. S. RANGANATHAN, A. SINGH, J. MEYER, and K. URBAN: *Philos. Mag. Lett.*, 1989, **60**, 261–267.
258. R. K. MANDAL and S. LELE: *Philos. Mag. B*, 1991, **63**, 513–527.
259. S. MULLER: *Europhys. Lett.*, 1987, **3**, 587–592.
260. S. MULLER: *Z. Phys. B*, 1989, **74**, 369–377.
261. R. J. SCHAEFER and L. BENDERSKY: *Scr. Metall.*, 1986, **20**, 745–750.
262. L. BENDERSKY, R. J. SCHAEFER, F. S. BIANCANIELLO, W. J. BEOTTINGER, M. J. KAUFMANN, and D. SHECHTMAN: *Scr. Metall.*, 1985, **19**, 909–914.
263. R. J. SCHAEFER: *Scr. Metall.*, 1986, **20**, 1187–1192.
264. V. van TENDELOO, A. SINGH, and S. RANGANATHAN: *Philos. Mag. A*, 1991, **64**, 413–427.
265. G. V. S. SASTRY and C. SURYANARAYANA: *Scr. Metall.*, 1986, **20**, 1359–1360.
266. C. SURYANARAYANA and J. MENON: *Scr. Metall.*, 1987, **21**, 459–460.
267. C. DONG, G. B. LI, and K. H. KUO: *J. Phys. F, Met. Phys.*, 1987, **17**, L189–L192.
268. A. R. KORTAN, F. A. THIEL, H. S. CHEN, A. P. TSAI, A. INOUE, and T. MASUMOTO: *Phys. Rev. B*, 1989, **40**, 9398–9399.

269. L. X. HE, Y. K. WU, X. M. MENG, and K. H. KUO: *Philos. Mag. Lett.*, 1990, **61**, 15–19.
270. K. H. KUO: *J. Non-Cryst. Solids*, 1990, **117/118**, 756–764.
271. P. LAUNOIS, M. AUDIER, F. DENOYER, C. DONG, J. M. DUBOIS, and M. LAMBERT: *Europhys. Lett.*, 1991, **3**, 629–634.
272. C. DONG, J. M. DUBOIS, M. DE BOISSIEU, and C. JANOT: *J. Phys. C, Solid State Phys.*, 1991, **3**, 1665–1673.
273. K. HIRAGA, W. SUN, and F. J. LINCOLN: *Jpn J. Appl. Phys.*, 1991, **30**, 2028–2034.
274. T. L. DAULTON and K. F. KELTON: *Philos. Mag. Lett.*, 1991, **63**, 257–265.
- 274a. T. L. DAULTON, K. F. KELTON, S. SONG, and E. RYBA: *Philos. Mag. Lett.*, 1992, **65**, 55–65.
275. S. SONG, E. R. RYBA, A. RAMANI, and P. R. HOWELL: *J. Mater. Sci. Lett.*, 1991, **10**, 237–240.
276. S. S. LU and T. CHANG: *Acta Phys. Sin. (China)*, 1957, **13**, 150.
277. M. VAN SANDE, R. DE RIDDER, J. VAN LANDUYT, and S. AMELINCKX: *Phys. Status Solidi(a)*, 1978, **50**, 587–599.
278. K. CHATTOPADHYAY, S. LELE, N. THANGARAJ, and S. RANGANATHAN: *Acta Metall.*, 1987, **35**, 727–733.
279. D. S. ZHOU, D. X. LI, H. Q. YE, and K. H. KUO: *Philos. Mag. Lett.*, 1987, **56**, 209–215.
280. L. X. HE, X. Z. LI, Z. ZHANG, and K. H. KUO: *Phys. Rev. Lett.*, 1988, **61**, 1116–1118.
281. D. R. NELSON: *Phys. Rev. Lett.*, 1983, **50**, 982–985.
282. D. R. NELSON: *Phys. Rev. B*, 1983, **28**, 5515–5535.
283. D. LEVINE and P. J. STEINHARDT: *Phys. Rev. Lett.*, 1985, **54**, 2477–2480.
284. R. PENROSE: *Bull. Inst. Math. Appl.*, 1974, **10**, 266–271.
285. R. PENROSE: *Math. Intelligencer*, 1974, **2**, 32.
286. A. L. MACKAY: *Phys. Bull.*, Nov. 1976, 495–497.
287. M. GARDNER: *Sci. Am.*, 1977, **236**, (1), 110–121.
288. B. GRUNBAUM and G. C. SHEPPARD: 'Tilings and patterns'; 1987, San Francisco, Freeman.
289. N. G. de BRUIJN: *Math. Proc. A*, 1981, **84**, 39–66.
290. A. L. MACKAY: *Sov. Phys. Crystallogr.*, 1981, **26**, 517–522.
291. D. LEVINE and P. J. STEINHARDT: *Phys. Rev. B*, 1986, **34**, 596–616.
292. V. ELSER: in 'Proc. 15th int. colloq. on group theoretical methods in physics', Vol. 1, (ed. R. Gilmore and D. H. Feng); 1987, Singapore, World Scientific.
293. A. L. MACKAY: *Physica*, 1982, **114A**, 609–613.
294. J. E. S. SOCOLAR and P. J. STEINHARDT: *Phys. Rev. B*, 1986, **34**, 617–647.
295. N. G. de BRUIJN: *Ned. Akad. Wet. Proc. Ser. A*, 1981, **43**, 39–66.
296. P. KRAMER and R. NERI: *Acta Crystallogr. A*, 1984, **40**, 580–587.
297. V. ELSER: *Acta Crystallogr. A*, 1986, **42**, 36–43.
298. P. A. KALUGIN, A. YU KITAEV, and L. S. LEVITOV: *JETP Lett. (USSR)*, 1985, **41**, 145–149.
299. A. KATZ and M. DUNEAU: *J. Phys. (Orsay)*, 1986, **47**, 181–196.
300. P. J. STEINHARDT and S. OSTLUND: 'The physics of quasicrystals', 29–31; 1987, Singapore, World Scientific.
301. P. BAK: *Scr. Metall.*, 1986, **20**, 1199–1204.
302. P. W. ANDERSON: 'Basic notions of condensed matter physics', 12–15; 1984, Menlo Park, CA, Benjamin/Cummings.
303. V. ELSER: *Phys. Rev. Lett.*, 1985, **54**, 1730.
304. C. L. HENLEY: *J. Phys. A*, 1988, **21**, 1649–1677.
305. P. BAK: *Phys. Rev. B*, 1985, **32**, 5764–5772.
306. N. D. MERMIN and S. TROIAN: *Phys. Rev. Lett.*, 1985, **54**, 1524–1527.
307. M. V. JARIĆ: *Phys. Rev. Lett.*, 1985, **55**, 607–610.
308. O. BIHAM, D. MUKAMEL, and S. SHTRIKMAN: *Phys. Rev. Lett.*, 1986, **56**, 2191–2194.
309. F. LANCON, L. BILLARD, and P. CHANDHARI: *Europhys. Lett.*, 1986, **2**, 625–629.
310. M. WIDOM, K. J. STRANDBURG, and R. H. SWENDSEN: *Phys. Rev. Lett.*, 1987, **58**, 706–709.
311. K. J. STRANDBURG: *Phys. Rev. B*, 1989, **40**, 6071–6084.
312. F. LANCON and L. BILLARD: *J. Phys. (Orsay)*, 1988, **49**, 249–256.
313. M. WIDOM, D. P. DENG, and C. L. HENLEY: *Phys. Rev. Lett.*, 1989, **63**, 310–313.
314. P. W. STEPHENS and A. I. GOLDMAN: *Phys. Rev. Lett.*, 1986, **56**, 1168–1172; **57**, 2331.
315. P. M. HORN, W. MALZFELDT, D. P. DIVINCENZO, J. TONER, and R. GAMBINO: *Phys. Rev. Lett.*, 1986, **57**, 1444–1447.
316. P. A. HEINEY, P. A. BANCEL, P. M. HORN, J. L. JORDAN, S. LAPLACA, J. ANGILELLO, and F. W. GAYLE: *Science*, 1987, **238**, 660–663.
317. V. ELSER: in 'Proc. 15th int. colloq. on group theoretical methods in physics', (ed. R. Gilmore and D. H. Feng); 1987, Singapore, World Scientific.
318. V. ELSER: in 'Aperiodicity and order', Vol. 3, (ed. M. V. Jarić and D. Gratias), 105–136; 1989, Boston, Academic Press.
319. J. L. ROBERTSON: *J. Non-Cryst. Solids*, 1988, **106**, 225–229.
320. J. L. ROBERTSON and S. C. MOSS: *Z. Phys. B*, 1991, **83**, 391–405.
321. J. L. ROBERTSON and S. C. MOSS: *Phys. Rev. Lett.*, 1991, **66**, 353–356.
322. C. L. HENLEY: *Phys. Rev. B*, 1991, **43**, 993–1020.
323. K. J. STRANDBURG, LEI-HAN TANG, and M. V. JARIĆ: *Phys. Rev. Lett.*, 1989, **63**, 314–317.
324. LEI-HAN TANG: *Phys. Rev. Lett.*, 1990, **64**, 2390–2393.
325. Y. HATWALNE and S. RAMASWAMY: *Phys. Rev. Lett.*, 1990, **65**, 68–71.
326. D. LEVINÉ, T. C. LUBENSKY, S. OSTLUND, S. RAMASWAMY, P. J. STEINHARDT, and J. TONER: *Phys. Rev. Lett.*, 1985, **54**, 1520–1523.
327. T. C. LUBENSKY, S. RAMASWAMY, and J. TONER: *Phys. Rev. B*, 1985, **32**, 7444–7452.
328. J. E. S. SOCOLAR, T. C. LUBENSKY, and P. J. STEINHARDT: *Phys. Rev. B*, 1986, **34**, 3345–3360.
329. T. C. LUBENSKY, J. E. S. SOCOLAR, P. J. STEINHARDT, P. A. BANCEL, and P. A. HEINEY: *Phys. Rev. Lett.*, 1986, **57**, 1440–1443.
330. B. E. WARREN: 'X-ray diffraction'; 1990, New York, Dover.
331. P. W. STEPHENS: in 'Aperiodicity and order', Vol. 3, (ed. M. V. Jarić and D. Gratias), 37–104; 1989, Boston, Academic Press.
332. P. A. BANCEL and P. A. HEINEY: *J. Phys. (Orsay)*, 1986, **47-C3**, 341–350.
333. K. URBAN, J. MAYER, M. RAPP, M. WILKENS, A. CSANADY, and J. FIDLER: *J. Phys. (Orsay)*, 1986, **47-C3**, 465–475.
334. J. E. S. SOCOLAR and D. C. WRIGHT: *Phys. Rev. Lett.*, 1987, **59**, 221–224.
335. M. AUDIER and P. GUYOT: *Acta Metall.*, 1988, **36**, 1321–1328.
336. M. AUDIER and P. GUYOT: in 'Quasicrystals and incommensurate structures in condensed matter', (ed. M. J. Yacaman et al.), 288–299; 1989, Singapore, World Scientific.
337. Y. ISHII: *Phys. Rev. B*, 1989, **39**, 11 862–11 871.
338. Y. ISHII: *Philos. Mag. Lett.*, 1990, **62**, 393–397.
339. J. ADAM and J. B. RICH: *Acta Crystallogr.*, 1954, **7**, 813–816.
340. W. B. PEARSON: 'The crystal chemistry and physics of metals and alloys'; 1972, New York, Wiley.
341. A. K. SINHA: *Prog. Mater. Sci.*, 1972, **15**, 75–185.
342. C. B. SHOEMAKER and D. P. SHOEMAKER: *Acta Crystallogr. B*, 1972, **28**, 2957–2905.
343. F. C. FRANK and J. S. KASPER: *Acta Crystallogr.*, 1958, **11**, 184–190; 1959, **12**, 483–499.
344. M. COOPER and K. ROBINSON: *Acta Crystallogr.*, 1966, **20**, 614–617.
345. P. GUYOT, M. AUDIER, and R. LEQUETTE: *J. Phys. (Orsay)*, 1986, **47-C3**, 389–404.
346. V. ELSER and C. L. HENLEY: *Phys. Rev. Lett.*, 1985, **55**, 2883–2886.
347. C. L. HENLEY: *Philos. Mag. B*, 1986, **53**, L59–L66.
348. M. AUDIER and P. GUYOT: in 'Aperiodicity and order', Vol. 3, (ed. M. V. Jarić and D. Gratias), 1–35; 1989, Boston, Academic Press.
349. N. K. MUKHOPADHYAY, K. CHATTOPADHYAY, and S. RANGANATHAN: *Metall. Trans.*, 1989, **20A**, 805–812.
350. A. L. MACKAY: *Acta Crystallogr.*, 1962, **15**, 916–918.
351. R. N. CORBY and P. S. BLACK: *Acta Crystallogr. B*, 1977, **33**, 3468.
352. P. GUYOT and M. AUDIER: *Philos. Mag. B*, 1985, **52**, L15–L19.
353. M. AUDIER and P. GUYOT: *Philos. Mag. B*, 1986, **53**, L43–L51.
354. M. AUDIER, P. SAINFORT, and B. DUBOST: *Philos. Mag. B*, 1986, **54**, L105–L111.
355. H. A. FOWLER, B. MOZER, and J. SIMS: *Phys. Rev. B*, 1987, **37**, 3906–3913.
356. Q. B. YANG: *Philos. Mag. Lett.*, 1988, **57**, 171–176.
357. Q. B. YANG: *Philos. Mag. B*, 1988, **58**, 47–57.
358. G. BERGMAN, J. L. T. WAUGH, and L. PAULING: *Acta Crystallogr.*, 1957, **10**, 254.
359. H. K. HARDY and J. M. SILCOCK: *J. Inst. Met.*, 1955–56, **84**, 423–428.
360. M. AUDIER, P. SAINFORT, and B. DUBOST: *Philos. Mag. B*, 1986, **54**, L105–L111.
361. A. KATZ: in 'Quasicrystalline materials', (ed. C. Janot and J. M. Dubois), 195; 1988, Singapore, World Scientific.

362. E. JEONG, J. C. HOLZER, A. E. CARLSSON, A. E. CONRADI, P. C. FEDDERS, and K. F. KELTON: *Phys. Rev. B*, 1990, **41**, 1695–1698.
363. L. E. LEVINE, J. C. HOLZER, P. C. GIBBONS, and K. F. KELTON: *Bull. Am. Phys. Soc.*, 1990, **35**, 331.
364. L. LEVINE, J. C. HOLZER, P. C. GIBBONS, and K. F. KELTON: *Philos. Mag. B*, 1992, **65**, 435–462.
365. J. C. HOLZER, K. F. KELTON, L. E. LEVINE, and P. C. GIBBONS: *Scr. Metall.*, 1989, **23**, 691–695.
366. J. L. LIBBERT, K. F. KELTON, P. C. GIBBONS, and A. I. GOLDMAN: *J. Non-Cryst. Solids*, 1993, **53**, 153–154.
367. P. A. KALUGIN: Personal communication, 1991.
368. D. D. KOFLAT, I. A. MORRISON, T. EGAMI, S. PREISCHE, S. J. POON, and P. J. STEINHARDT: *Phys. Rev. B*, 1987, **35**, 4489–4492.
369. D. GRATIAS, J. W. CAHN, and B. MOZER: *Phys. Rev. B*, 1988, **38**, 1643–1646.
370. J. W. CAHN, D. GRATIAS, and B. MOZER: *J. Phys. (Orsay)*, 1988, **49**, 1225–1233.
371. M. V. JARIĆ and S. NARASIMHAN: *Phase Transitions*, 1989, **16/17**, 351–365.
372. Z. OLAMI and S. ALEXANDER: *Phys. Rev. B*, 1988, **37**, 3973–3978.
373. C. OGUEY and M. DUNEAU: *Europhys. Lett.*, 1988, **7**, 49–54.
374. M. DUNEAU and C. OGUEY: *J. Phys. (Orsay)*, 1989, **50**, 135–146.
375. R. A. BRAND, G. LE CAËR, and J. M. DUBOIS: *J. Phys. C, Solid State Phys.*, 1990, **2**, 6413–6431.
376. R. C. O'HANDLEY, R. A. DUNLAP, and M. E. McHENRY: *Philos. Mag. B*, 1990, **61**, 677–690.
377. C. L. HENLEY: in 'Quasicrystals', (ed. T. Fujiwara and T. Ogawa); 1990, Berlin, Springer-Verlag.
378. K. F. KELTON: *Phase Transitions*, 1989, **16/17**, 367–381.
379. B. G. BAGLEY and H. S. CHEN: in 'Phase transitions in condensed systems – Experiments and theory', (ed. C. S. Cargill III et al.), *Mater. Res. Soc. Symp. Proc.*, 1985, **57**, 451–463.
380. K. KIMURA, T. HASHIMOTO, K. SUZUKI, K. NAGAYAMA, H. INO, and S. TAKEUCHI: *J. Phys. Soc. Jpn.*, 1986, **55**, 534.
381. A. J. MCALISTER, L. A. BENDERSKY, R. J. SCHAEFER, and F. S. BIANCANIELLO: *Scr. Metall.*, 1987, **21**, 103–106.
382. K. YU-ZHANG, M. HARMELIN, A. QUIVY, Y. CALVAYRAC, J. BIGOT, and R. PORTIER: *Mater. Sci. Eng.*, 1988, **99**, 385–388.
383. K. URBAN, N. MOSER, and H. KRANMULLER: *Phys. Status Solidi (a)*, 1985, **91**, 411–422.
384. K. F. KELTON and J. C. HOLZER: *Phys. Rev. B*, 1988, **37**, 3940–3947.
385. K. F. KELTON and J. C. HOLZER: *Mater. Sci. Eng.*, 1988, **99**, 389–392.
386. U. KOSTER and B. SCHUMACHER: *Mater. Sci. Eng.*, 1988, **99**, 417–421.
387. H. S. CHEN, C. H. CHEN, A. INOUE, and J. T. KRAUSE: *Phys. Rev. B*, 1985, **32**, 1940.
388. D. TURNBULL: *J. Appl. Phys.*, 1950, **21**, 1022.
389. K. F. KELTON: *Solid State Phys.*, 1991, **45**, 75–177.
390. H. GLEITER and B. CHALMERS: *Prog. Mater. Sci.*, 1972, **16**, 13–39.
391. K. K. FUNG and Y. Q. ZHOU: *Philos. Mag. B*, 1986, **54**, L27–L31.
392. P. A. BANCER: *Phys. Rev. Lett.*, 1989, **63**, 2741–2744.
393. M. AUDIER and P. GUYOT: in 'Proc. of Adriatico research conf. on quasicrystals', (ed. M. V. Jarić and S. Lundqvist); 1989, Singapore, World Scientific.
394. Z. ZHANG, N. C. LI, and K. URBAN: *J. Mater. Res.*, 1991, **6**, 366–370.
395. Y. ISHII: *J. Non-Cryst. Solids*, 1989, **117/118**, 840–843.
396. M. WIDOM: in 'Proc. of Adriatico research conf. on quasicrystals', (ed. M. V. Jarić and S. Lundqvist); 1989, Singapore, World Scientific.
397. L. D. LANDAU and E. M. LIFSHITZ: 'Statistical physics', Chap. 14; 1978, Oxford, Pergamon Press.
398. F. H. LI, G. Z. PAN, S. Z. TAO, M. S. HUI, Z. H. MAI, X. S. CHEN, and L. Y. CAI: *Philos. Mag. B*, 1989, **59**, 535–542.
399. Z. ZHANG, N. C. LI, and K. URBAN: *J. Mater. Res.*, 1991, **6**, 366–370.
400. Z. R. HUANG, K. K. FUNG, and Y. Q. ZHOU: *Philos. Mag. B*, 1991, **63**, 485–491.
401. H. ZHANG and K. H. KUO: *Phys. Rev. B*, 1990, **41**, 3482–3487.
402. V. T. SWAMY, S. RANGANATHAN, and K. CHATTOPADHYAY: *J. Mater. Res.*, 1989, **4**, 539–551.
403. T. A. BHASKARAN, R. V. KRISHNAN, S. RANGANATHAN, and K. F. KELTON: in 'Metastable microstructures', (ed. D. Banerjee and L. A. Jacobson), 93–102; 1993, New Delhi, Oxford and IBH Publishing.
404. L. E. LEVINE, P. C. GIBBONS, and K. F. KELTON: *Bull. Am. Phys. Soc.*, 1990, **35**, 331.
405. F. DENOYER, G. HEGER, M. LAMBERT, J. M. LANG, and P. SAINFORT: *J. Phys. (Orsay)*, 1987, **48**, 1357–1361.
406. A. I. GOLDMAN, C. A. GURYAN, P. W. STEPHENS, J. M. PARSEY Jr., G. AEPPLI, H. S. CHEN, and F. W. GAYLE: *Phys. Rev. Lett.*, 1988, **61**, 1962–1965.
407. P. C. GIBBONS, K. F. KELTON, L. E. LEVINE, and R. B. PHILLIPS: *Philos. Mag. B*, 1989, **59**, 593–618.
408. N. K. MUKHOPADHYAY, S. RANGANATHAN, and K. CHATTOPADHYAY: *Philos. Mag. Lett.*, 1989, **60**, 207–211.
409. K. CHATTOPADHYAY and N. K. MUKHOPADHYAY: *Mater. Sci. Forum*, 1987, **22–24**, 639.
410. C. L. HENLEY: *Philos. Mag. Lett.*, 1988, **58**, 87–89.
411. S. EBALARD and F. SPAEPEN: *J. Mater. Res.*, 1989, **4**, 39–43.
412. C. A. GURYAN, A. I. GOLDMAN, P. W. STEPHENS, K. HIRAGA, A. P. TSAI, A. INOUE, and T. MASUMOTO: *Phys. Rev. Lett.*, 1989, **62**, 2409–2412.
413. K. F. KELTON, P. C. GIBBONS, and L. E. LEVINE: in 'Quasicrystals and incommensurate structures in condensed matter', (ed. M. J. Yacaman et al.), 524–531; 1989, Singapore, World Scientific.
414. K. F. KELTON and P. C. GIBBONS: *Philos. Mag. B*, 1992, **66**, 639–651.
415. R. DE RIDDER, G. VAN TENDELOO, and S. AMELINCKX: *Acta Crystallogr.*, 1976, **32**, 216.
416. R. DE RIDDER, G. VAN TENDELOO, D. VAN DYCK, and S. AMELINCKX: *Phys. Status Solidi (a)*, 1976, **38**, 663–674.
417. P. J. STEINHARDT: Personal communication, 1987.
418. L. S. LEVITOV: *Europhys. Lett.*, 1988, **6**, 419–424.
419. M. V. JARIĆ and D. R. NELSON: *Phys. Rev. B*, 1988, **37**, 4458–4472.
420. P. C. GIBBONS, K. F. KELTON, L. E. LEVINE, and R. B. PHILLIPS: in 'Quasicrystals and incommensurate structures in condensed matter', (ed. M. J. Yacaman et al.), 516–523; 1989, Singapore, World Scientific.
421. S. K. SIKKA, Y. K. VOHRA, and R. CHIDAMBARAM: *Prog. Mater. Sci.*, 1982, **27**, 245–310.
422. S. J. POON: *Adv. Phys.*, 1992, **41**, 303–363.
423. A. I. GOLDMAN and K. F. KELTON: *Rev. Mod. Phys.*, 1993, **65**, 213–230.
424. *J. Non-Cryst. Solids*, 1993, **153–154**, 1–674.